ATTACHMENT 8

Brannon A. Seay et al., *Per- and Polyfluoroalkyl Substances Fate and Transport at a Wastewater Treatment Plant with a Collocated Sewage Sludge Incinerator*, 847 SCI. TOTAL ENV'T 1 (2023) ("Battelle Study") and Supporting Information

Science of the Total Environment 874 (2023) 162357

Contents lists available at ScienceDirect

Science of the Total Environment

journal homepage: www.elsevier.com/locate/scitotenv

Per- and polyfluoroalkyl substances fate and transport at a wastewater treatment plant with a collocated sewage sludge incinerator

Brannon A. Seay *, Kavitha Dasu, Ian C. MacGregor [1], Matthew P. Austin, Robert T. Krile, Aaron J. Frank, George A. Fenton, Derik R. Heiss, Rhett J. Williamson, Stephanie Buehler [1]

Battelle Memorial Institute, 505 King Ave, Columbus, OH 43201, United States

HIGHLIGHTS

- The fate and transport of PFAS at WWTPs operating SSIs is an important data gap.
- Study measured PFAS and IF at all influents/effluents of a WWTP operating an SSI.
- Statistical analyses characterized concentrations and mass flows at the WWTP/SSI.
- Most PFAS mass discharged in aqueous effluent; small contributions to air/landfill.
- The SSI may inadequately destroy PFAS, as the observed thermal removal was 51 %.

GRAPHICAL ABSTRACT

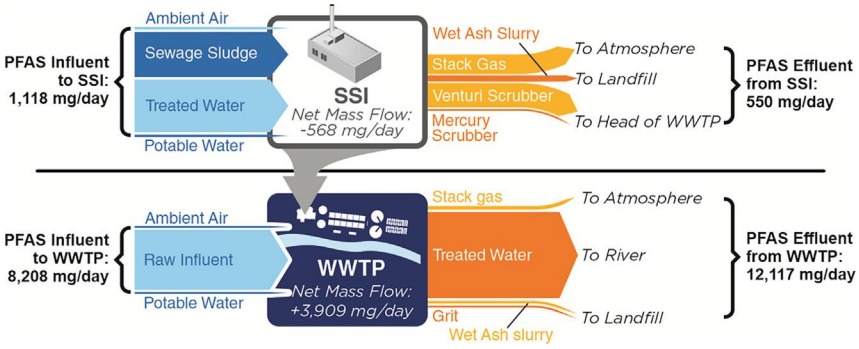

ARTICLE INFO

Editor: Damià Barceló

Keywords:
PFAS
Inorganic fluoride
WWTP
SSI
Raw influent
Treated water

ABSTRACT

This study aims to understand the fate and transport of per- and polyfluoroalkyl substances (PFAS) and inorganic fluoride (IF) at an undisclosed municipal wastewater treatment plant (WWTP) operating a sewage sludge incinerator (SSI). A robust statistical analysis characterized concentrations and mass flows at all WWTP and SSI primary influents/effluents, including thermal-treatment derived airborne emissions. WWTP-level net mass flows (NMFs) of total PFAS were not statistically different from zero. SSI-level NMFs indicate that PFAS, and specifically perfluoroalkyl acids (PFAAs), are being broken down. The NMF of perfluoroalkyl sulfonic acids (PFSAs; -274 ± 34 mg/day) was statistically significant. The observed breakdown primarily occurred in the sewage sludge. However, the total PFAS destruction and removal efficiency of 51 % indicates the SSI may inadequately remove PFAS. The statistically significant IF source (NMF $= 16 \pm 4.2$ kg/day) compared to the sink of PFAS as fluoride (NMF $= -0.00036$ kg/day) suggests that other fluorine-containing substances are breaking down in the SSI. WWTP PFAS mass discharges were primarily to the aquatic environment (>99 %), with <0.5 % emitted to the atmosphere/landfill. Emission rates for formerly phased-out PFOS and PFOA were compared to previously reported levels. Given the environmental persistence of these compounds, the observed decreases in PFOS and PFOA discharge rates from prior reports implies regional/local differences in emissions or possibly their accumulation elsewhere. PFAS were observed in stack gas emissions, but modestly contributed to NMFs and showed negligible contribution to ambient air concentrations observed downwind.

Abbreviations: ASE, accelerated solvent extraction; AWOS, Automatic Weather Observing Station; DoD/DOE QSM 5.3, Department of Defense/Department of Energy Quality Systems Manual Version 5.3; DRE, destruction and removal efficiency; GC/MS, gas chromatography/mass spectrometry; HF, hydrogen fluoride; IC, ion chromatography; IF, inorganic fluoride; ISC-PRIME, Industrial Source Complex – Plume Rise Model Enhancements; ISE, ion selective electrode; LC/MS/MS, liquid chromatography tandem mass spectrometry; MDL, measurement detection limit; NC, negative control; NMF, net mass flow; PCI, positive chemical ionization mode; PIC, products of incomplete combustion; PFAA, perfluoroalkyl acid; PFAS, per- and polyfluoroalkyl substances; PFCA, perfluoroalkyl carboxylic acid; PFSA, perfluoroalkyl sulfonic acids; SPE, solid phase extraction; SSI, sewage sludge incinerator; TF, total fluorine; WWTP, wastewater treatment plant.

* Corresponding author.
E-mail address: seay@battelle.org (B.A. Seay).
[1] Formerly from Battelle Memorial Institute, 505 King Ave., Columbus, OH 43201, United States.

http://dx.doi.org/10.1016/j.scitotenv.2023.162357
Received 12 December 2022; Received in revised form 15 February 2023; Accepted 16 February 2023
Available online 27 February 2023

1. Introduction

Nearly 15,000 wastewater treatment plants (WWTPs), serving 238.2 million people, and processing 25 billion gallons/day of liquid raw influent (i.e., municipal wastewater, landfill leachate, and industrial waste (Stoiber et al., 2020)) were in operation in the United States in 2012 (EPA, 2016a). Given per- and polyfluoroalkyl substances (PFAS) have been used in diverse industrial and consumer applications since 1940, with over 600 PFAS in current commercial use in the United States (EPA, 2020), WWTP raw influents often contain elevated levels of PFAS. Furthermore, previous studies have found higher concentrations of PFAS in treated wastewater effluent as compared to the raw influent (Eriksson et al., 2017; Gallen et al., 2018; Kim Lazcano et al., 2019; Loganathan et al., 2007; Schultz et al., 2006; Venkatesan and Halden, 2013; Wang et al., 2018), likely due to the wastewater treatment's biological and physical processes converting precursor compounds to terminal PFAS (Stoiber et al., 2020; Schultz et al., 2006; Arvaniti and Stasinakis, 2015). It has been reported that WWTPs discharge PFAS into aquatic environments through the direct release of treated water, the atmosphere via aeration tank treatment and other processes (Stoiber et al., 2020; Vierke et al., 2011), and soil and groundwater through the leaching of landfilled biosolids. One byproduct of the wastewater treatment process, sewage sludge, can be either landfilled with other solid wastes, spread on agricultural fields as a fertilizer, or incinerated.

While various factors influence PFAS sorption potential, generally longer chain PFAS more readily adsorb to solids, and hence show greater accumulation in sewage sludge, while shorter chain PFAS partition to liquids, providing greater accumulation in treated water effluent (Coggan et al., 2019). Further, higher partitioning of perfluoroalkyl sulfonic acids (PFSAs) as compared to perfluoroalkyl carboxylic acids (PFCAs) to sewage sludge has previously been observed (Coggan et al., 2019; Higgins et al., 2005). Millions of tons of sewage sludge per year are applied on agricultural fields in the United States (NEBRA, 2007), and studies (Blaine et al., 2013; Ghisi et al., 2019; Sepulvado et al., 2011; Wang et al., 2020a) have found that PFAS can bioaccumulate in plants during this process. With the potential of PFAS-laden sewage sludge contaminating crops, the State of Maine has temporarily banned the practice (Burns, 2019) until further testing can be conducted.

Sewage sludge incinerators (SSIs) are currently in operation at approximately 200 WWTPs in the United States, in which over one million tons of WWTP processed sludge are incinerated annually (NEBRA, 2007). Previously reported studies have shown that waste incineration of fluorotelomer based polymers mineralized PFAS to inorganic fluoride at high temperatures (>870 °C) (Aleksandrov et al., 2019; Taylor et al., 2014). However, more research is required regarding the incomplete combustion and ash byproduct from sewage sludge incineration to fully understand the fate and transport of PFAS during thermal treatment (Stoiber et al., 2020; EPA, 2019). Laboratory studies have found that the required incineration temperature to degrade a given PFAS compound increases with increasing perfluoroalkyl chain lengths (Rayne and Forest, 2009), with 99 % of PFAS degrading at 600 °C (Taylor and Yamada, 2003) and higher destruction requiring temperatures exceeding 1000 °C and residence times >2 seconds (Taylor et al., 2014). Few field studies have investigated PFAS incineration at full-scale operating facilities (Stoiber et al., 2020). One study found that concentrations declined two to 10-fold from pre-incineration sewage sludge to post-incineration wet ash slurry (Loganathan et al., 2007). Another study found that leachates from wet ash slurry landfills had significantly lower PFAS levels than from solid waste landfills, and the lower ash leachate concentrations correlated to higher incineration temperatures (Solo-Gabriele et al., 2020). Elevated PFOA concentrations have also been measured onsite as compared to upwind of municipal solid waste incinerators (Wang et al., 2020b). However, to fully understand the fate and transport of PFAS during thermal treatment, specifically at SSIs, full-scale field studies that quantify mass flows of all applicable effluents, including stack gas emissions and wet ash slurry, are needed. Further, while mineralization of PFAS is dependent on incineration operating conditions, such as temperature and residence time (Aleksandrov et al., 2019; Taylor et al., 2014), it is not well understood whether current incineration processes generate products of incomplete combustion (PICs) or completely mineralize PFAS compounds (Tsang et al., 1998). Further research in analytical methods capable of capturing and characterizing PICs potentially formed during thermal destruction processes is needed. Given the current state of the science, it is important to measure fluoride coincidentally with PFAS to better understand if incineration is generating PICs or fully mineralizing PFAS. To the best of our knowledge, there are no published studies regarding the fate and transport of PFAS and fluoride through all primary influents and effluents of an SSI (Winchell et al., 2020), which represents an important data gap (Stoiber et al., 2020).

To address this gap, this study measured up to 30 different PFAS and inorganic fluoride (IF) in the influents and effluents of a full-scale WWTP operating a fluidized bed SSI. We aim to improve the understanding of the fate and transport of these compounds at both the level of the WWTP, which is inclusive of the SSI, and through the SSI alone. Herein, we (1) report concentrations of PFAS and IF at all influents and effluents streams, (2) estimate net mass flows (NMFs) from the WWTP and SSI, (3) investigate the efficacy with which PFAS are destroyed in the SSI under typical operating conditions, (4) estimate PFAS emission rates in all effluent streams, and (5) estimate stack gas contributions to downwind ambient air PFAS concentrations to understand thermal treatment's potential contribution to ambient air.

2. Materials and methods

2.1. Study design and sampling approach

The two-day field study occurred on August 28–29, 2019, at an undisclosed U.S. WWTP (Fig. S1) operating a fluidized bed SSI. The SSI actively processed and incinerated approximately 160,000 kg of sewage sludge under its typical operating conditions (830 °C internal temperature and ~ 8 s residence time) during the entirety of the study. Municipal waste incineration is typically operated at temperatures >810 °C and residence time of >2 s. A schematic of the WWTP's treatment process along with the ten influent and effluent matrices which were assayed are shown in Fig. 1. The sampling schedules, flow rates, and other details for each matrix are provided in Table S1.

Discrete stack gas samples were collected in the morning and afternoon on both days of the study. The SSI airborne effluent was assayed for total fluorine (TF; Modified EPA Method 18 (EPA, U. S, n.d.)), hydrogen fluoride (HF; EPA Method 26A (EPA, U. S, n.d.)), and 30 PFAS compounds (Modified EPA Method 0010 (EPA, 1986), adapted for PFAS analysis). Table S2 lists every compound measured from the stack and each of the other nine matrices. One field blank train was also prepared and collected for each of the sampling methods described above. A detailed description of the stack gas sampling approach is provided in the supplemental information (SI; Text S1).

Grab sampling was performed for each of the eight solid and aqueous matrices. Three sewage sludge, potable water, treated water, venturi scrubber water, mercury scrubber water, and wet ash slurry sampling events occurred approximately at the beginning, middle, and end of each stack gas run, for a total of 12 sampling events per matrix. Excluding potable water, each of these matrices was expected to be temporally correlated to one another and the stack gas. One raw influent and grit sampling event occurred at the beginning and end of each day. No temporal correlation was expected between either the raw influent or grit with any other sampled matrix. Identical field samples were collected during each sampling event to allow for both duplicate measurements of a given compound class and the assay for various compound classes, i.e., both target PFAS and IF. One negative quality control sample on each day for each matrix and compound class was also collected. Additional discrete samples of aqueous matrices were collected for use as positive controls.

Collocated ambient air samplers were positioned both north (~275 m) and south (~450 m) of the SSI (Fig. S1) and operated at approximately 12 m^3/h for 24 h both days. The custom high-volume sampling method was based on a modification of EPA Method TO-13A (EPA, 1999) and similar

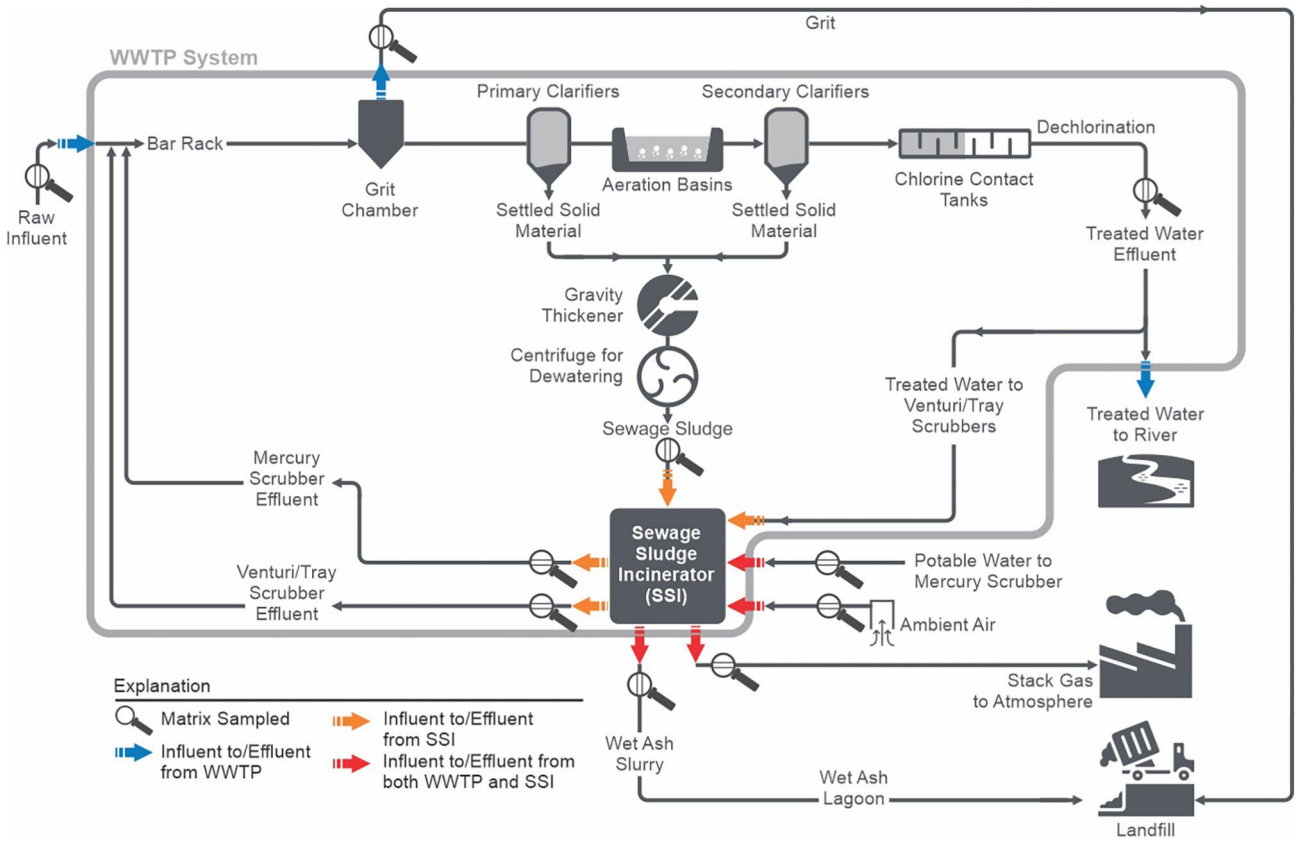

Fig. 1. Flow diagram of the WWTP and SSI treatment process from initial waste input (raw influent; upper left) to the final discharge location (river, atmosphere, landfill; lower right) of the various effluents. Both the larger WWTP system (grey outer box) and the incorporated SSI system (dark grey square) are illustrated along with the various material influent and effluent streams (colored arrows). Arrow colors indicate if the influent/effluent is to/from the WWTP (blue), SSI (orange), or both (red) systems. Magnifying glass symbols indicate matrices sampled in the study.

to methods previously described (Piekarz et al., 2007; Wong et al., 2018). Each sampler was loaded with a 102 mm diameter quartz fiber filter (Whatman) atop a PUF/XAD/PUF "sandwich" (Sigma-Aldrich) for collection and analysis of 24 ionic (Tables S2, S4-S5) and seven neutral (Table S2-S3) PFAS, respectively. A total of eight discrete field samples were collected along with two field blanks and a trip blank.

2.2. Sample extraction and analysis

The sample extraction and analysis methodology for each matrix are briefly described here. Additional details are provided in the SI (Text S2).

2.2.1. Aqueous and solid matrices

Extraction and analysis of the aqueous and solid matrices were performed for target PFAS and IF. The wet ash samples were biphasic, consisting of an aqueous layer overlying a small amount (~0.5 to ~1 g) of wet solid material. The aqueous and solid phases were separated and analyzed independently for target PFAS, whereas only the aqueous fraction was assayed for IF. The measured concentrations for all solid matrices are reported on a dry weight basis.

Target ionic PFAS analysis in all the sample matrices was performed using isotope dilution liquid chromatography tandem mass spectrometry (LC/MS/MS). Target PFAS (18 PFAS analytes, Table S2) in potable water samples were extracted and analyzed following EPA Method 537.1 (Shoemaker and Tettenhorst, n.d.). Non-potable water samples were analyzed for 27 PFAS analytes (Table S2) using weak anion exchange solid phase extraction (SPE) cartridges following an extraction method compliant with the U.S. Department of Defense/Department of Energy Quality Systems Manual Version 5.3 (DoD/DOE QSM 5.3) Table B-15 criteria (DoD and DOE, 2009). Solid (grit and sewage sludge) matrix samples were analyzed for 28 PFAS analytes (Table S2) using solvent extraction followed by ENVI-Carb™ clean-up procedure compliant with DoD/DOE QSM 5.3 Table B-15 criteria (DoD and DOE, 2009).

IF was measured in the aqueous matrices by ion chromatography (IC) with conductivity detection. Due to the presence of coeluting chromatographic interferences, positive bias was suspected in the sewage sludge extracts' measured fluoride concentrations; therefore, reanalysis of the sewage sludge was performed with a potentially more selective technique using an ion selective electrode (ISE; Text S2).

2.2.2. Stack gas matrix

Stack gas was assayed for 30 target ionic PFAS, HF, and TF (Table S2). The PFAS collected on the MM0010 sampling trains were extracted with alkaline methanol and analyzed by isotope dilution LC/MS/MS using modified EPA Method 537 (EPA, 2009). Analysis of HF in the Method 26A trains was performed by IC following EPA Method 9056A (EPA, 2007). An aliquot of methanol from each of the six impingers in the modified Method 18 sampling train was combined into a single, composited sample, after which the fluorinated species in this composite were converted to free fluoride using EPA Method 5050 (bomb combustion) followed by fluoride analysis by EPA Method 9056A (EPA, 2007).

2.2.3. Ambient air matrix

Neutral PFAS collected on PUF/XAD/PUF were extracted using accelerated solvent extraction (ASE) with ethyl acetate followed by analysis using gas chromatography/mass spectrometry (GC/MS) in positive chemical ionization mode (PCI) with methane as the reagent gas.

Ionic PFAS (Table S4 and S5) collected on QFFs were extracted by fortifying the filters with extraction internal standards and serially extracted twice using methanol and cleaned using Supelclean™ Envi-Carb™ SPE cartridges (Millipore Sigma, Burlington, MA). Extracts were concentrated to dryness under nitrogen and reconstituted with 50:50 methanol/water (*V*/V) and fortified with injection internal standards for analysis by isotope dilution LC/MS/MS.

2.3. Dispersion modeling

Site meteorological data assessment and ambient dispersion modeling was performed to predict 24-h incinerator stack concentration contributions at the two ambient air monitoring locations. A Met One model 034B weather station sited adjacent to the WWTP stack and Automatic Weather Observing Station (AWOS) data from a Regional Airport, located approximately 1 mile southeast of the WWTP, were the sources of meteorological data. The Industrial Source Complex – Plume Rise Model Enhancements (ISC-PRIME) ambient dispersion model (Schulman et al., 2000) was applied to estimate the 24-h average dilution of a unit emission from the SSI stack at both ambient air monitoring locations for both days of the study. Applying the model predicted dilutions to the measured stack gas concentrations provided an estimate of the incinerator's contribution to the downwind ambient air concentrations. Further details on the dispersion modeling are provided in the SI (Text S3).

2.4. Data analysis

For each sampling matrix and compound, concentration and mass flow central tendencies were calculated as the average negative control (NC) corrected measurement from all unique sampling events performed over both study days. For sampling events containing duplicate measurements, the duplicate concentrations were averaged prior to the event level averaging. Any measurement qualified as a non-detect was zero substituted and included in the calculation. This conservative approach, as opposed to substitution of one half the measurement detection limit (MDL) for non-detects, for example, or omitting non-detects from calculations altogether, prevented biasing results high and protected against false positive results. Furthermore, to minimize bias, all numerical results were retained and included, even those less than applicable MDLs, so long as qualitative identification criteria were met. The NC correction was made by subtracting the maximum NC from the averaged value. All negative NC corrected central tendency concentrations were set to zero. Per matrix PFAS class (PFCAs, PFSAs, precursors/intermediates, new alternatives, and total PFAS) central tendencies were then derived as the sum of all individual NC corrected compound values for PFAS belonging to a specific class.

The concentration central tendency (*C*) for each matrix (*m*) and compound (*p*) was derived as:

$$C(m,p) = \frac{1}{n}\sum_{i=1}^{n}(c_i) - NC, \tag{1}$$

where c_i is the concentration of an individual sampling event, *NC* is the maximum negative control (Tables S11 – S21), and *n* is the number of unique events aggregated across both study days for the given matrix and compound. The NC corrected mass flow central tendency (*MF*) was derived as:

$$MF(m,p) = \frac{1}{n}\sum_{i=1}^{n} f_i(c_i - NC), \tag{2}$$

where *f* is the averaged flow rate (Table S1) for the matrix, *m*. The per compound net mass flow (*NMF*) was calculated at both the WWTP and SSI levels as the difference between sums of *MFs* in the effluent and influent matrices:

$$NMF(p) = \sum_{e=1}^{E}(MF)_e - \sum_{i=1}^{I}(MF)_i, \tag{3}$$

where *e* and *i* represent an effluent or influent matrix, respectively. Fig. 1 and Table S1 identify the influents to and effluents from both the WWTP and SSI. At the SSI level only, PFAS-specific destruction and removal efficiencies (DREs) were calculated as:

$$DRE(p) = 100 \times \left(1 - \left(\frac{\sum_{e=1}^{E}(MF)_e}{\sum_{i=1}^{I}(MF)_i}\right)\right) \tag{4}$$

Uncertainty of the central tendencies (*C* and *MF*) and *NMF* were estimated as the standard error based on the concentration, matrix flow rate, and covariance between the two. For the *NMF* uncertainties, covariances between daily averages were also considered. Hypothesis testing was applied to derive 95 % confidence intervals for the *NMF* point estimates. Both unadjusted and adjusted *p*-values were derived, where the latter was calculated following the Holm-Bonferroni method (Holm, 1979). Further details on the central tendencies, uncertainties, and hypothesis testing are provided in the SI (Text S4).

3. Results and discussion

3.1. PFAS concentrations

Individual and total PFAS concentrations (Eq. (1), Fig. S2, Tables S11-S21) in the raw influent (117 ± 39 ng/L; study average ± uncertainty) were within the range of measured concentrations at other WWTPs reported in the literature (Schultz et al., 2006; Coggan et al., 2019; Nguyen et al., 2019), and comprised mostly of perfluoroalkyl acids (PFAAs; 88 %), with considerable concentrations of short-chain compounds as well as PFOA and PFOS. Of the precursors/intermediates and new alternatives, 6:2 FTS and HFPO-DA accounted for over 10 % of the total PFAS concentration.

The WWTP separates and processes the raw influent into grit, sewage sludge, and treated water. The grit contained traces of PFAS (1.3 ± 2.5 ng/g), namely PFBA, PFHxA, and PFOA. Sewage sludge concentrations were >20 times higher (31 ± 3.7 ng/g), where PFAS tend to accumulate through sorption, with long-chain PFAS generally partitioning to the sludge more readily (Coggan et al., 2019). PFOS, a long-chain PFSA, represented 48 % of the total PFAS concentrations in the sewage sludge, followed by PFHxA (18 %) and PFPeA (12 %) (two short-chain PFCAs). While these short-chained compounds provided a large absolute percentage of the total PFAS in the sewage sludge, concentrations in the treated water were greater than that in the raw influent for both, indicating PFHxA and PFPeA primarily remained bound in the liquid phase (plus additional transformation). Total PFAS concentration in the treated water (167 ± 83 ng/L) was greater than but not statistically different than in the raw influent. This concentration increase was primarily attributed to increases in PFBA (19.6 ± 29.8 ng/L to 72.0 ± 75.9 ng/L) and to a lesser extent HFPO-DA (7.5 ± 2.5 ng/L to 18.6 ± 6.9 ng/L), suggesting their formation during wastewater treatment, as previously observed (Eriksson et al., 2017; Gallen et al., 2018; Loganathan et al., 2007; Schultz et al., 2006; Venkatesan and Halden, 2013; Wang et al., 2018; Kim Lazcano et al., 2020; Sun et al., 2016). The long-chain PFCAs and all PFSAs, however, exhibited lower concentrations in the treated water, which may be attributable to their sorption to sewage sludge (Coggan et al., 2019).

An intercomparison of SSI matrix concentrations shows that total PFAS concentrations of treated water (167 ± 83 ng/L), which is admitted to the venturi/tray scrubber and contributes approximately 99 % of the wet ash slurry volume, were within the measurement uncertainties of both the venturi/tray scrubber (86.9 ± 17.9 ng/L) and wet ash slurry (136 ± 44.7 ng/L), as expected. All applicable individual PFAS from the potable water measured below both state (Cordner et al., 2019; Legislature, 2020) and 2016 U.S. EPA(EPA, 2016b) advisory levels, however, both PFOA and PFOS measured above the updated 2022 U.S. EPA interim lifetime health advisory levels (EPA, 2022). The potable water total PFAS influent (9.9 ± 0.6 ng/L) was not statistically different than the mercury scrubber

effluent (13.2 ± 3.6 ng/L) across like-measured compounds. These results are discussed in more detail in the SI (Text S5).

The total sum ionic PFAS (Table S20) measured in ambient air across both days of the study and from both sampling locations averaged 56.2 ± 34.8 pg/m^3, with the largest contributions from PFOA (26.3 ± 31.9 pg/m^3) and PFBA (22.5 ± 6.6 pg/m^3). The limited number of previous studies regarding PFAS in WWTP ambient air have shown that compared to non-contaminated reference sites the PFAS concentrations on WWTP sites were 1.5 to 15 times higher (Hamid, 2016). However, results here were more similar to previously reported reference sites than onsite WWTPs. Across like measured compounds, the average PFCA concentration observed here (50.1 pg/m^3) was similar to that measured at a distant reference site (59.1 pg/m^3) located approximately 600 m from an Ontario, Canada WWTP (Ahrens et al., 2011) and lower than that at near reference sites (70.4–134 pg/m^3), primary clarifiers (95.7–208 pg/m^3), aeration tanks (202–237 pg/m^3), and secondary clarifiers (106–121 pg/m^3). Similarly, PFOS (2.15 pg/m^3) was most similar to the distant reference site (3.05 pg/m^3) and lower than those at near reference sites (4.68–34.2 pg/m^3), primary clarifiers (42.7–120 pg/m^3), aeration tanks (126–171 pg/m^3), and secondary clarifiers (93.9–108 pg/m^3). The total sum neutral PFAS (Table S21) measured in the ambient air averaged 780.3 ± 488.2 pg/m^3, primarily from 6:2 FTOH (89 %) and 8:2 FTOH (7 %). The dominance of 6:2 FTOH followed by 8:2 FTOH has been observed at various Ontario, Canada WWTPs (Vierke et al., 2011; Ahrens et al., 2011; Shoeib et al., 2016). Conversely, two WWTPs in northern Germany (Weinberg et al., 2011) observed 8:2 FTOH >6:2 FTOH, which is typical to that observed in ambient urban air not influenced by WWTPs (Piekarz et al., 2007; Barber et al., 2007; Jahnke et al., 2007; Shoeib et al., 2006). Shoeib et al. (2016) provided possible explanations for the higher 6:2 FTOH levels observed at the Canadian WWTPs, including higher 6:2 FTOH levels in the raw influent (FTOH was not measured in the liquid matrices in this study), differences in the compounds' chemical properties, and transition from long- to short-chain PFAS in industrial practices. As primary sources of atmospheric FTOHs are manufacturing facilities and/or other commercial product usage, the higher 6:2 FTOH compared to 8:2 FTOH observed here could be due to nearby industries' transition to short-chain PFAS. Like the ionic compounds, the neutral PFAS concentrations were most similar to previously observed reference sites nearby WWTP features (442–1095 pg/m^3) and lower than those by primary clarifiers (9354–22,677 pg/m^3), aeration tanks (4334–11,541 pg/m^3), and secondary clarifiers (1414–1909 pg/m^3) (Ahrens et al., 2011).

3.2. Inorganic fluoride concentrations

IF concentrations at the WWTP (Eq. (1), Tables S11-S19, Fig. S3) were most notably observed in the wet ash slurry (30.2 ± 7.82 mg/L), with measured concentrations >20 times greater than the next closest aqueous matrix. This large disparity could indicate mineralization of fluorinated compounds during thermal treatment of the sewage sludge, but nonetheless was unanticipated and is not fully explainable within the scope of this study.

The potable water IF concentration (0.64 ± 0.06 mg/L) was consistent with that from fluoridation of the public water supply (Health and Human Services Federal Panel on Community Water F, 2015). The elevated concentration in the raw influent (1.06 ± 0.07 mg/L) suggests contributions from additional sources beyond potable water fluoridation. The raw influent consisted of residential wastewater (65.4 %) mostly comprised of potable water, stormwater (19.2 %), and industrial wastewater (15.4 %). IF in the treated water (0.82 ± 0.19 mg/L) was not statistically different than in the raw influent, coinciding with previous research indicating that conventional wastewater treatment does not remove fluorides (Gehr and Leduc, 1992; Tafu et al., 2016).

3.3. Stack gas PFAS emission contributions to downwind ambient air concentrations

On Day One, the stack gas plume was estimated to contribute 0.15 pg/m^3 (0.17 %) to the total ionic PFAS (83.6 pg/m^3) measured at the North sampling site (Fig. S4, Table S22). Changing meteorological conditions on Day Two resulted in an estimated plume contribution of 0.27 pg/m^3 (0.83 %) to the total PFAS (32.7 pg/m^3) observed at the South location. The estimated concentration contributions from the plume at the downwind sites for both days and for every PFAS compound were less than both the uncertainty in the daily averaged ambient concentrations and the ambient air analysis MDLs (Table S22). Further, when considering the daily location of maximum downwind plume impact within the modeled domain, all concentration contributions were still below the MDLs. These results indicate the plume's contribution to ambient air concentrations within the modeled domain were negligible on both study days.

Neutral PFAS concentrations (Table S23) exhibited similar spatial and temporal trends as the ionic PFAS. While neutral PFAS were not measured in the stack gas, given the dispersion results and observed ambient concentrations on both days, the stack's influence on downwind ambient air concentrations appears to be minimal compared to other potential sources. Concentrations of 6:2 FTOH and 8:2 FTOH, particularly at the North site, are greater than that previously measured at rural and urban locations (Barber et al., 2007) and more similar to monitoring nearby WWTP features (e.g., aeration tanks, clarifiers) (Ahrens et al., 2011). This suggests a potential onsite source, other than the stack plume, of these neutral PFAS. These results are discussed in more detail in the SI (Text S6).

3.4. PFAS mass flow at the WWTP, including the SSI

PFAS mass flows (Eq. (2); Figs. 2, S5, and S6; Tables S11-S20) at the WWTP were driven primarily by the raw influent and treated water effluent. Both PFCA (4004 ± 5808 mg/day) and total PFAS (3909 ± 5815 mg/day) NMFs were positive (Eq. (3), Fig. 2, Table 1), consistent with previous studies (Eriksson et al., 2017; Houtz et al., 2016) showing that transformation of unmeasured PFAS precursor species, such as fluorotelomers, to target terminal PFAS is likely occurring during wastewater treatment. The NMF of PFCAs was driven largely by the formation of PFBA (3872 ± 5778 mg/day), with 1 to 2 orders of magnitude lower net positive contributions from PFPeA, PFHxA, and PFDA (Figs. S5-S6, Table 1). The remainder of the PFCAs behaved more similarly to the PFSAs, which exhibited a negative NMF (−872 ± 748 mg/day), demonstrating partial loss during water treatment, as previously observed (Lenka et al., 2021; Wang et al., 2020c). This sink, particularly for the longer chained terminal PFAS, could be at least in part due to sorption onto the sewage sludge and transformation prior to incineration (Coggan et al., 2019; Lenka et al., 2021; Sun et al., 2012; Zhou et al., 2019). Primary contributors to the loss of PFSAs included PFBS, PFHxS, and PFOS (Table 1). Across the PFAAs (PFCAs and PFSAs), the influent mass flows of even chain-length PFAS were larger than odd chain-length PFAS, e.g., PFBA > PFPeA, PFBS > PFPeS, etc. Such a pattern is consistent with that observed previously during wastewater treatment (Loganathan et al., 2007; Sinclair and Kannan, 2006).

Among the measured PFAS precursors/intermediates, NEtFOSAA, which is an aerobic biotransformation intermediate of N-EtFOSE (Mejia Avendaño and Liu, 2015) and an immediate precursor of PFOS, appears to be formed during wastewater treatment. Conversely, the fluorotelomer sulfonates (e.g., 6:2 FTS) are being broken down, potentially into PFCAs (e.g., PFHxA) due to aerobic biotransformation in the activated sludge (Wang et al., 2011). Primarily due to the loss of 6:2 FTS during wastewater treatment, the NMF of the precursor species is negative (−198 ± 315 mg/day). Among the new alternatives, only HFPO-DA was measured to an appreciable extent, with a positive NMF (976 ± 596 mg/day), suggesting it was formed and released during treatment of the raw influent. However, HFPO-DAs NMF was not statistically significantly different than zero at the 95 % confidence level, and while studies have found that conventional wastewater treatment does not adequately remove HFPO-DA (Vakili et al., 2021), to the authors' knowledge there has been no prior research supporting or observing HFPO-DAs formation during treatment.

The qualitative trends in formation and removal noted above notwithstanding, none of the PFAS classes, total PFAS, or the individual species

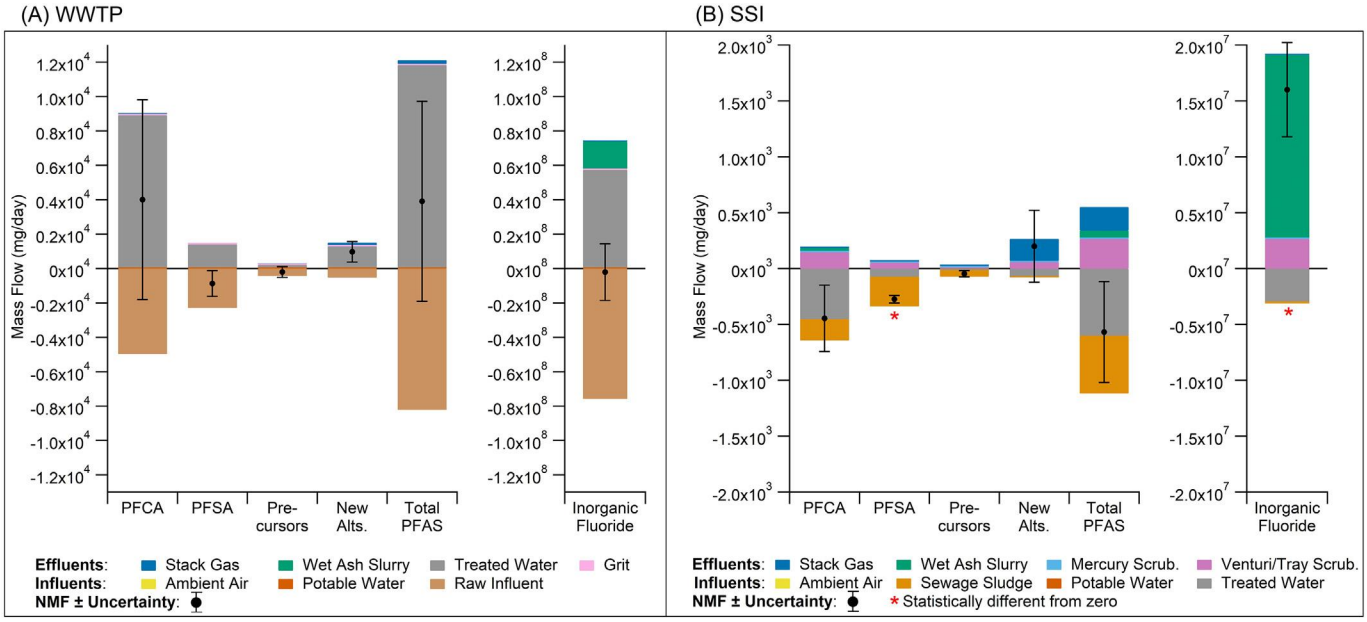

Fig. 2. Study average mass flows for each PFAS class and IF at the level of the WWTP (A), which is inclusive of the SSI, and the SSI alone (B). Each colour indicates a separate influent and effluent source. Influents are shown as negatives and effluents as positives on the y-axes. The black circles represent the NMF for a given pollutant group, i.e., the sum of all effluents minus the sum of all influents. A positive (negative) NMF indicates the WWTP or SSI is a source (sink) of the PFAS class or IF. The black error bars represent the NMF uncertainty. Red asterisks (*) denote NMFs that are statistically different from zero at the 95 % confidence interval. Note that the IF y-axes are scaled 10^4 times larger than the PFAS class y-axes for both subplots (A) and (B).

exhibited NMFs that were statistically significantly different from zero at the 95 % confidence level (Tables 1, S24, and S25). Therefore, based on the observed variability in flow rates and PFAS concentrations over the duration of this field study, it is not possible to draw definitive conclusions regarding the net production or breakdown of PFAS during the water treatment process.

3.5. PFAS mass flow and DREs at the SSI

SSI NMFs for PFCA (−446 ± 297 mg/day) and all individual PFCA species were negative, except for PFTeDA, whose NMF was negligible (< 0.2 mg/day; Table 1). The negative NMF was driven by the loss of PFBA from the treated water introduced into the venturi/tray scrubber, along with losses of PFPeA, PFHxA, and PFOA from both the treated water influent and the sewage sludge. Exclusive of PFTeDA, SSI DREs ranged from 16 to 99 % (Table 1). Such suggests that PFCAs are mineralizing to some extent in the SSI, offering an explanation as to the observed negative NMFs of PFHpA, PFOA, PFNA, PFUnA and other longer-chain PFCAs at the level of the WWTP, which includes thermal treatment in the SSI. Net loss of the PFCAs was also the major contributor to the negative NMF for total PFAS (−568 ± 452 mg/day, 51 % DRE). While the NMFs of PFCA and total PFAS were not statistically significant (Tables 1 and S24), NMFs for two individual PFCAs, PFHxA (−99 ± 12 mg/day, 53 % DRE) and PFDA (−9.7 ± 2.5 mg/day, 87 % DRE), were statistically significant (Tables 1 and S26, Fig. S6). Excluding PFBA, PFCAs with higher DREs were those with significant contributions from sewage sludge. Given long-chain PFAS generally partition to sewage sludge more readily (Coggan et al., 2019), this explains why higher DREs were observed for some of the longer-chained homologs.

Among the precursor/intermediate species, statistically significant NMFs of NMeFOSAA (−35 ± 6 mg/day, 96 % DRE) and NEtFOSAA (−27 ± 5 mg/day, 96 % DRE) suggest they are breaking down, primarily in the sewage sludge, during incineration (Tables 1 and S26, Fig. S6). These losses drove the observed negative NMF for the precursor/intermediate family (−46 ± 28 mg/day, 65 % DRE). Conversely, there is evidence that 6:2 FTS (14 ± 25 mg/day) was formed in the SSI, albeit its NMF was not statistically significant (Tables 1 and S26, Fig. S6). Other unmeasured precursors/intermediates, e.g., 6:2 FTAA, 6:2 FTAB, 6:2 FTSAS, may be transforming to 6:2 FTS during thermal treatment(Xiao et al., 2021).

While the SSI also appears to be a net source of the new alternatives (Table 1), and specifically HFPO-DA (198 ± 321 mg/day), these results should be observed with caution. The positive NMF for HFPO-DA, and the class of new alternatives taken together, was driven almost entirely by stack gas emissions of HFPO-DA (Table S19; mass flow = 196 ± 331 mg/day, concentration = 488 ± 827 ng/m^3). However, a potential mechanism for HFPO-DAs formation is unknown, as it is unexpected to survive thermal treatment (Alinezhad et al., 2022; EPA, 2021; Sasi et al., 2021; Xiao et al., 2020) and contributions from the potential vaporization of treated and potable water introduced at the scrubbers cannot fully account for that observed in the stack gas. The variability in the observed stack gas concentrations, potentially due in part to the application of the substantial maximum negative control correction, may have confounded these results and contributed to the lack of statistical significance for the NMFs of new alternatives as a class and HPFO-DA specifically.

The one PFAS class that showed a statistically significant negative NMF from the SSI was the PFSAs (−274 ± 34 mg/day, 81 % DRE; Tables 1 and S24). The loss of PFOS, the majority of which was introduced into the SSI in the sewage sludge, was primarily responsible and its NMF (−274 ± 30 mg/day, 91 % DRE) was also statistically significant (Tables 1 and S26, Fig. S6). Conversely, PFBS and PFHxS showed little net change, as neither were substantially observed in the sewage sludge, and the other PFSAs were modest contributors with mass flows of <0.3 mg/day.

As this is the first study, to the authors' knowledge, to assess the DRE of PFAS in an SSI, direct comparison to results reported elsewhere in the literature is not possible. Theoretical considerations suggest that temperatures of at least 1000 °C and potentially >1400 °C may be required to fully mineralize PFAS, including the CF_4 that may be formed during thermal treatment of PFAS (Tsang et al., 1998; Ryan and Gullet, 2020; Winchell et al., 2020). Previous bench-scale work (Taylor et al., 2014; Yamada et al., 2005) demonstrated 99.9 % destruction of fluorotelomer-based polymers (based on measurements of PFOA) at 1000 °C and field-scale work at facilities equipped with thermal oxidizers or secondary combustors at >1000°C

Table 1
Matrix aggregated mass flows and statistical confidence[a] at the Wastewater Treatment Plant (WWTP) and Sewage Sludge Incinerator (SSI) levels, and SSI destruction and removal efficiencies (DREs).

Compound	WWTP Level (mg/day ± 1σ) [b]			SSI Level (mg/day ± 1σ) [b]			SSI DRE (%) [d]
	Influent [c]	Effluent [c]	NMF [d]	Influent [c]	Effluent [c]	NMF [d]	
PFBA †	1284 ± 1966	5156 ± 5434	3872 ± 5778	259 ± 273	17 ± 18	-242 ± 271	93
PFPeA †	416 ± 476	572 ± 411	156 ± 629	90 ± 31	34 ± 14	-55 ± 30	62
PFHxA	1620 ± 661	1904 ± 123	284 ± 672	186 ± 21	88 ± 14	**-99 ± 12**	53
PFHpA	393 ± 65	331 ± 30	-62 ± 72	17 ± 3.4	14 ± 2.7	-2.7 ± 1.9	16
PFOA	1097 ± 54	859 ± 133	-237 ± 143	60 ± 16	38 ± 9.1	-22 ± 9.2	37
PFNA	107 ± 26	89 ± 7.6	-17 ± 27	4.5 ± 0.90	3.0 ± 0.62	-1.5 ± 0.51	32
PFDA	39 ± 16	59 ± 19	20 ± 24	11 ± 2.6	1.4 ± 0.30	**-9.7 ± 2.5**	87
PFUnA	0.45 ± 6.8	0.037 ± 0.090	-0.41 ± 6.8	6.5 ± 5.0	0.037 ± 0.090	-6.4 ± 5.0	99
PFDoA	4.9 ± 8.2	0.057 ± 0.065	-4.9 ± 8.2	8.3 ± 3.6	0.057 ± 0.065	-8.2 ± 3.5	99
PFTrDA	2.0 ± 6.0	0.047 ± 0.088	-2.0 ± 6.0	0.056 ± 3.6	0.047 ± 0.088	-0.0089 ± 3.6	16
PFTeDA	3.7 ± 6.1	0.062 ± 0.071	-3.7 ± 6.1	3.8E-5 ± 1.5E-5	0.17 ± 0.82	0.17 ± 0.82	< 0
ΣPFCA	4966 ± 1868	8970 ± 5500	4004 ± 5808	642 ± 301	196 ± 37	-446 ± 297	69
PFBS	853 ± 758	416 ± 29	-437 ± 759	21 ± 5.5	20 ± 4.8	-1.6 ± 2.3	7.4
PFPeS †	0	0.31 ± 0.15	0.31 ± 0.15	0	0.31 ± 0.15	0.31 ± 0.15	N/A
PFHxS	341 ± 114	275 ± 16	-66 ± 115	15 ± 8.0	16 ± 5.1	0.86 ± 8.9	< 0
PFHpS †	3.5 ± 21	0.0094 ± 0.040	-3.5 ± 21	0	0.0094 ± 0.040	0.0094 ± 0.040	N/A
PFOS	1086 ± 610	720 ± 64	-366 ± 614	302 ± 30	28 ± 6.4	**-274 ± 30**	91
PFNS †	0	0.0048 ± 0.0096	0.0048 ± 0.0096	0	0.0048 ± 0.0096	0.0048 ± 0.0096	N/A
PFDS †	6.6E-7 ± 1.8E-6	0.021 ± 0.12	0.021 ± 0.12	6.6E-7 ± 1.8E-6	0.021 ± 0.12	0.021 ± 0.12	< 0
PFDoS §	0	0.035 ± 0.055	0.035 ± 0.055	0	0.035 ± 0.055	0.035 ± 0.055	N/A
ΣPFSA	2283 ± 741	1411 ± 100	-872 ± 748	338 ± 34	64 ± 15	**-274 ± 34**	81
NMeFOSAA	17 ± 20	61 ± 11	44 ± 23	36 ± 6.2	1.3 ± 0.69	**-35 ± 5.8**	96
NEtFOSAA	16 ± 18	17 ± 5.2	1.7 ± 19	28 ± 4.5	1.1 ± 1.4	**-27 ± 4.7**	96
PFOSA †	3.4E-4 ± 1.2E-4	0.10 ± 0.17	0.10 ± 0.17	3.4E-4 ± 1.2E-4	0.10 ± 0.17	0.10 ± 0.17	< 0
4:2 FTS †	0	0.032 ± 0.029	0.032 ± 0.029	0	0.032 ± 0.029	0.032 ± 0.029	N/A
6:2 FTS †	387 ± 301	153 ± 79	-234 ± 311	7.0 ± 3.8	21 ± 24	14 ± 25	< 0
8:2 FTS †	11 ± 14	1.1 ± 2.1	-9.6 ± 14	0.021 ± 0.058	1.2 ± 1.3	1.2 ± 1.3	< 0
10:2 FTS §	0	0.10 ± 0.15	0.10 ± 0.15	0	0.10 ± 0.15	0.10 ± 0.15	N/A
ΣPrecursors/ intermediates	430 ± 306	232 ± 78	-198 ± 315	71 ± 8.9	25 ± 24	-46 ± 28	65
HFPO-DA ‡	528 ± 99	1503 ± 588	976 ± 596	67 ± 25	265 ± 340	198 ± 321	< 0
Adona ‡	0	0.043 ± 0.045	0.043 ± 0.045	0	0.043 ± 0.045	0.043 ± 0.045	N/A
11Cl-PF3OUdS ‡	0	0.040 ± 0.030	0.040 ± 0.030	0	0.040 ± 0.030	0.040 ± 0.030	N/A
9Cl-PF3ONS ‡	0	0.0055 ± 0.014	0.006 ± 0.014	0	0.0055 ± 0.014	0.0055 ± 0.014	N/A
ΣNew Alts.	528 ± 99	1503 ± 588	976 ± 596	67 ± 25	265 ± 340	199 ± 321	< 0
ΣPFAS	8208 ± 1735	12,117 ± 5551	3909 ± 5815	1118 ± 332	550 ± 376	-568 ± 452	51
Inorganic Fluoride	7.6E+7 ± 4.8E+6	7.4E+7 ± 1.6E+7	-2.1E+6 ± 1.7E+7	3.1E+6 ± 7.1E+5	1.9E+7 ± 4.5E+6	**1.6E+7 ± 4.2E+6**	< 0

[a]Bold red text indicates NMF point estimates statistically significantly different from 0 at the 95 % confidence level (unadjusted *p*-values <0.05). The per compound and compound class 95 % confidence intervals and p-values are provided in Tables S24, S25, and S26.
[b]σ = standard deviation.
[c]Matrix influents to and effluents from both the WWTP and SSI are identified in Fig. 1 and Table S1.
[d]NMF and SSI DRE equations are provided in Section 2.4 (Eqs. (3) and (4), respectively).
† Compound not measured in potable water.
§ Compound only measured in stack gas.
‡ Compound not measured in ambient air.

(Ryan and Gullet, 2020; Focus Environmental Inc., 2020). The single most comparable study is that of Loganathan et al. (2007), which reported PFAS concentrations in sewage sludge 2 to 10 times higher than in ash following incineration, suggesting their removal. Results of the present work were similar, with total PFAS mass flows in sewage sludge 7 times higher than the wet ash slurry and 2 times higher than the combination of wet ash slurry and stack gas. However, the SSI-level NMFs and DREs presented here consider all SSI influent (sewage sludge, treated water, potable water, and ambient air) and effluent (wet ash slurry, stack gas, venturi/tray scrubber, and mercury scrubber) matrices, rather than just the influents thermally treated in the fluidized bed incinerator (sewage sludge) and the thermal treatment effluent byproducts (wet ash slurry and stack gas). The matrices that do not undergo thermal treatment (treated water, potable water) were also considered as influents, as they contribute to the PFAS observed in the thermally treated byproduct effluents. For example, the treated water influent is expected to contribute to both the stack gas (via water vaporization at the venturi/tray scrubber), the wet ash slurry (approximately 99 % of the volume of wet ash slurry was treated water), and venturi/tray scrubber effluents. Excluding the treated water influent and venturi/tray scrubber effluent would therefore bias the NMF and DRE results low. Considering all SSI matrices provides the most holistic and unbiased NMF and DRE estimates of the entire SSI system processes. With that said, excluding PFBA, compounds that exhibited a large DRE were those with substantial contributions from the sewage sludge, which indicates, as expected, that the majority of PFAS removal through the SSI were from the sewage sludge incineration.

The DRE results provide evidence for the removal of several individual PFAS species (PFHxA, PFDA, PFOS, NMeFOSAA, and NEtFOSAA) in the

SSI. Such is based on hypothesis testing in which *p*-values were unadjusted for multiple tests being completed simultaneously. Following application of the relevant adjustments to control for false positives, these results were not statistically significant, therefore caution is suggested in their interpretation. Overall, this study found that PFAS removal through the SSI system varies between DREs <0 up to 99 % for individual PFAS compounds. The total PFAS DRE was 51 %. The only PFAS class with a statistically significant NMF was PFSA, which had a DRE of 81 %. Such suggests that an SSI may inadequately remove PFAS and that process optimization, such as updating incinerator temperature and/or residence time or replacing PFAS-laden treated water introduced to the venturi/tray scrubber with PFAS-free water, is required to achieve consistent and higher removal efficiencies.

3.6. PFAS mass discharges to the environment

The population-normalized WWTP effluent mass flows of PFAS (Table S27) allow for comparison of emission rates to those reported elsewhere. The total PFAS discharge rate (97 ± 45 μg/day/person) was within the range of that reported by Loganathan et al. (2007) at two southeastern U.S. WWTPs in the summer (37 to 872 μg/day/person), by Campo et al. (2014) at 16 WWTPs in Spain (33 to 148 μg/day/person), and by Kim et al. (2012) at 15 WWTPs in Korea (44 μg/day/person). Agreement with the latter study improves following exclusion of PFBA (42 ± 44 μg/day/person) and HFPO-DA (11 ± 2.7 μg/day/person), which were unmeasured by Kim et al. (2012). Given PFOS and PFOA have been phased out from U.S. commerce over the past two decades (Company, 2000; EPA, 2000), discharge rate comparisons between the Loganathan et al. (2007) study and the current study can provide a qualitative assessment of the environmental change of these PFAS over this time. The discharge rate of PFOS from the current study (5.8 ± 0.52 μg/day/person) is approximately 36 times lower than that from Loganathan et al. (2007) (206 μg/day/person). Similarly, the discharge rate of PFOA from the current study (6.9 ± 1.1 μg/day/person) is approximately 19 times lower than that from Loganathan et al. (2007) (132 μg/day/person). Since PFOS and PFOA do not environmentally degrade (Post et al., 2012), the observed discharge reductions could be due to the compounds accumulating in other matrices (Ghisi et al., 2019). Given PFOS has a higher tendency to accumulate than PFOA (Cui et al., 2009), the larger decrease observed for PFOS corroborates this hypothesis. Alternatively, regional/local differences in emissions of these compounds could explain the observed differences.

The majority (> 99 %; 96.2 ± 44.7 μg/day/person) of total PFAS was discharged to the aquatic environment (via treated water to the adjacent river), with ~0.4 % and ~ 0.2 % emitted to the atmosphere (through stack gas emissions) and terrestrial (via landfilling of the wet ash slurry and grit) environments, respectively. In general, discharges to treated water dominated those to air or land for the individual PFAS species with discharges >1 μg/day/person, with the exceptions being 6:2 FTS and HFPO-DA (~2 % to landfills and ~ 4 % to the air, respectively). The contribution of 6:2 FTS to the landfill (via wet ash slurry) potentially resulted from the transformation of other unmeasured precursors during thermal treatment (Xiao et al., 2021), whereas the contribution of HFPO-DA to air (via stack gas) should be observed with caution for the reasons discussed in Section 3.5. Consistent with the results of the dispersion modeling, airborne emissions of target PFAS from the SSI were modest compared to those to the aquatic environment.

3.7. Inorganic fluoride mass flow at the WWTP and SSI

The NMF of fluoride at the WWTP level was nearly zero (−2.1 ± 17 kg/day) and driven by a small difference between the raw influent and the sum of the treated water and wet ash slurry effluents. At the SSI level, the overall NMF of fluoride was 16 ± 4.2 kg/day and statistically significant at the 95 % confidence interval. The total influent mass flow was driven primarily by treated water (94 %) and sewage sludge (5.6 %), whereas the major effluent sources were wet ash slurry (86 %) and venturi/tray scrubber water (14 %). While a small effluent source, the fluoride emissions from the stack gas produced interesting results. The mass emission rate of IF from the stack gas was 0.0041 ± 0.0030 kg/day and total PFAS as fluoride was 0.00013 kg/day, whereas the mass emission rate of TF from the stack was >1000 times larger at 5.08 ± 10.2 kg/day (Table S19). The observed TF mass flow being substantially larger than the sum of IF and total PFAS as fluoride could be due to a combination of multiple factors. We offer three possible explanations: (1) the IF measurements were biased low (see Section 2.2.1 and Text S2), (2) this was an analytical artifact of the TF field measurements given they were highly variable and included only one measurement larger than the substantial maximum NC correction, and/or (3) there may have been a significant gas-phase emission of PFAS products of incomplete combustion and/or other fluorine containing chemicals. Note, TF was only measured in the stack gas matrix as access to a total fluoride method for the solid/aqueous matrices was not commercially available at the time of the study.

The large statistically significant positive NMF of fluoride from the SSI (16 ± 4.2 kg/day) was unanticipated. While the NMF of total PFAS at the SSI was not statistically significantly different from zero, the result was −0.00057 ± 0.00045 kg/day, indicating PFAS were potentially being mineralized. On a fluoride basis, this NMF was −0.00036 kg/day, meaning the IF NMF was approximately 44,000 times larger than the loss of all target PFAS as fluoride, indicating other mechanisms must be responsible for the large IF NMF. While the data produced in this study do not provide insights into the possible mechanism(s), we provide two possible explanations. The first being that previously uncharacterized PFAS or other fluorine-containing compounds (e.g., pharmaceuticals, pesticides, and herbicides) may have been present in the influent to the SSI and thermally degraded to IF. While common PFAS compounds were well characterized by the methodologies used in this study, the total universe of PFAS compounds characterized is a small percentage, lending this as a possibility. For this to be practical, however, the mass of the previously uncharacterized PFAS would need to exceed the fluence for the known PFAS compounds. Alternatively, only water soluble, extractable IF was measured in these matrices. Fluorine atoms covalently bound in other compounds and water insoluble IF salts (e.g., CaF_2) were not measured. Therefore, a second possible explanation is that IF present in the influent to the SSI but otherwise sequestered as an insoluble IF salt or other IF bound to organic matter prevented the fluoride from being analyzed in the influent by the analytical methodologies used in this study. The thermal treatment by the SSI may have liberated the fluoride, thus providing a form that is amenable to IC or ISE and therefore analyzed in the effluent. Additional effort is recommended to understand the fluoride mass balance through the SSI.

4. Conclusion

During a two-day field study at a WWTP operating an SSI, PFAS and IF concentrations and mass flows from all primary influents/effluents were characterized. PFAS concentrations were within the range of that observed at other WWTPs, with total PFAS in the treated water effluent exceeding that in the raw influent. However, while PFAS NMF was positive at the WWTP level as observed in previous studies, the robust hypothesis testing found that no statistically significant net production or breakdown of PFAS occurred. The NMF of fluoride at the WWTP level was nearly zero.

At the SSI level, DREs for individual PFAS varied between <0 up to 99 %, with five compounds (PFHxA, PFDA, PFOS, NMeFOSAA, and NEtFOSAA) and one class (PFSA) having a statistically significant negative NMF. Each of these compounds had significant influent contributions from sewage sludge, the primary matrix in which destruction is expected through the SSI. Nonetheless, the total PFAS DRE was 51 % and not statistically significant, suggesting the entire SSI system may inadequately remove PFAS and might require process optimization to achieve consistent and higher removal efficiencies. Such optimizations could include updating

incinerator temperature, incinerator residence time, and/or replacing PFAS-laden treated water introduced to the venturi/tray scrubber with PFAS-free water. IF was primarily observed in the wet ash slurry, and the statistically significant positive NMF indicate other uncharacterized PFAS or fluorine-containing compounds were potentially breaking down, or unextractable/unmeasurable organically bound IF present in the influents potentially released measurable IF in the effluent after thermal treatment. Additional effort is recommended to understand the fluoride mass balance through the SSI.

Nearly all environmental discharges of PFAS from the WWTP went to the adjacent river, with <0.5 % being landfilled or emitted to the atmosphere. Consistent with these results, dispersion modeling showed the stack gas plume's contribution to ambient air PFAS concentrations within the modeled domain were negligible on both study days.

5. Future research needs

While the present study is, to the authors' best knowledge, the most thorough assessment of PFAS at the various inflows and outflows of a WWTP/SSI, inclusive of the gas phase emissions released from the SSI, future studies can expand on the matrices sampled and compounds measured. While the bar rack effluent is likely a small source of PFAS and IF to the overall WWTP system, future assays of this matrix can nonetheless provide a more complete account of the fate and transport of these pollutants. The volatilization of PFAS can also be quantified from the aeration tanks, clarifiers, and wet ash slurry lagoons to further characterize WWTP features' (alongside the incinerator stack gas) influence on downwind ambient air concentrations. Further, future research performing high resolution mass spectral techniques can identify many additional PFAS not included in the standard targeted analysis performed here, which measured between 18 and 30 target PFAS per matrix.

The DREs reported here represent the losses of a given target PFAS or PFAS class, without respect to the potential for species to be partially broken down into unmeasured products of incomplete combustion. Future research measuring full mineralization can provide a more complete understanding of the breakdown of PFAS during incineration. Further, only water-soluble fluoride, a subset of inorganic fluoride, was measured in the solid and aqueous matrices as access to a total fluoride method at the time of the study was not commercially available. Therefore, additional research could provide a more complete understanding of the fluoride mass balance through the WWTP and SSI.

Conclusions regarding the net production or loss of some PFAS families could not be drawn given elevated background levels, concentration variability, and the limited study period. Future extended studies utilizing more sensitive analytical methods could provide more definitive conclusions. Lastly, care should be taken to avoid extrapolation of these results to different seasons, other publicly-owned treatment works, or incineration of AFFF and other PFAS-containing matrices.

CRediT authorship contribution statement

Brannon A. Seay: Conceptualization, Methodology, Software, Validation, Formal analysis, Investigation, Data curation, Writing – original draft, Visualization. **Kavitha Dasu:** Conceptualization, Methodology, Validation, Data curation, Writing – original draft, Visualization, Supervision. **Ian C. MacGregor:** Conceptualization, Methodology, Validation, Formal analysis, Investigation, Data curation, Writing – original draft, Visualization, Supervision, Project administration. **Matthew P. Austin:** Conceptualization, Methodology, Software, Validation, Formal analysis, Data curation, Writing – original draft. **Robert T. Krile:** Conceptualization, Methodology, Validation, Formal analysis, Writing – original draft. **Aaron J. Frank:** Conceptualization, Methodology, Validation, Writing – original draft. **George A. Fenton:** Methodology, Software, Formal analysis, Writing – original draft. **Derik R. Heiss:** Investigation, Writing – original draft. **Rhett J. Williamson:** Investigation, Writing – original draft. **Stephanie Buehler:** Conceptualization, Writing – original draft.

Data availability

Data will be made available on request.

Declaration of competing interest

The authors declare that they have no known competing financial interests or personal relationships that could have appeared to influence the work reported in this paper.

Acknowledgements

The authors would like to acknowledge Jon Eastep from Battelle Memorial Institute for his assistance in the field sampling. We'd like to also acknowledge the following Battelle Analytical laboratory staff who contributed to analyzing hundreds of non-potable water, potable water, solid, and ambient air samples: Jonathan Thorn, Matthew Schumitz, Denise Schumitz, Martha McCauley, Kristara Abrams, Chad Cucksey, Nate Burkitt, Alan Lewis, and Larry Mullins. We also thank Leo Chiques, a graphic designer at Battelle Memorial Institute, for his assistance in developing various figures and schematics. The authors thank Paul Meter, Wes Fritz, Lisa Kammer, and the other staff members from Weston Solutions for conducting the onsite stack gas sampling. Laboratory analysis of the stack gas samples was conducted by Eurofins and led by Courtney Atkins and William Anderson, who the authors acknowledge for their contributions. We would also like to thank Kelley Begin of Woodard and Curran for her support and contributions as well as the undisclosed wastewater treatment plant staff for allowing us access to the facility for three days and assisting during various matrix grab sampling.

The study was supported by Battelle Memorial Institute. The authors declare that they have no known competing financial interests or personal relationships that could have appeared to influence the work reported in this paper.

Appendix A. Supplementary data

Supplementary data to this article can be found online at https://doi.org/10.1016/j.scitotenv.2023.162357.

References

Ahrens, L., Shoeib, M., Harner, T., Lee, S.C., Guo, R., Reiner, E.J., 2011. Wastewater treatment plant and landfills as sources of polyfluoroalkyl compounds to the atmosphere. Environ. Sci. Technol. 45 (19), 8098–8105.

Aleksandrov, K., Gehrmann, H.-J., Hauser, M., Mätzing, H., Pigeon, D., Stapf, D., Wexler, M., 2019. Waste incineration of polytetrafluoroethylene (PTFE) to evaluate potential formation of per- and poly-fluorinated alkyl substances (PFAS) in flue gas. Chemosphere 226, 898–906.

Alinezhad, A., Challa Sasi, P., Zhang, P., Yao, B., Kubátová, A., Golovko, S.A., Golovko, M.Y., Xiao, F., 2022. An investigation of thermal air degradation and pyrolysis of per- and Polyfluoroalkyl substances and aqueous film-forming foams in soil. ACS ES&T Eng. 2 (2), 198–209.

Arvaniti, O.S., Stasinakis, A.S., 2015. Review on the occurrence, fate and removal of perfluorinated compounds during wastewater treatment. Sci. Total Environ. 524–525, 81–92.

Barber, J.L., Berger, U., Chaemfa, C., Huber, S., Jahnke, A., Temme, C., Jones, K.C., 2007. Analysis of per- and polyfluorinated alkyl substances in air samples from Northwest Europe. J. Environ. Monit. 9 (6), 530–541.

Blaine, A.C., Rich, C.D., Hundal, L.S., Lau, C., Mills, M.A., Harris, K.M., Higgins, C.P., 2013. Uptake of perfluoroalkyl acids into edible crops via land applied biosolids: field and greenhouse studies. Environ. Sci. Technol. 47 (24), 14062–14069.

Burns, D., 2019. In: Protection, S.O.M.D.O.E. (Ed.), Requirement to Analyze for PFAS Compounds.

Campo, J., Masiá, A., Picó, Y., Farré, M., Barceló, D., 2014. Distribution and fate of perfluoroalkyl substances in Mediterranean Spanish sewage treatment plants. Sci. Total Environ. 472, 912–922.

Coggan, T.L., Moodie, D., Kolobaric, A., Szabo, D., Shimeta, J., Crosbie, N.D., Lee, E., Fernandes, M., Clarke, B.O., 2019. An investigation into per- and polyfluoroalkyl substances (PFAS) in nineteen Australian wastewater treatment plants (WWTPs). Heliyon 5 (8), e02316.

Company, M., 2000. Voluntary Use and Exposure Information Profile for Perfluorooctanoic Acid and Salts. AR226-0595. U. A. R.

Cordner, A., De La Rosa, V.Y., Schaider, L.A., Rudel, R.A., Richter, L., Brown, P., 2019. Guideline levels for PFOA and PFOS in drinking water: the role of scientific uncertainty, risk assessment decisions, and social factors. J. Expo. Sci. Environ. Epidemiol. 29 (2), 157–171.
Cui, L., Zhou, Q.F., Liao, C.Y., Fu, J.J., Jiang, G.B., 2009. Studies on the toxicological effects of PFOA and PFOS on rats using histological observation and chemical analysis. Arch. Environ. Contam. Toxicol. 56 (2), 338–349.
DoD, U.S., DOE, U.S., 2009. DoD Quality Systems Manual Version 5.3.
EPA, U.S., 1986. SW-846 Test Method 0010: Modified Method 5 Sampling Train.
EPA, U.S., 1999. Compendium Method TO-13A: Determination of Polycyclic Aromatic Hydrocarbons (PAHs) in Ambient Air Using Gas Chromatography/Mass Spectrometry (GC/MS). Second edition. .
EPA, 2000. U. S., EPA and 3M Announce Phase out of PFOS.
EPA, U.S., 2007. SW-846 Test Method 9056A: Determination of Inorganic Anions by Ion Chromatography.
EPA, U.S., 2009. Method 537: Determination of Selected Perfluorinated Alkyl Acids in Drinking Water by Solid Phase Extraction and Liquid Chromatography/Tandem Mass Spectrometry (LC/MS/MS).
EPA, U.S., 2016. Clean Watersheds Needs Survey 2012 Report to Congress.
EPA, U.S., 2016. . No. 101In: Register, F. (Ed.), Lifetime Health Advisories and Health Effects Support Documents for Perfluorooctanoic Acid and Perfluorooctane Sulfonate. 81.
EPA, U.S., 2019. Per- and Polyfluoroalkyl Substances (PFAS): Incineration to Manage PFAS Waste Streams.
EPA, U.S., 2020. In: EPA, U.S. (Ed.), EPA PFAS Action Plan: Program Update.
EPA, 2021. U. S. Human Health Toxicity Values for Hexafluoropropylene Oxide (HFPO) Dimer Acid and Its Ammonium Salt (CASRN 13252-13-6 and CASRN 62037-80-3) Also Known as "GenX Chemicals".
EPA, U.S., 2022. . No. 118In: Register, F. (Ed.), Lifetime Drinking Water Health Advisories for Four Perfluoroalkyl Substances. 87, p. 2.
EPA, U. S., Method 18-Measurement of gaseous organic compound emissions by gas chromatography. In Title 40, Part 60, Appendix A-6, Regulation, C. o. F., Ed.
EPA, U. S., Method 26A-Determination of hydrogen halide and halogen emissions from stationary sources isokinetic method. In Title 40, Part 60, Appendix A-8, Regulations, C. o. F., Ed.
Eriksson, U., Haglund, P., Karrman, A., 2017. Contribution of precursor compounds to the release of per- and polyfluoroalkyl substances (PFASs) from waste water treatment plants (WWTPs). J. Environ. Sci. 61, 80–90.
Focus Environmental Inc., 2020. Thermal Oxidizer Performance Test Report: Chemours Company Fayetteville Works.
Gallen, C., Eaglesham, G., Drage, D., Nguyen, T.H., Mueller, J.F., 2018. A mass estimate of perfluoroalkyl substance (PFAS) release from Australian wastewater treatment plants. Chemosphere 208, 975–983.
Gehr, R., Leduc, R., 1992. Assessing effluent fluoride concentrations following physicochemical wastewater treatment. Can. J. Civ. Eng. 19 (4), 649–659.
Ghisi, R., Vamerali, T., Manzetti, S., 2019. Accumulation of perfluorinated alkyl substances (PFAS) in agricultural plants: a review. Environ. Res. 169, 326–341.
Hamid, H., 2016. Role of wastewater treatment plant (WWTP) in environmental cycling of poly- and perfluoroalkyl (PFAS) compounds. Ecocycles 2.
Health, U.S.D.O., Human Services Federal Panel on Community Water F, 2015. U.S. public health service recommendation for fluoride concentration in drinking water for the prevention of dental caries. Public Health Rep. 130 (4), 318–331.
Higgins, C.P., Field, J.A., Criddle, C.S., Luthy, R.G., 2005. Quantitative determination of perfluorochemicals in sediments and domestic sludge. Environ. Sci. Technol. 39 (11), 3946–3956.
Holm, S., 1979. A simple sequentially rejective multiple test procedure. Scand. J. Stat. 6 (2), 65–70.
Houtz, E.F., Sutton, R., Park, J.-S., Sedlak, M., 2016. Poly- and perfluoroalkyl substances in wastewater: significance of unknown precursors, manufacturing shifts, and likely AFFF impacts. Water Res. 95, 142–149.
Jahnke, A., Ahrens, L., Ebinghaus, R., Temme, C., 2007. Urban versus remote air concentrations of fluorotelomer alcohols and other polyfluorinated alkyl substances in Germany. Environ. Sci. Technol. 41, 745–752.
Kim Lazcano, R., de Perre, C., Mashtare, M.L., Lee, L.S., 2019. Per- and polyfluoroalkyl substances in commercially available biosolid-based products: the effect of treatment processes. Water Environ. Res. 91 (12), 1669–1677.
Kim Lazcano, R., Choi, Y.J., Mashtare, M.L., Lee, L.S., 2020. Characterizing and comparing per- and Polyfluoroalkyl substances in commercially available biosolid and organic non-biosolid-based products. Environ. Sci. Technol. 54 (14), 8640–8648.
Kim, S.K., Im, J.K., Kang, Y.M., Jung, S.Y., Kho, Y.L., Zoh, K.D., 2012. Wastewater treatment plants (WWTPs)-derived national discharge loads of perfluorinated compounds (PFCs). J. Hazard. Mater. 201–202, 82–91.
Legislature, N.H.S., 2020. Extending the commission on the seacoast cancer cluster investigation, setting the maximum contaminant levels for certain perfluorochemicals in drinking water, establishing a per and polyfluoroalkyl substances fund and programs and making an appropriation therefor, requiring insurance coverage for PFAS and PFC blood tests, and expanding the statute governing ambient groundwater quality standards. In: NHS (Ed.), NH HB1264, Legislature Chapter 30; I. Sec. 12 & 14, II. Sec 9/ 10/ 11 & 13, III. Rem.
Lenka, S.P., Kah, M., Padhye, L.P., 2021. A review of the occurrence, transformation, and removal of poly- and perfluoroalkyl substances (PFAS) in wastewater treatment plants. Water Res. 199, 117187.
Loganathan, B.G., Sajwan, K.S., Sinclair, E., Senthil Kumar, K., Kannan, K., 2007. Perfluoroalkyl sulfonates and perfluorocarboxylates in two wastewater treatment facilities in Kentucky and Georgia. Water Res. 41 (20), 4611–4620.
Mejia Avendaño, S., Liu, J., 2015. Production of PFOS from aerobic soil biotransformation of two perfluoroalkyl sulfonamide derivatives. Chemosphere 119, 1084–1090.
NEBRA, 2007. A National Biosolids Regulation, Quality, End Use & Disposal Survey.
Nguyen, H.T., Kaserzon, S.L., Thai, P.K., Vijayasarathy, S., Bräunig, J., Crosbie, N.D., Bignert, A., Mueller, J.F., 2019. Temporal trends of per- and polyfluoroalkyl substances (PFAS) in the influent of two of the largest wastewater treatment plants in Australia. Emerging Contam. 5, 211–218.
Piekarz, A.M., Primbs, T., Field, J.A., Barofsky, D.F., Simonich, S., 2007. Semivolatile fluorinated organic compounds in asian and Western U.S. Air masses. Environ. Sci. Technol. 41 (24), 8248–8255.
Post, G.B., Cohn, P.D., Cooper, K.R., 2012. Perfluorooctanoic acid (PFOA), an emerging drinking water contaminant: a critical review of recent literature. Environ. Res. 116, 93–117.
Rayne, S., Forest, K., 2009. Perfluoroalkyl sulfonic and carboxylic acids: a critical review of physicochemical properties, levels and patterns in waters and wastewaters, and treatment methods. J. Environ. Sci. Health A 44 (12), 1145–1199.
Ryan, J., Gullet, B., 2020. Analysis of Fate of PFAS During Incineration; ER19-1408. EPA, U.S., p. 1193.
Sasi, P.C., Alinezhad, A., Yao, B., Kubátová, A., Golovko, S.A., Golovko, M.Y., Xiao, F., 2021. Effect of granular activated carbon and other porous materials on thermal decomposition of per- and polyfluoroalkyl substances: mechanisms and implications for water purification. Water Res. 200, 117271.
Schulman, L.L., Strimaitis, D.G., Scire, J.S., 2000. Development and evaluation of the PRIME plume rise and building downwash model. J. Air Waste Manage. Assoc. 50 (3), 378–390.
Schultz, M.M., Higgins, C.P., Huset, C.A., Luthy, R.G., Barofsky, D.F., Field, J.A., 2006. Fluorochemical mass flows in a municipal wastewater treatment facility. Environ. Sci. Technol. 40 (23), 7350–7357.
Sepulvado, J.G., Blaine, A.C., Hundal, L.S., Higgins, C.P., 2011. Occurrence and fate of perfluorochemicals in soil following the land application of municipal biosolids. Environ. Sci. Technol. 45 (19), 8106–8112.
Shoeib, M., Harner, T., Vlahos, P., 2006. Perfluorinated chemicals in the arctic atmosphere. Environ. Sci. Technol. 40 (24), 7577–7583.
Shoeib, M., Schuster, J., Rauert, C., Su, K., Smyth, S.-A., Harner, T., 2016. Emission of poly and perfluoroalkyl substances, UV-filters and siloxanes to air from wastewater treatment plants. Environ. Pollut. 218, 595–604.
Shoemaker, J.; Tettenhorst, D., Method 537.1: Determination of Selected Per- and Polyfluorinated Alkyl Substances in Drinking Water by Solid Phase Extraction and Liquid Chromatography/Tandem Mass Spectrometry (LC/MS/MS). U.S. Environmental Protection Agency, O. o. R. a. D., National Center for Environmental Assessment, Ed.
Sinclair, E., Kannan, K., 2006. Mass loading and fate of perfluoroalkyl surfactants in wastewater treatment plants. Environ. Sci. Technol. 40 (5), 1408–1414.
Solo-Gabriele, H.M., Jones, A.S., Lindstrom, A.B., Lang, J.R., 2020. Waste type, incineration, and aeration are associated with per- and polyfluoroalkyl levels in landfill leachates. Waste Manag. 107, 191–200.
Stoiber, T., Evans, S., Naidenko, O.V., 2020. Disposal of products and materials containing per- and polyfluoroalkyl substances (PFAS): a cyclical problem. Chemosphere 260, 127659.
Sun, H., Zhang, X., Wang, L., Zhang, T., Li, F., He, N., Alder, A.C., 2012. Perfluoroalkyl compounds in municipal WWTPs in Tianjin, China—concentrations, distribution and mass flow. Environ. Sci. Pollut. Res. 19 (5), 1405–1415.
Sun, M., Arevalo, E., Strynar, M., Lindstrom, A., Richardson, M., Kearns, B., Pickett, A., Smith, C., Knappe, D.R.U., 2016. Legacy and emerging perfluoroalkyl substances are important drinking water contaminants in the cape fear river watershed of North Carolina. Environ. Sci. Technol. Lett. 3 (12), 415–419.
Tafu, M., Arioka, Y., Takamatsu, S., Toshima, T., 2016. Properties of sludge generated by the treatment of fluoride-containing wastewater with dicalcium phosphate dihydrate. Euro-Mediterr. J.Environ. Integr. 1 (1), 4.
Taylor, P.H., Yamada, T., 2003. Laboratory-scale Thermal Degradation of Perfluoro-octanyl Sulfonate and Related Precursors. 3M Company.
Taylor, P.H., Yamada, T., Striebich, R.C., Graham, J.L., Giraud, R.J., 2014. Investigation of waste incineration of fluorotelomer-based polymers as a potential source of PFOA in the environment. Chemosphere 110, 17–22.
Tsang, W., Burgess, D.R., Babushok, V., 1998. On the incinerability of highly fluorinated organic compounds. Combust. Sci. Technol. 139 (1), 385–402.
Vakili, M., Bao, Y., Gholami, F., Gholami, Z., Deng, S., Wang, W., Kumar Awasthi, A., Rafatullah, M., Cagnetta, G., Yu, G., 2021. Removal of HFPO-DA (GenX) from aqueous solutions: a mini-review. Chem. Eng. J. 424, 130266.
Venkatesan, A.K., Halden, R.U., 2013. National inventory of perfluoroalkyl substances in archived U.S. biosolids from the 2001 EPA National Sewage Sludge Survey. Journal of Hazardous Materials 252-253, 413–418.
Vierke, L., Ahrens, L., Shoeib, M., Reiner, E.J., Guo, R., Palm, W.-U., Ebinghaus, R., Harner, T., 2011. Air concentrations and particle–gas partitioning of polyfluoroalkyl compounds at a wastewater treatment plant. Environ. Chem. 8 (4), 363–371.
Wang, N., Liu, J., Buck, R.C., Korzeniowski, S.H., Wolstenholme, B.W., Folsom, P.W., Sulecki, L.M., 2011. 6:2 fluorotelomer sulfonate aerobic biotransformation in activated sludge of waste water treatment plants. Chemosphere 82 (6), 853–858.
Wang, Y., Yu, N., Zhu, X., Guo, H., Jiang, J., Wang, X., Shi, W., Wu, J., Yu, H., Wei, S., 2018. Suspect and nontarget screening of per- and Polyfluoroalkyl substances in wastewater from a fluorochemical Manufacturing Park. Environ. Sci. Technol. 52 (19), 11007–11016.
Wang, W., Rhodes, G., Ge, J., Yu, X., Li, H., 2020a. Uptake and accumulation of per- and polyfluoroalkyl substances in plants. Chemosphere 261, 127584.
Wang, B., Yao, Y., Chen, H., Chang, S., Tian, Y., Sun, H., 2020b. Per- and polyfluoroalkyl substances and the contribution of unknown precursors and short-chain (C2–C3) perfluoroalkyl carboxylic acids at solid waste disposal facilities. Sci. Total Environ. 705, 135832.
Wang, X., Yu, N., Qian, Y., Shi, W., Zhang, X., Geng, J., Yu, H., Wei, S., 2020c. Non-target and suspect screening of per- and polyfluoroalkyl substances in Chinese municipal wastewater treatment plants. Water Res. 183, 115989.

Weinberg, I., Dreyer, A., Ebinghaus, R., 2011. Waste water treatment plants as sources of polyfluorinated compounds, polybrominated diphenyl ethers and musk fragrances to ambient air. Environ. Pollut. 159 (1), 125–132.

Winchell, L.J., Ross, J.J., Wells, M.J.M., Fonoll, X., Norton Jr., J.W., Bell, K.Y., 2020. PFAS thermal destruction at wastewater treatment facilities: a state of the science review. Water Environ. Res. 93, 826–843.

Wong, F., Shoeib, M., Katsoyiannis, A., Eckhardt, S., Stohl, A., Bohlin-Nizzetto, P., Li, H., Fellin, P., Su, Y., Hung, H., 2018. Assessing temporal trends and source regions of per- and polyfluoroalkyl substances (PFASs) in air under the Arctic monitoring and assessment programme (AMAP). Atmos. Environ. 172, 65–73.

Xiao, F., Sasi, P.C., Yao, B., Kubátová, A., Golovko, S.A., Golovko, M.Y., Soli, D., 2020. Thermal stability and decomposition of perfluoroalkyl substances on spent granular activated carbon. Environ. Sci. Technol. Lett. 7 (5), 343–350.

Xiao, F., Sasi, P.C., Alinezhad, A., Golovko, S.A., Golovko, M.Y., Spoto, A., 2021. Thermal decomposition of anionic, zwitterionic, and cationic polyfluoroalkyl substances in aqueous film-forming foams. Environ. Sci. Technol. 55 (14), 9885–9894.

Yamada, T., Taylor, P.H., Buck, R.C., Kaiser, M.A., Giraud, R.J., 2005. Thermal degradation of fluorotelomer treated articles and related materials. Chemosphere 61 (7), 974–984.

Zhou, Y., Meng, J., Zhang, M., Chen, S., He, B., Zhao, H., Li, Q., Zhang, S., Wang, T., 2019. Which type of pollutants need to be controlled with priority in wastewater treatment plants: traditional or emerging pollutants? Environ. Int. 131, 104982.

Supporting information for

Per- and polyfluoroalkyl substances fate and transport at a wastewater treatment plant with a collocated sewage sludge incinerator

Brannon A. Seay[a]*, Kavitha Dasu[a], Ian C. MacGregor[b], Matthew P. Austin[a], Robert T. Krile[a], Aaron J. Frank[a], George A. Fenton[a], Derik R. Heiss[a], Rhett J. Williamson[a], Stephanie Buehler[b]

[a]Battelle Memorial Institute, 505 King Ave, Columbus, OH 43201, United States

[b]Formerly Battelle Memorial Institute, 505 King Ave, Columbus, OH 43201, United States

*Corresponding author email : seay@battelle.org

58 Pages, 6 Texts, 27 Tables, 6 Figures

Table of Contents

Text S1. Stack Gas Sampling

Pre-Test Determinations

Preliminary test data was obtained at the test location. Stack geometry was measured and recorded, and traverse point distances verified. A preliminary velocity traverse was performed utilizing a calibrated S-type pitot tube and an inclined manometer to determine velocity profiles. Flue gas temperatures were observed with a calibrated direct readout panel meter equipped with a chromel-alumel thermocouple. A preliminary measurement of the stack gas moisture content was conducted in accordance with EPA Method 4 (EPA 2023a). A check for the presence or absence of cyclonic flow was also conducted. Preliminary test data was used for nozzle sizing and sampling rate determinations for isokinetic sampling procedures. Calibration of probe nozzles, pitot tubes, metering systems, and temperature measurement devices were as specified in Section 5 of EPA Method 5 (EPA 2023b) test procedures.

Modified EPA Method 0010 (MM0010) for PFAS

A modified SW-846 EPA Method 0010 (EPA 1986) sampling train was utilized to perform the PFAS sampling. MM0010 is itself a modification of US EPA Method 5 (EPA 2023b). The Method 0010 consists of a borosilicate nozzle that was attached directly to a heated borosilicate probe. To minimize possible thermal degradation of the HFPO-DA, the probe and particulate filter were heated above the stack temperature to minimize water vapor condensation before the filter. The probe was connected directly to a heated borosilicate filter holder containing a solvent extracted glass fiber filter.

A section of borosilicate glass connected the filter holder exit to a Grahm (spiral) type ice water cooled condenser, followed by an ice water-jacketed sorbent module containing approximately 40 grams of XAD-2 resin. The XAD-2 resin tube was equipped with an inlet temperature sensor. The XAD-2 resin trap was followed by a condensate knockout impinger and a series of two impingers containing 100-ml of high purity distilled water. The train also included a second XAD-2 resin trap behind the impinger section to evaluate possible sampling train breakthrough. Each XAD-2 resin trap was connected to a 1-L condensate knockout trap. The final impinger contained 300 grams of dry pre-weighed silica gel. All impingers and condensate traps were maintained in an ice bath. Ice water was continuously circulated in the condenser and the XAD-2 module to maintain method required temperature. A control console with a leakless vacuum pump, a calibrated orifice, and dual inclined manometers were connected to the final impinger via an umbilical cord to complete the sample train.

During sampling, gas stream velocities were measured by attaching a calibrated S-type pitot tube into the gas stream adjacent to the sampling nozzle. The velocity pressure differential was observed immediately after positioning the nozzle at each traverse point, and the sampling rate adjusted to maintain isokineticity ± 10%. The flue gas temperature was monitored at each point with a calibrated meter and thermocouple. Isokinetic test data were recorded at each traverse point during all test periods, as appropriate. Leak checks were performed on the sampling apparatus according to reference method instructions prior to and following each run, during component changes (if required), and/or during midpoint port changes. The flow rate was controlled at approximately 18 L/min over each of the four ~120 min sampling events such that a total volume of ~2.2 m^3 of stack effluent was collected.

At the conclusion of each test, the MM0010 sampling train was dismantled, the openings sealed, and the components transported to the field laboratory trailer for recovery. Each container was labeled to clearly identify its contents. All samples were maintained cool. During each test, a M0010 blank train was setup near the test location, leak checked twice, and recovered along with the respective sample train.

EPA Method 26A for Hydrogen Fluoride (HF)

HF was determined following procedures outlined in EPA Method 26A (EPA 2023d). For comparison with concentrations and mass flows of free, or inorganic, fluoride in other matrices, HF was stoichiometrically converted to IF.

The sampling train nozzle and heated probe were constructed of borosilicate glass and connected to a heated filter holder containing a quartz filter, which was connected to an impinger train. The first and second impingers were each charged with 100 mL of 0.1 N H_2SO_4. The third and fourth impingers contained 100 mL of 0.1 N NaOH. The fifth impinger was charged with 200-300 grams of indicating silica gel. All impingers were maintained in a crushed ice bath. A gas measuring control console with a leakless vacuum pump, a calibrated dry gas meter, a calibrated orifice, and inclined manometers were connected to the final impinger via an umbilical cord to complete the train. The flow rate was controlled at approximately 20 L/min over each of the four ~120 min sampling events such that a total volume of ~2.4 m^3 of stack effluent was collected.

Flue gas velocity was measured with a calibrated S-type pitot tube (provided with extensions) fastened alongside the sampling nozzle. Flue gas temperature was monitored with a calibrated direct readout pyrometer equipped with a chromel-alumel (Type K) thermocouple positioned near the sampling nozzle. The impinger exit gas temperature was monitored with a calibrated direct readout pyrometer equipped with Type K thermocouples positioned in the sample gas stream after the last impinger. The sampling rate was adjusted, based on stack velocity, at each point to ensure the sample was collected within ± 10% of isokineticity. After completion of the sample run, the sample train was leak checked. Following a successful leak check, the contents of the first and second impingers were measured volumetrically and transferred to a sample container. The third and fourth impingers were measured volumetrically and transferred to a separate sample container. The impingers were then rinsed with deionized water into the appropriate sample containers.

Modified Method 18 (MM18) for total fluorine (TF)

The sampling train employed six (6) midget impingers in series and was based on a modification of EPA Method 18 (EPA 2023c). Aliquots of each impinger were combined into a single composited sample for TF analysis.

All impingers, probes, and connecting tubing were thoroughly cleaned and rinsed with a pure grade of methanol prior to use. All tubing connecting the sampling probe to the impinger train were new parts. Train components and samples were stored and handled in a clean sampling trailer. The impingers and connectors were protected from contamination by placement in separate clean coolers during storage in the trailer and shipping.

The sample collection procedure set-up generally followed standard EPA protocols. The dry gas meter was calibrated before arriving at the test site, and the sample train components were cleaned and assembled before charging the impingers with methanol. The train was leak tested at approximately 10 inches of Hg using a system isolation valve that prevented exposure of the train to possible contamination in the ambient air. Leak tests were conducted before and after the sampling interval for each run.

Before the start of each run, each of the six (6) impingers was charged with approximately 100 mL of methanol. The impinger train was set in a dry ice/methanol bath for the duration of sample collection. The methanol level in each impinger was positioned to maintain an operational level of approximately one inch below the dry ice bath external fluid level to maximize cooling efficiency of the methanol trapping solution. The temperature of the chilling bath was monitored throughout the sampling event to maintain a bath temperature of ≤ -70°C.

The probe of the sampling train was inserted into an appropriate sampling port and purged with stack gas to fill the dead volume of the train before the actual sampling was started. Non-isokinetic sample collection occurred at a single point probe location. The probe was heated to approximately 10 °C above the stack gas temperatures to prevent the condensation of moisture in the probe during the run. The stack gas was sampled at a rate of ~1.0 L/min for 120 minutes to collect a nominal sample volume of ~120 L for each run.

At the completion of each sampling event, the sampling train was disconnected from the probe assembly, remaining sealed and immersed in the dry ice bath until being transported to the sampling trailer, at which point the train fractions were broken down and placed into individual 250 mL (or larger) HDPE vials. The sample fractions included rinses of the probe and all connecting tubing.

The contents of Impinger #1 were placed into the 250 mL HDPE sample container clearly labeled with the run and fraction number. The impinger was rinsed with three (3) small aliquots of methanol. The probe and connecting tubing also received three (3) methanol rinses using a clean (or new) HDPE squirt bottle. Each rinse was added to the Impinger #1 sample container.

During a sampling run, a complete field blank train was set up to simulate the handling of the four stack gas samples. The methanol remained in an identical train for the approximate length of time required to complete a sampling run. The beginning and end leak checks were performed on the blank train, and the probe was heated to the standard operating temperature. The methanol was recovered from the blank train by the same operator and in the same location as those for the four test runs.

Samples were stored on regular wet ice (approximately 4°C) from the time they were collected from the impingers and placed into sampling bottles.

Stack Gas Quality Control

Calibration and leak checks of the appropriate sampling equipment, including meter boxes, temperature sensors, nozzles, pitot tubes, and umbilicals, were performed according to the requirements specified in EPA's Quality Assurance Handbook, Volume III (EPA 1984). The results were documented and retained.

Dry gas meters were calibrated before and after sampling. Thermocouples were calibrated against mercury thermometers, and aneroid barometers were calibrated against a mercury barometer. The temperature of the gas leaving the impinger train was kept at ≤ 20°C throughout the sampling by maintaining the ice bath. Care was taken to prevent sample loss during sample recovery. Sample storage bottles were purchased new or cleaned prior to use and were kept sealed at all times. Samples were transported to the laboratory under chain-of-custody.

Text S2. Sample Extraction and Analysis

Target PFAS Extraction

Non-Potable Water. The water samples were spiked with extraction internal standard (EIS) in the original sample container from the field. The water was extracted using a weak ion exchange solid phase extraction (SPE) cartridge and eluted from the SPE with 0.5% NH_3 in methanol. Extracts were concentrated to dryness under nitrogen and reconstituted with 80:20 methanol/water (V/V) and fortified with internal standard. Extracts were transferred for liquid chromatography tandem mass spectrometry (LC/MS/MS) analysis.

Solids. Percent moisture in solid samples was determined prior to extraction, using an aliquot from a well-homogenized solid sample. For extractions, an aliquot from a well-homogenized sample was fortified with EIS (Table S7) and serially extracted twice using 0.4% NH_3 in methanol and cleaned using ENVI-Carb™ SPE cartridges. Extracts were concentrated to dryness under nitrogen and reconstituted with 80:20 methanol/water (V/V) and fortified with internal standard for LC/MS/MS analysis.

Target PFAS Analysis

Target PFAS in both the solid and non-potable water samples were measured using liquid chromatography with tandem mass spectrometry (LC/MS/MS) operated in a negative electrospray ionization mode using multiple reaction monitoring (MRM). The high-performance liquid chromatograph (HPLC) included a 1260 SL (Agilent, USA) connected to a QTRAP 5500 triple quadrupole mass spectrometer (AB Sciex, USA). The analytical column used to perform the chromato-graphic peak separation of the analytes was a Gemini® C18 3 μm; 50 × 2 mm (Phe-nomenex, USA). The analytes were identified by comparing the acquired mass spectra and retention times to reference spectra and retention times for calibration standards acquired under identical LC/MS/MS conditions.

An initial calibration consisting of representative target analytes, EIS, and internal standards was analyzed prior to analysis to demonstrate the linear range of analysis. Calibration verification was performed at the beginning and end of 10 injections and at the end of each sequence. The concentration of each analyte is determined using the isotope dilution quantitation technique following the Department of Defense/Department of Energy Quality Systems Manual Version 5.3 (DoD/DOE QSM 5.3) Table B-15 criteria (DoD and DOE 2009). The isotopically labeled analog of an analyte (EIS) was used for quantitation if commercially available. If a labeled analog was not commercially available, internal standard quantitation was performed using the surrogate analyte with the closest retention time to the analyte. Two transitions were monitored for all analytes excluding perfluorobutanoic acid (PFBA) and perfluoropentanoic acid (PFPeA). One transition was for quantitation and the other for confirmation. The ion ratios were monitored for all analytes. EIS analytes were added to all field and quality control samples (laboratory control spikes, method blanks, and matrix spike samples and duplicates) to monitor the extraction efficiency of the method analytes.

Ambient Air Extraction and Analysis

Ambient air samples were collected both north and south of the SSI (Figure S1) on both days of the field study using four Tisch PS-1 high-volume air samplers (HVASs). Two HVASs were collocated on the roof of a building (~6 m above ground level [agl]) near the northern boundary of the WWTP approximately 275 meters (m) from the SSI stack. The other two HVASs were collocated on the roof of a building (~9 m agl) near the southern boundary of the WWTP approximately 450 m from the SSI stack. Each HVAS was loaded with a 102 mm diameter quartz fiber filter (QFF; Whatman) atop a pre-cleaned PUF/XAD/PUF "sandwich" (Sigma-Aldrich) containing XAD-2 sandwiched between 2 sections of PUF

contained in a glass cartridge. PUF/XAD/PUF were purchased pre-cleaned and QFF were muffled at 460°C for 3 hours prior to use. Each HVAS was operated at approximately 12 m^3/hour for 24 hours (~288 m^3 total), starting at approximately 08:30 local time on each of the two study days. A total of eight discrete field samples were collected along with two field blanks (one on each day of the study) and a trip blank. Field blank samples were collected by momentarily exposing blank QFFs and PUF/XAD/PUF cartridges to the atmosphere at the sampling site. Trip blanks were collected by taking additional sealed sampling media to the sampling site and shipping these sealed matrices to the laboratory with the field samples.

Neutral PFAS Extracted from PUF/XAD/PUF. Neutral PFAS collected on PUF/XAD/PUF were extracted using accelerated solvent extraction (ASE) (Dionex ASE350). ASE cells (100 mL) were filled with 10g of muffled Accusand (Fisher) sand and then a PUF/XAD/PUF cartridge was transferred to the cells and spiked with a total of 100 ng of a laboratory surrogate recovery standards (LSRS) mix consisting of d_9 N-EtFOSE, ^{13}C 6:2 FTOH, and ^{13}C 10:2 FTOH. The SRS spike quantity was split equally between the PUF and XAD and distributed evenly throughout the matrices. The LSRS was used to track extraction efficiency and method performance. Additional muffled sand was added to the ASE cell to remove headspace. PUF/XAD/PUF samples were extracted with ethyl acetate twice at 100°C and 1500psi, with a 60% flush and 120 second purge. The resulting extracts were concentrated to <1 mL using TurboVap (Biotag 415001), 50 ng of internal standard (IS) consisting of d_5 N-EtFOSA, d_7 N-MeFOSE, and ^{13}C 8:2 FTOH, was added to the sample extract, and brought up to a final volume of 1 mL with ethyl acetate. Aliquots (100 µL) of each extract were transferred to GC vials for analysis and stored at < -10°C until analysis.

Analysis of neutral PFAS extracted from PUF/XAD/PUF. Neutral PFAS extracts were analyzed using gas chromatography/mass spectrometry (GC/MS) (Agilent 6890/5973) in positive chemical ionization mode (PCI) with methane as the reagent gas at a constant flow of 1 mL/min. An HP Innowax column (15m x 0.25mm, x 0.25um film) was used for separation with a temperature program of 50°C for 1 min, 3°C/min to 70°C, 10°C/min to 130°C, 20°C/min to 225°C, and a 11.5 min hold, for a total run time of 29.92 min. A 1 mL injection volume was used. The instrument was operated in splitless mode at 220°C with a 40 mL/min purge for 0.75 min. The transfer line temperature was 225°C. Samples were analyzed in selected ion monitoring (SIM) mode by monitoring a quantitation ion for each neutral PFAS compound, as well as a confirmation ion for most. Table S2 lists the monitored ions. A 7-point linear/quadratic calibration curve was used for each set of samples analyzed. Neutral PFAS were quantitated using the IS approach, based on the IS most close in retention time to the native PFAS of interest (Table S3).

Ionic PFAS Extraction from QFFs. Ionic PFAS collected on QFFs were extracted by spiking the filters with enough EIS, consisting of a correlate mass labelled analog for each ionic PFAS being measured (Table S2), to achieve a final concentration of 5 ng/mL for each compound. QFFs were placed into 50 mL polypropylene (PP) centrifuge tubes, 15 mL of methanol was added, and they were sonicated for 10 minutes. The extract was transferred to a separate PP tube over glass wool. The extraction was repeated two more times, using 15 mL of fresh methanol for each serial extraction. All extracts were combined and concentrated to ~1 mL under nitrogen. Extracts were cleaned using Supelclean™ Envi-Carb™ cartridges (MilliporeSigma, Burlington, MA) and 3 mL of methanol rinse. All eluent (sample extract + methanol rinse) was collected together and concentrated to 0.5 mL under nitrogen. The extract was then brought up to 1 mL with Milli-Q water.

Analysis of Ionic PFAS extracted from QFFs. Ionic PFAS were analyzed by ultra-high performance liquid chromatography with tandem mass spectrometry (UHPLC-MS/MS; Waters Xevo TQMS) operated in a negative electrospray ionization mode using multiple reaction monitoring (MRM; Table S2, S4-S5). A 5-

point linear/quadratic calibration curve was used for each set of samples analyzed. Each curve had a coefficient of determination (R^2) > 0.99 for all analytes. The concentration of each analyte was determined by using the isotope dilution quantitation technique (Table S4 and S5).

IF in aqueous and solid matrices

IF Measurement using ion chromatography (IC). Both potable and non-potable water samples were prepared by filtering 5 mL of each sample through a 0.2 µm nylon membrane filter (Fisher item #13-100-109). A 2 g (wet mass) aliquot of each solid matrix (sewage sludge and grit) was homogenized and serially extracted with 5 mL of water three times using a Geno/Grinder 2010. The resulting aqueous leachates were then similarly filtered, combined, and adjusted to a final volume of 15 mL. The filtrates (aqueous matrices) or extracts (solid matrices) were analyzed for soluble inorganic fluoride (IF) by IC with conductivity detection using a Dionex DX-500 IC system consisting of an EG40 eluent generator, AS3500 autosampler with 100 µL sample loop, GP40 gradient pump, and ED40 electrochemical detector operating in conductivity mode. Table S9 includes details on the IC method.

Quantitative analysis was performed using the method of external standards. Solutions were prepared in ultra-high purity water (18.2 MΩ*cm resistivity) using a certified fluoride standard (Inorganic Ventures product # ICF1). A six-point calibration curve from 0.1 to 5 mg/L fluoride was generated by plotting peak areas against the nominal concentrations of the calibration standards and applying $1/x^2$ weighting to the linear regression. Each calibration curve had an R^2 > 0.99 and all calibration standards deviated less than 15% from nominal concentration.

IF Measurement using ion selective electrode (ISE). The ISE was an Orion Fluoride Electrode (Part # 9609BNWP, ThermoFisher) and its potential was measured with an Orion Star A214 pH/ISE Benchtop Meter (ThermoFisher). The electrode was maintained in a solution containing 10 mg/L fluoride prepared from a 1000 mg/L standard solution (TraceCert, Sigma Aldrich) prepared in a matrix of Optimum Results A Fill solution for cadmium, calcium, fluoride, and sulfide ISE (ThermoFisher) and conditioned daily using the same solution. Calibration curves were linear as established with a least-squares regression of $E_{measured}$ vs. log [F^-] across five concentrations ranging from 0.1 to 2.5 mg/L using standards prepared in high-purity water and diluted 1:1 with total ionic strength adjustment buffer (TISAB II, ThermoFisher Scientific). Observed electrode potentials were between 54 to 60 mV for calibration points differing by one order of magnitude in concentration, consistent with a theoretical value of 59.2 mV. Acceptable electrode performance was confirmed daily by analysis of known fluoride standards. Fluoride concentrations in the sewage sludge extracts were determined with the external standard method of quantification (ES-ISE).

IF Matrix Interferences. Fluoride is only poorly retained on IC and as a result may be biased because of coeluting chromatographic interferences such as acetate anions. Such interferences were assessed by the preparation and analysis of positive quality controls such as laboratory control samples and duplicates (LCS, LCSD; reagent water or sand spiked with 1 mg/L equivalent F-) and matrix spikes (a separate aliquot of a field sample, spiked to increase its fluoride concentration by 1 mg/L, then extracted and analyzed). Apart from sewage sludge, no such bias was observed: recoveries of positive controls ranged from 55% to 120%. Note that this overall recovery range was that for the matrix spike (MS) and matrix spike duplicate (MSD) results for grit, and suggests that the heterogeneity of this matrix, even after homogenization, adversely impacted precision and that some signal suppression may occur in this complex matrix. Excluding the grit, recoveries ranged from 64 to 113%. However, for the sewage sludge extracts, visual inspection of the chromatograms revealed substantial likely interferences and lack of bias

could not be confirmed since the MS/MSD recoveries were unable to be determined due to the dilution required for analysis of the prospective fluoride peak.

Thus, the sludge extracts were subsequently reanalyzed using an ISE method as an orthogonal technique for quantification, one that was anticipated to minimize the potential for positive bias in the reported fluoride concentrations. Results demonstrated that IF in the sludge extracts by IC was likely biased high by a factor of ~50 to ~100. However, the MS/MSD recoveries of IF by ISE were 34 and 49%, indicating that the ISE-derived fluoride concentrations were likely biased low. While such is consistent with a known limitation of ISE, i.e., signal suppression, especially in complex matrices, the MS/MSD results called into question the fitness-for-use of the ES-ISE-derived concentrations.

To investigate the potential for negative bias of IF in sewage sludge by ES-ISE, the fluoride in two field sample extracts and the MS/MSD was quantified by the method of standard addition (SA-ISE). A known volume (0.5 mL) of each extract was diluted 1:1 with TISAB II, the initial electrode response was determined, and responses were again measured after each of 4 sequential additions of 10 µL of a 100 mg/L fluoride standard. The volume change was negligible (~4%), thereby permitting calculation of fluoride in each of the non-fortified extracts, [C_{unk}], as the reciprocal of the observed extract-specific slope of $(V_0 + V_{std})10^{\frac{E_2-E_1}{S}}$ plotted against $C_{std}V_{std}$, corrected for TISAB II dilution (Skoog, West, and James 1996). While F- by SA-ISE was consistently greater than by ES-ISE, ranging from +3 to 20%, indicating a modest fluoride suppression, fluoride concentrations by IS-ISE for the MS/MSD were only greater than ES-ISE by no more than 2%. Such suggests that the observed negative IF bias in the sewage sludge extracts by ISE was likely due to only a modest extent to signal suppression, and that inefficient fluoride extraction from the matrix itself could instead be the principal cause.

The results of a sensitivity analysis of the IF mass flow at the level of the incinerator demonstrated that study outcomes were unchanged, i.e., IF net mass flows remained statistically significantly negative, even when sewage sludge concentrations were multiplied by a factor of three to account for the likely under recovery of soluble fluoride from the sewage sludge extracts. Based on this result, combined with the age of the sludge (~2 years) at the time of the follow-up ISE analyses, and the comparability of the ES-ISE and SA-ISE results (within 20%), re-extraction of the sludge was not performed and the IF concentrations in the sludge extracts reported in this study are those determined by ES-ISE.

Stack Gas Extraction and Analysis.

Extraction of the five Modified Method 0010 (EPA 1986) sampling trains (four test runs and one field blank) resulted in four separate analytical fractions for PFAS analysis:

- Front-Half Composite (FH) – comprised of the particulate filter, and the probe, nozzle, and front-half of the filter holder solvent rinses;
- Back-half Composite (BH) – comprised of the first XAD-2 resin material and the solvent rinses of the back-half of the filter holder, both condensers, both condensate impingers, and the connecting glassware;
- Condensate Composite (COND) – comprised of the aqueous condensates contained in impingers 1 and 2; and
- Breakthrough XAD-2 Resin Tube (BT) – comprised of the resin tube behind the series of impingers.

In addition to the field blank train generated onsite at the WWTP, laboratory quality control (QC) consisted of method blanks (MBs; negative controls), LCSs (positive controls), and in some instances,

LCDs, MSs, and MSDs. At least one MB and one LCS was prepared with each extraction batch which consisted of a group of similarly processed samples, e.g., a set of FH composites for PFAS, all M26A sampling trains for HF, or the set of composited impinger samples from the MM18 trains for TF. A blank filter and XAD-2 cartridge were also extracted and analyzed to assess PFAS background levels.

Text S3. Dispersion Modeling

Initial dispersion modeling was performed to (1) estimate the potential downwind PFAS concentration profiles, including concentration maxima, for PFAS emissions from the sewage sludge incinerator (SSI) and (2) to assess ideal ambient air sample locations (maximum SSI plume concentrations/minimum dilutions) as well as the suitability of proposed sample locations at the WWTP site. The primary challenge of positioning ambient air monitors within the WWTP was corresponding dispersion conditions (combined wind direction, wind speed, and atmospheric stability) were needed to mix the elevated stack plume (stack outlet ~36.6 m above ground level [AGL]) to the near-ground sampling locations. Prior to modeling, typical site dispersion conditions were derived from 5 years of Automatic Weather Observing Station (AWOS) data from a regional airport, located approximately 1 mile SE of the WWTP. These data were assessed to identify typical ambient dispersion conditions for daytime, nighttime and 24-hour time periods. Subsequently, the minimum dilutions and their downwind locations from the stack emission source were estimated with the SCREEN3 gaussian dispersion model, the screening version of the Industrial Source Complex – Plume Rise Model Enhancements (ISC-PRIME) model (Schulman, Strimaitis, and Scire 2000).

Following the preliminary and screening work, the average dilution of a unit emission from the SSI for each of two periods, corresponding to the 2 x 24-h sampling durations of the consecutive ambient air sampling events, was estimated with ISC-PRIME. These dilutions are the ratios of the predicted ambient air monitoring site concentration contributions from the SSI plume to the observed stack gas concentration. The dilution factor (DF) is the reciprocal of this ratio. Four 24-hour averaged dilutions were estimated, one for each of the ambient air sampling locations on each day of the study.

The SSI atmospheric plume concentration profiles (peak hourly and 24-hour averaged) were calculated using hourly site dispersion conditions derived from measurements of temperature, wind speed, and wind direction made with a MetOne model 034B (S/N x21858) weather station located on the roof (~12 m AGL) of a building 63 m south of the incinerator stack (outlet ~36.6 m AGL). Technical issues prevented the station from recording measurements during the first two hours of the first day of the study. During this time, AWOS data from the airport were utilized to extrapolate the missing on-site data. Two methods were utilized to derive time varying atmospheric stability over the sampling period. One method derives atmospheric stability as a function of wind direction variability (sigma theta) and the other as a function of sky cover (effective solar heating). The average dilution values derived from these two methods were used in the concentration estimates. Modeling applied a unit stack emission rate (1 g/s) since actual stack emissions (constituents and rates) were not known. The unit emission based plume concentration results are scalable, yielding an effective equivalent DF from the emitted stack concentration of a constituent to the estimated and/or measured downwind concentration. Since the downwind samples were acquired over a 24-hour duration, the ISC-Prime results applied for stack/sampler correlation assessment were 24-hour averaged concentrations.

Stack release plume dispersion on Day One was initially to the North progressing through to the West and finishing toward the South. Day One daytime dispersion conditions were slightly unstable with above average wind speeds, and nighttime conditions were stable with below average wind speeds. Modeled Day One minimum plume dilution (peak concentrations) occurred during the daytime approximately 440 meters NNE of the stack. During Day One sampling, the North sampler was within the dispersion plume around sunset, under neutrally stable atmosphere with above average wind speeds. These conditions yielded an average modeled 24-hour plume dilution at the North sampler of $2.8*10^{-6}$; DF = (1/dilution) = $3.6*10^{5}$, which was approximately ten times greater dilution than at the Day One minimum dilution location (location of maximum downwind plume impact).

Stack release plume dispersion on Day Two was initially toward the S-SE, under a slightly unstable atmosphere and average wind speeds during the daytime, shifting toward the NE under a stable atmosphere and near calm winds during nighttime. Day Two minimum dilution during the daytime was >

340 meters South of the stack. The South sampler was within the dispersion plume from mid-afternoon to sunset, under slightly to moderately unstable atmosphere and near average wind speeds. These conditions yielded an average modeled 24-hour plume dilution at the South sampler of $1.7*10^{-5}$; DF = $5.8*10^{4}$, which was approximately two time greater than the dilution at the Day Two minimum dilution location.

The sample event results indicate that due to the height of the incinerator stack and proximity of the North and South sampler locations, that unstable (daytime) conditions would yield the greatest sampler exposure to stack emissions over each 24-hour monitoring period. Modeling of the two-day period indicate that for a constant stack emission rate, the South sampler would be more likely to detect stack emissions on Day Two than the North sampler would on Day One (i.e., smaller plume DFs on Day 2 vs. Day 1), consistent with the southern ambient air sampling location on Day 2 being more consistently in the plume.

Text S4. Data Analysis

Individual Compound Qualifiers

A qualifier was applied to the individual compound measurements from each sampling event. Qualifiers were determined based on concentrations before negative control (NC) correction. The individual compound qualifiers were:

- No qualifier: The reported result was > LOQ. A nonqualified result was interpreted as the compound being present, with the highest confidence in the reported concentration.
- J: The reported result was ≤ LOQ and > MDL. A J-qualified result was interpreted as the compound being present, with a marginal confidence in the reported concentration.
- U: The reported result was ≤ MDL and > 0. A U-qualified result was interpreted as the compound being present, with low confidence in the reported concentration.
- ND: The analyte was not detected by the laboratory. An ND-qualified result was interpreted as the compound being absent and treated as zero in calculations.

All concentration data, regardless of qualifier, were treated as numerical and included in downstream calculations. Nonqualified, U-, and J-qualified values were treated as numerical and used as presented. ND-qualified data were zero (0) substituted and also treated as numerical. This approach prevents central tendencies from being biased high, which follows a conservative approach to protect against false positive results.

For the 30 PFAS compounds measured in the stack gas matrix, the approach for qualifying and reporting results were different from the other matrices. Note that this does not apply to IF measured in the stack gas and the following is only applicable to the PFAS compounds.

Here, qualifiers were first applied to each of the four sampling trains, or analytical fractions (FH, BH, COND, BRK), in each run. The qualifier for a given run was then selected as the "highest order" qualifier from the four individual fractions. We define the highest order qualifier as nonqualified, followed by J, U, and ND. For example, if a run's four individual fraction qualifiers were J, U, U, and ND, the given run would be J-qualified.

Following the "highest order" approach as implemented for the stack gas fractions, the "highest order" individual pollutant qualifier included in each of the summed PFAS (PFCA, PFSA, new alternatives, precursors, and total sum PFAS) was selected as the qualifier for that sum.

Central Tendency Qualifiers

The central tendency qualifiers differed from the individual compound qualifiers in three ways:

1. The qualifiers were determined from the NC corrected central tendency measurement as opposed to the non-NC corrected value.
2. The NC corrected central tendency was compared against the maximum MDL and LOQ from the population of all measurements with which the arithmetic mean was calculated.
3. NC corrected central tendencies < zero (0) were ND-qualified.

The central tendency qualifiers were defined as:

- No qualifier: The mean concentration following NC correction was greater than the maximum LOQ.

- J: The mean concentration following NC correction was greater than the maximum MDL and less than or equal to the maximum LOQ.
- U: The mean concentration following NC correction was greater than zero (0) and less than or equal to the maximum MDL.
- ND: The compound was not detected in the laboratory analysis or had a mean concentration less than zero following NC correction.

Estimating Central Tendencies

For each sampling matrix and compound, the central tendency for concentrations and mass flows was taken as the average NC corrected measurement from all unique sampling events performed during the two-day study. NCs for the solid and liquid matrices included field blanks, field reagent blanks, instrument blanks, and procedural blanks. NCs for the stack gas matrix included blank trains, media checks, and method blanks. For the ambient air matrix, NCs included lab reagent, filter matrix, trip, and field blanks.

A few distinctions to the derivations of the concentration central tendency, mass flow central tendency, and net mass flow (NMF), as described in Section 2.4, are provided here.

Wet Ash Slurry: For the biphasic wet ash slurry matrix, the solids and liquids were isolated and analyzed separately. The solid and liquid ash concentrations were then combined to determine a total wet ash slurry concentration via:

$$c_{\text{ash}} = \frac{max(0, c_{\text{solid}}) * mass_{\text{solid}} + max(0, c_{\text{liquid}}) * vol_{\text{liquid}}}{vol_{\text{liquid}}},$$

where $mass_{\text{solid}}$ is the total mass of solids isolated from the biphasic specimen and vol_{liquid} is the total volume of water after separating the solids. This equation assumes the volume of ash solids in the biphasic matrix was negligible. Based on inspection of the wet ash slurry matrix, 99% of the volume was assumed to be water.

To determine the wet ash slurry MDL, the smaller MDL of the liquid and solid matrices was selecting, following the equation:

$$MDL_{\text{ash}} = min(\frac{MDL_{solid} * mass_{solid}}{vol_{liquid}}, \frac{MDL_{liquid} * vol_{liquid}}{vol_{liquid}}),$$

The same approach was used to determine the wet ash slurry LOQ. In every case, it was found that the liquid phase provided the lower MDL and LOQ.

Stack Gas: An initial laboratory analysis of all stack gas sampling trains from all four runs was performed directly following the field study. Approximately 10 months later, replicate analyses of the BH fractions from all four runs and the COND fractions from runs 1-3 were performed. These later analyses were completed to achieve greater measurement sensitivity, however, given the elapsed time between analyses, there was an added risk of species loss and transformation. Greater sensitivity was achieved in the re-analysis, in that of the 116 NDs from the initial laboratory analysis, numerical (non-ND) results were available for 41 (35%) in the later analysis. These considerations prompted the data treatment decision to use the results from the more recent analysis for a given pollutant, unless the result was ND-qualified, in which case the original analysis result was used.

For the PFAS compounds measured in the stack gas matrix, the four analytical fractions (FH, BH, COND, BRK) within a run were summed prior to averaging the four runs. To not decrement and bias low the reported stack gas concentration by a single fraction's large NC correction, the NC correction was

applied at the individual fraction level and negative concentrations were truncated to zero (0) prior to summing the four fractions. This approach is consistent with the fact that each fraction functions independently of the other three.

Ambient Air: For PFHxS and PFOS, both a linear and branched compound were analyzed. The linear and branched results for both field samples and negative controls were summed prior to selecting a maximum NC and performing NC subtraction.

Estimating uncertainties

Concentrations were measured for chemical compounds and evaluated to determine estimates of central tendency (i.e., weighted mean). Flow rate measurements were made for sampling matrices that contained the chemical compounds. The concentration and flow rate measurements were multiplied to yield mass flow rate measurements, and central tendencies were estimated for these mass flow rates. Both the concentration, matrix flow rates, and covariance between the two were evaluated to determine uncertainty (as the standard error [SE]) of the reported central tendency values. The components of uncertainty are denoted: σ_c, the concentration uncertainty; σ_f, the sample matrix flow rate uncertainty; and σ_{cf}, the covariance between the concentrations and sample matrix flow rates.

Uncertainty was estimated for each individual compound i within each matrix m. Uncertainties were also estimated across compounds within a matrix, across matrices for a compound, among aggregates of chemical compounds, and across the entire WWTP and SSI. The methodology for this estimation is provided below.

Within-matrix uncertainties: For a given compound i in matrix m, the concentration variance σ^2_{cmi} was estimated from a general linear model fitted to the *non-NC corrected* concentration measurements. For those matrices with multiple replicates within an event (treated water, raw influent, potable water, and mercury scrubber), the sampling event was modeled as a random effect predictor and σ^2_{cmi} was the sum of the two model-based variance components (event-level and residual). For the matrices with only a single discrete sample per event (grit, sewage sludge, venturi scrubber, wet ash slurry, stack gas, and ambient air), σ^2_{cmi} was the estimated residual variance from the linear model. The concentration measurements were weighted in the model so that each event was equally weighted; thus, the resulting model intercept matches the central tendency.

The sample matrix mass flow variance σ^2_{fm} was estimated from each matrix's two daily mass flow rates with a few exceptions. In the case of the stack gas matrix, the value was based on the mass flow rates of the four runs. For the ambient air matrix, the daily flow rate was the average of the two stack gas run flow rates on that particular day. For matrices with only a single flow measurement, the variance was based on coefficients of variance (*cv*) with an estimated variance equal to percent *cv* multiplied by the mean flow rate and divided by 100. For the wet ash slurry matrix, a conservative engineering estimate of 10% *cv* was used, and for the grit matrix, the *cv* was assumed to be consistent with the raw influent stream from which it was extracted (i.e., 11.5%).

The average concentration measurements and the paired sample matrix mass flow rates for those same average concentrations were used to estimate the covariance between concentration and flow σ_{cfm}. Since the flow rates (with one exception) were estimated by day, the average concentrations used in these calculations also had to be aggregated accordingly so that the paired structure with the factor of least resolution (i.e., flow rates) was retained.

Once these variance and covariance estimates were obtained, the uncertainty of mean mass flow for any two compounds, i and j, within a single matrix, m, was estimated using the methods for propagation of uncertainties in Taylor (1997):

$$\sigma_{mij} = \sqrt{\bar{f}_m^2 \sigma_{cmi} \sigma_{cmj} + \bar{c}_{mi} \bar{c}_{mj} \sigma_{fm}^2 + \bar{f}_m^2 \bar{c}_{mi} \bar{c}_{mj} \sigma_{cfm}},$$

where in addition to the variance terms identified above, $\bar{f}_m$ is the average sample matrix mass flow rate, and $\bar{c}_{mi}, \bar{c}_{mj}$ are the estimated central tendency (i.e., weighted mean) concentrations.

For the each of the summed PFAS groups, the uncertainty was $\sqrt{\sum_i \sum_j \sigma_{mij}}$ for that particular group; any compound with a negative NC corrected concentration was excluded from the sum.

Among-matrix uncertainties: Within a matrix, measured concentrations and flow rates were generally associated by sampling event, which provided the paired correlation structure for the covariance estimates described above. For mass flow estimates of aggregated matrices, covariances were only estimated where the field sampling design provided scientific rationale for there to possibly be a measurable correlation. The correlation structure among matrices was defined such that correlation would be estimated from the data for all paired matrices with the exceptions of grit, raw influent, and potable water—which were uncorrelated with any other matrix—and ambient air, which was only correlated with the stack gas matrix.

For cross-matrix aggregate mean concentration covariance estimates, using the correlation structure above, the *NC corrected* concentrations were averaged on a per-event basis and used to compute the corresponding covariances among all matrices and compounds. These are called concentration-concentration covariances. Each matrix-compound combination had four events with the following exceptions:

- Mercury scrubber 6:2 FTS was missing the first event, so all covariances involving this exclude the first event from the other matrix-compound combinations.
- Raw influent PFOA was missing its third event (the first sampling event on the second day), so its covariances exclude the third event from the other matrix-compound combinations.
- Raw influent PFUnA and PFDoA are both missing the fourth event (the second sampling event on the second day), so its covariances exclude the final event from the other matrix-compound combinations.
- All ambient air compounds had four events (each in duplicate). However, in considering the correlation with the stack gas, the ambient air measurements on a given day could not be uniquely paired to a particular stack gas run, but only some unknown combination of the two stack gas runs on that day. Thus, the covariance is based only on the two daily measurements in these matrices—the average of stack gas Runs 1 and 2 was paired with the average of the two ambient air events on Day 1, and the average of stack gas Runs 3 and 4 were paired with the average of the two ambient air events on Day 2.

In a similar manner, the cross-matrix aggregate mean sample flow rate covariances, using the structure above, were based on the two daily flow rates for each matrix (in the case of stack gas, the Day 1 flow rate was the average flow rate for Runs 1 and 2, and the Day 2 flow rate was the average flow rate for Runs 3 and 4). These are called flow-flow covariances.

For the cross-matrix sample concentration and sample matrix flow rate covariances, the NC corrected concentrations were averaged on a daily (rather than per-event) basis and paired with the daily flow rates to compute the covariance of all matrix-compound combinations. These are called concentration-flow covariances.

Once the concentration-concentration, flow-flow, and concentration-flow covariances were computed, the full two-dimensional covariance matrix was $\mathrm{V} = \mathrm{V}_c + \mathrm{V}_f + 2\mathrm{V}_{cf}$, where V_c was the matrix of concentration-concentration covariances, V_f was the matrix of flow-flow covariances, and V_{cf} was the matrix of concentration-flow covariances.

For each of the summed groups of compounds and matrices, the total uncertainty was $\sqrt{\sum_i \sum_j v_{ij}}$, where v_{ij} is the ij^{th} element of V. Only the matrix-compound elements belonging to both group g (a set of compounds; e.g., PFCA) and system s (a set of matrices; e.g., SSI or WWTP) were included in the sum. As with the within-matrix sum, any compounds with negative NC corrected mass flows were excluded.

Hypothesis testing: Hypothesis testing was carried out for each compound group in the two systems using the mean mass flows and the corresponding uncertainties as derived above to conduct a series of individual t-tests. Since the concentration and flow rates are correlated, the appropriate degree of freedom for each test was derived using the generalized Satterthwaite approximation of Willink (2007). The tests were controlled at an overall $\alpha = 0.05$ for the WWTP and SSI systems separately. Although these two systems are actually nested, the interest is in investigating them separately; thus, they are treated as such solely for testing purposes. Both unadjusted and adjusted p-values were derived, where the latter was calculated following the Holm-Bonferroni method (Holm 1979), which adjusts for the fact that multiple tests are completed simultaneously (e.g., all PFCA or all SSI compounds together, etc.) and is a more conservative approach that protects against false positives.

Mean mass flows as determined above were assessed for statistical significance (i.e., greater than zero with 95% confidence) by comparing the lower confidence bound to zero and concluding evidence of significance if greater than zero.

Text S5. PFAS Concentrations

Individual PFAS concentration central tendencies, uncertainties, and PFAS class contributions for each of the ten sampled matrices are presented in Figure S2 and Tables S11 to S21.

The WWTP's treated water effluent (167 ± 83 ng/L) exhibited a 42% higher total PFAS concentration than the raw influent (117 ± 39 ng/L). Elevated PFAA concentrations in treated water have been previously observed (Eriksson, Haglund, and Karrman 2017; Gallen et al. 2018; Kim Lazcano et al. 2020; Loganathan et al. 2007; Schultz et al. 2006; Venkatesan and Halden 2013; Wang et al. 2018) and attributed to wastewater treatment processes (e.g., activated sludge treatment) transforming longer-chained precursors into smaller PFAS (Arvaniti and Stasinakis 2015), namely PFCAs and PFSAs (Schultz et al. 2006). Comparison between raw influent and treated water effluent concentrations shows a 48% net decrease in precursor concentrations (primarily 6:2 FTS) and an increase in three of the four short-chain PFCAs (PFBA, PFPeA, and PFHxA), corroborating previous reports (Wang et al. 2011; Zhao et al. 2013) of 6:2 FTS biotransforming into short-chain PFCAs. The remaining long-chain PFCAs and all PFSAs, however, exhibited lower concentrations in the treated water concentrations as compared to the raw influent. Notably, PFOA and PFOS concentrations decreased by 24% and 32%, respectively, which may be attributable to their sorption to the sewage sludge as previously discussed. Of the new alternatives, HFPO-DA concentrations were more than two times higher in the treated water (18.6 ± 6.9 ng/L) as compared to the raw influent (7.5 ± 2.5 ng/L), suggesting its formation during wastewater treatment, as previously observed(Sun et al. 2016).

Considering SSI matrices, the wet ash slurry contained elevated levels of 6:2 FTS (22.2 ± 42.9 ng/L) as compared to the treated water (1.95 ± 1.05 ng/L), and although within the statistical uncertainty of the measurements, suggests that 6:2 FTS may be forming from other unmeasured precursor PFAS (e.g., 6:2 FTAA, 6:2 FTAB, 6:2 FTSAS) during thermal treatment (Xiao et al. 2021). From the potable water influent to mercury scrubber effluent a substantial increase in PFHxA (1.3 ng/L to 4.6 ng/L) and HFPO-DA (0.05 ng/L to 2.2 ng/L), and a decrease in PFOA (4.5 ng/L to 2.0 ng/L) was observed. Stack gas emissions, from which HFPO-DA contributed over 93% to the total PFAS concentrations (523 ± 869 ng/m^3), may be a source of HFPO-DA deposition in the mercury scrubber water. However, the concentration of HFPO-DA measured in the stack gas was highly uncertain (488 ± 827 ng/m^3) and has been previously report as not expected to survive thermal treatment during incineration (Alinezhad et al. 2022; EPA 2021; Sasi et al. 2021; Xiao et al. 2020). These confounding results may be in part due to analyzed artifacts resulting from elevated HFPO-DA levels in field collected negative controls (Table S19).

Text S6. Stack Gas PFAS Emission Contributions to Downwind Ambient Air Concentrations

Figure S4 and Table S22 provide ionic PFAS concentration results from the incinerator stack and both ambient sampling locations for both days of the study. Table S23 provides the neutral PFAS concentration results.

Stack release plume dispersion on Day One yielded an average modeled 24-hour plume dilution of $2.8*10^{-6}$ at the North sampling site and zero at the South sampling site. The plume was therefore estimated to contribute 0.15 pg/m^3 to the total PFAS measured at the North sampling site, accounting for only 0.17% of the 83.6 pg/m^3 observed. Individual PFAS with the largest estimated stack contribution were PFDS (1.9%), PFPeA (1.5%), and PFTrDA (1.1%). However, the estimated concentration contribution for every compound was less than the uncertainty in the averaged ambient concentration and the ambient air analysis MDLs (Table S22). Further, when considering the model predicted minimum dilution ($3.2*10^{-5}$), i.e., the locations of maximum downwind plume impact within the modeled domain, all concentration contributions were still below the MDLs.

In comparing concentrations on Day One from downwind (North location) to outside of the plume (South location), the downwind total PFAS concentration was 45.3 pg/m^3 greater than outside of the plume. Only 0.3% of this concentration difference could be attributed to the stack, suggesting that on this day the local background and/or other PFAS sources were many times more influential on ambient PFAS concentrations than the incinerator stack. Other nearby WWTP features (e.g., aeration tanks, primary and secondary clarifiers, chlorine contact tanks) could have been significant sources to these concentrations. Further, in comparing the North location's Day 1 (downwind) and Day 2 (upwind) concentrations, the downwind total PFAS concentration was 13.1 pg/m^3 greater than upwind. Only 1.1% of this concentration difference could be attributed to the stack, suggesting that the inter-day concentration variability may be attributable more to background ambient PFAS concentrations from non-incinerator stack sources.

Changing meteorological conditions on Day Two resulted in 24-hour plume dilutions of zero at the North sampling site and $1.7*10^{-5}$ at the South sampling site. The plume was therefore estimated to contribute 0.27 pg/m^3 to the total PFAS measured at the South location, which accounts for only 0.83% of the 32.7 pg/m^3 observed. Individual PFAS with the largest estimated stack contributions were 6:2 FTS (16.0%), 8:2 FTS (13.5%), and NMeFOSA (7.3%). While the plume accounted for a larger fractional contribution to these individual PFAS, its absolute ambient concentration contribution was small and below the analysis method MDL for each of these compounds. Also, as with Day One, when considering the model predicted minimum dilution ($3.1*10^{-5}$), all concentration contributions were still below the MDLs.

In comparing Day Two concentrations downwind (South location) to outside of the plume (North location), the downwind total PFAS concentration was 37.9 pg/m^3 lower than outside of the plume. This clearly suggests that other background PFAS sources were many times more influential on ambient PFAS concentrations than the plume. Further, in comparing the South location's Day Two (downwind) and Day One (upwind) concentrations, the downwind total PFAS concentration was 5.7 pg/m^3 lower than upwind, again suggesting that the inter-day concentration variability attributable to background source(s) was more influential on ambient PFAS concentrations than the incinerator stack emissions.

The incinerator stack's contribution to downwind ambient air concentrations was minimal during the two sampling days. Applying the dispersion model estimated dilutions to the sampled stack emissions, the plumes only contributed an estimated 0.15-0.27 pg/m^3 of total PFAS to the ambient air at the downwind locations, with these contributions at the individual compound level being below the sampling analysis method MDLs. Both the background differences on both days (37.9-45.3 pg/m^3) and the daily

concentration differences at both sites (5.7-13.1 pg/m^3) were many times greater than could be attributed to the plume alone. These results suggest the incinerator PFAS emissions minimally influences ionic PFAS concentrations in the nearby ambient air.

Other potential sources to the observed PFAS in ambient air include the aeration tanks, primary and secondary clarifiers, and chlorine contact tanks, all located between the incinerator stack and South sampling location. While previously measured source emissions at aeration tanks and clarifiers were approximately two orders of magnitude lower than the incinerator source emissions measured here (Ahrens et al. 2011), these features could still provide a greater contribution to concentrations at the two ambient sampling locations given likely higher dilutions from these sources. Higher dilutions from these sources are probable due to their proximity, smaller relative source/receptor height difference, and potential for greater concentrations associated with stable conditions (counter to the elevated stack requiring unstable conditions to mix the plume to the near surface-based samplers). Interestingly, the total PFAS concentrations were more than two times greater at the North sampling location as compared to the South, even though the North site is further away from these features.

Table S23 presents the downwind and upwind measured neutral PFAS concentrations for both study days. The sampling location and per day concentrations observed for the neutral PFAS exhibited a similar pattern as the ionics. Net concentrations at the North site were 2.7 times greater than the South site, with only Me-FOSE and Et-FOSE concentrations greater at the South location. FTOHs made up 97% of the total neutral PFAS at the North location and 80-89% at the South location. The net Day One concentrations were 1.3 times greater than Day Two, although the daily difference is attributable mostly to the South location. The Day One levels at the North site were generally the same as Day Two for all compounds, while Day One levels at the South site were greater for all compounds as compared to Day Two. Day One total neutral PFAS were 2.7 times greater than Day Two at the South site, despite Day One having been downwind. While neutral PFAS were not measured in the stack gas, given the location of the plume on both days and the observed ambient concentrations, the stack's influence on downwind ambient air concentrations appears to have been minimal compared to other potential sources.

Supplementary Tables

Table S1. WWTP and SSI influent and effluent streams, descriptions, sampling schedule, and flow rates.

Matrix	Matrix sub-type	Discrete sampling events (#)	Description	Influent/Effluent stream	Day One flow rate [a]	Day Two flow rate [a]	Flow rate unit
Raw influent [b]	Non-potable water	4	Untreated wastewater	Influent to WWTP	$6.58*10^7$	$7.75*10^7$	L/day
Ambient air [c]	Ambient	4	Sampling locations N and S of WWTP/SSI	Influent to both the WWTP and SSI	R1: 4.68 R2: 4.50	R3: 4.45 R4: 4.53	m^3/sec (at 25°C, 1 atm)
Potable water	Potable water	12	To mercury scrubber	Influent to both the WWTP and SSI	$1.89*10^3$	$1.87*10^3$	L/day
Sewage sludge	Solid	12	Dewatered, 24-28% solids by weight	Influent to SSI	$7.80*10^7$	$8.13*10^7$	g/day (wet)
Treated water	Non-potable water	12	To venturi/tray scrubber	Influent to SSI	$3.60*10^6$	$3.59*10^6$	L/day
			Discharged to river	Effluent from WWTP	$6.58*10^7$	$7.75*10^7$	L/day
Venturi/Tray scrubber water [d]	Non-potable water	12	Returned to head of WWTP	Effluent from SSI	$3.06*10^6$	$3.05*10^6$	L/day
Mercury scrubber water [e]	Non-potable water	12	Returned to head of WWTP	Effluent from SSI	$1.89*10^3$	$1.87*10^3$	L/day
Stack gas	Stack gas	4	100°F, 100% RH, vented at stack, condensable and noncondensable	Effluent from both the WWTP and SSI	R1: 4.68 R2: 4.50	R3: 4.45 R4: 4.53	m^3/sec (at 25°C, 1 atm)
Wet ash slurry [f]	Solid/non-potable water slurry	12	Water/solid slurry, to wet ash lagoon	Effluent from both the WWTP and SSI	$5.45*10^5$		L/day
Grit	Solid	4	Sand, coffee grounds, eggshells, other organics	Effluent from WWTP	$5.10*10^5$		g/day (wet)

[a] Daily flow rate data were averaged from midnight-to-midnight local time. For matrices in which daily flow data were not available, a single longer-term average was derived (wet ash slurry and grit). For stack gas sampling, flow rates were averaged for each of the four discrete sampling events (R1 – R4).

[b] Raw influent flow rates were not directly measured at the WWTP. Rather, the influent flow rates were assumed to equal the effluent flow rates of treated water discharged to the river. We acknowledge that the raw influent flow rate should equal the sum of the treated water, wet ash, and grit effluents minus the potable water influent. However, given treated water accounts for ≳99% of the total flow through the WWTP, we estimated the raw influent flow rate as ≈ treated water.

[c] Ambient air influent was not directly measured. The influent flow rates were assumed to equal the effluent flow rate of stack gas emitted from the SSI.

[d] Venturi/Tray scrubber water effluent from the SSI was not directly measured at the WWTP. The effluent flow rates were estimated as Venturi/Tray influent flow rate less the flow rate of the wet ash slurry effluent that was water. Based on inspection of the wet ash slurry matrix, 99% of the volume of slurry was assumed to be water.

[e] Mercury scrubber water effluent from the SSI was not directly measured. The effluent flow rates were assumed to equal the influent flow rate to the mercury scrubber.

[f] Wet ash slurry effluent was not directly measured at the WWTP. The effluent flow rate was estimated based on the SSI's design specifications.

Table S2. PFAS names, abbreviations, CAS numbers, and matrices in which each were measured.

PFAS Type (Family)	Compound Abbreviation	Full Compound Name	CAS #	Fluoride Mass Fraction	Ambient Air	Stack Gas	Potable Water	Non-potable Water	Solids
Ionic (PFCA)	PFBA	Perfluoro-n-butanoic acid	375-22-4	0.62	x	x		x	x
	PFPeA	Perfluoro-n-pentanoic acid	2706-90-3	0.65	x	x		x	x
	PFHxA	Perfluoro-n-hexanoic acid	307-24-4	0.67	x	x	x	x	x
	PFHpA	Perfluoro-n-heptanoic acid	375-85-9	0.68	x	x	x	x	x
	PFOA	Perfluoro-n-octanoic acid	335-67-1	0.69	x	x	x	x	x
	PFNA	Perfluoro-n-nonanoic acid	375-95-1	0.70	x	x	x	x	x
	PFDA	Perfluoro-n-decanoic acid	335-76-2	0.70	x	x	x	x	x
	PFUnA	Perfluoro-n-undecanoic acid	2058-94-8	0.71	x	x	x	x	x
	PFDoA	Perfluoro-n-dodecanoic acid	307-55-1	0.71	x	x	x	x	x
	PFTrDA	Perfluoro-n-tridecanoic acid	72629-94-8	0.72	x	x	x	x	x
	PFTeDA	Perfluoro-n-tetradecanoic acid	376-06-7	0.72	x	x	x	x	x
Ionic (PFSA)	PFBS	Perfluorobutane-1-sulfonic acid	375-73-5	0.57	x	x	x	x	x
	PFPeS	Perfluoropentane-1-sulfonic acid	2706-91-4	0.60	x	x		x	x
	PFHxS	Perfluorohexane-1-sulfonic acid	355-46-4	0.62	x*	x	x	x	x
	PFHpS	Perfluoroheptane-1-sulfonic acid	375-92-8	0.63	x	x		x	x
	PFOS	Perfluorooctane sulfonic acid	1763-23-1	0.65	x*	x	x	x	x
	PFNS	Perfluorononane-1-sulfonic acid	68259-12-1	0.66	x	x		x	x
	PFDS	Perfluorodecane-1-sulfonic acid	335-77-3	0.66	x	x		x	x
	PFDoS	Perfluorododecanesulfonic acid	79780-39-5	0.68		x			
Ionic (Precursors/ Intermediates)	N-MeFOSAA	N-methylperfluoro-1-octanesulfonamidoacetic acid	2355-31-9	0.57	x	x	x	x	x
	N-EtFOSAA	N-ethylperfluoro-1-octanesulfonamidoacetic acid	2991-50-6	0.55	x	x	x	x	x
	4:2 FTS	1H,1H,2H,2H-perfluorohexane-1-sulfonic acid	757124-72-4	0.52	x	x		x	x
	6:2 FTS	1H,1H,2H,2H-perfluorooctane-1-sulfonic acid	27619-97-2	0.58	x	x		x	x
	8:2 FTS	1H,1H,2H,2H-perfluorodecane-1-sulfonic acid	39108-34-4	0.61	x	x		x	x
	10:2 FTS	1H,1H,2H,2H-perfluorododecane-1-sulfonic acid	120226-60-0	0.64		x			
Ionic (New Alternatives)	HFPO-DA	2,3,3,3-Tetrafluoro-2-(heptafluoropropoxy)propanoic acid	13252-13-6	0.63		x	x	x	x

PFAS Type (Family)	Compound Abbreviation	Full Compound Name	CAS #	Fluoride Mass Fraction	Ambient Air	Stack Gas	Potable Water	Non-potable Water	Solids
	ADONA	3H-perfluoro-3-[(3-methoxy-propoxy)propanoic acid]	919005-14-4	0.60		x	x	x	x
	11Cl-PF3OUdS	11-Chloroeicosafluoro-3-oxaundecane-1-sulfonic acid	763051-92-9	0.57		x	x	x	x
	9Cl-PF3ONS	9-Chlorohexadecafluoro-3-oxanonane-1-sulfonic acid	756426-58-1	0.53		x	x	x	x
Neutral (Precursors/ Intermediates)	N-MeFOSA	N-methyl perflourooctane sulfonamide	31506-32-8	0.63	x				
	N-EtFOSA	N-ethyl perfluorooctane sulfonamide	4151-50-2	0.61	x				
	N-MeFOSE	N-methyl perflourooctane sulfonamidoethanol	24448-09-7	0.58	x				
	PFOSA	Perfluorooctane sulfonamide	754-91-6	0.65	x	x		x	x
	N-EtFOSE	N-ethyl perfluorooctane sulfonamidoethanol	1691-99-2	0.57	x				
	4:2 FTOH	4:2 fluorotelomer alcohol	2043-47-2	0.65	x				
	6:2 FTOH	6:2 fluorotelomer alcohol	647-42-7	0.68	x				
	8:2 FTOH	8:2 fluorotelomer alcohol	678-39-7	0.70	x				
N/A	IF	Inorganic fluoride	N/A	1			x	x	x
	IF	Hydrogen fluoride	7664-39-3	0.95		x			
	TF	Total fluorine	N/A	1		x			

* Includes separate concentration values for branched isomers. Individual results for linear and branched isomers were summed prior to data analysis and reporting.

Table S3. Neutral PFAS measured in ambient air: Ion transitions, surrogates, and retention times.

Analyte	Retention time (min)	Ions monitored (target/qualifier 1/qualifier 2)	Applicable internal standard (IS)*
Native Analytes			
4:2 FTOH	3.96	265/227	$^{13}C_2$-d_2-8:2 FTOH
6:2 FTOH	5.79	365/327	$^{13}C_2$-d_2-8:2 FTOH
8:2 FTOH	8.67	465/427	$^{13}C_2$-d_2-8:2 FTOH
EtFOSA	14.97	528	d_5-EtFOSA
MeFOSA	15.35	514	d_5-EtFOSA
MeFOSE	16.04	540/558	d_7-MeFOSE
Et-FOSE	16.09	554/572	d_7-MeFOSE
Mass Labeled Analytes			
d_4-4:2 FTOH (SRS) (spiked pre-sampling)	3.89	269/231/230	$^{13}C_2$-d_2-8:2 FTOH
$^{13}C_2$-d_2-6:2 FTOH (SRS) (spiked pre-extraction)	5.72	369/331	$^{13}C_2$-d_2-8:2 FTOH
$^{13}C_2$-d_2-8:2 FTOH (IS)*	8.53	469/431/497	N/A
$^{13}C_2$-d_2-10:2 FTOH (SRS) (spiked pre-extraction)	10.64	569/531	$^{13}C_2$-d_2-8:2 FTOH
d_5-EtFOSA (IS)	14.94	533	N/A
d_3-MeFOSA (SRS) (spiked pre-sampling)	15.33	517	d_5-EtFOSA
d_7-MeFOSE (IS)	16.02	547/565	N/A
d_9-EtFOSE (SRS) (spiked pre-extraction)	16.07	563/581	d_7-MeFOSE

* The mass labeled PFAS identified as internal standards (IS) were used for quantification. For example, the observed response ratio of 4:2 FTOH to $^{13}C_2$-d_2-8:2 FTOH was calculated and compared against the known concentration ratio to generate the calibration models.

Table S4. Ionic PFAS measured in ambient air: Ion transitions and extracted internal standards (EIS).

Full PFAS Name	PFAS Abbreviation	Quantitative transition	Qualitative transition	EIS
Perfluoro-n-butanoic acid	PFBA	213>169	N.A.	MPFBA M3PFBA
Perfluoro-n-pentanoic acid	PFPeA	263>219	N.A.	M5PFPeA
Perfluoro-n-hexanoic acid	PFHxA	313>269	313>119	M5PFHxA MPFHxA
Perfluoro-n-heptanoic acid	PFHpA	363>319	363>169	M4PFHpA
Perfluoro-n-octanoic acid	PFOA	413>369	413>169	M2PFOA M8PFOA
Perfluoro-n-nonanoic acid	PFNA	463>419	463>219	M9PFNA
Perfluoro-n-decanoic acid	PFDA	513>469	513>219	M6PFDA MPFDA
Perfluoro-n-undecanoic acid	PFUdA	563>519	563>269	M7PFUdA
Perfluoro-n-dodecanoic acid	PFDoA	613>569	613>319	MPFDoA
Perfluoro-n-tridecanoic acid	PFTrDA	663>619	663>169	MPFTeDA
Perfluoro-n-tetradecanoic acid	PFTeDA	713>669	713>169	MPFTeDA MPFDoA
Perfluror-1-octanesulfonamide	FOSA	498>78	498>169	M8FOSA
N-methylperfluoro-1octancesulfonamidoacetic acid	N-MeFOSAA	570>419	570>512	d_3-N-MeFOSAA
N-ethylperfluroro-1-octanesulfonamidoacetic acid	N-Et-FOSAA	584>419	584>483	d_3-N-MeFOSAA
Potassium perfluoro-1-butanesulfonate	L-PFBS	299>80	299>99	M3PFBS
Sodium perfluoro-1-pentanesulfonate	L-PFPeS	349>80	349>99	M4PFHpA
Potassium perfluorohexanesulfonate	PFHxS	399>80	399>99	M3PFHxS
Sodium perfluoro-1-heptanesulfonate	L-PFHpS	449>80	449>99	M8PFOS
Potassium perfluorooctanesulfonate	PFOS	499>80	499>90	M8PFOS
Sodium perfluoro-1-nonanesulfonate	L-PFNS	549>80	549>99	d_3-N-MeFOSAA
Sodium perfluoro-1-decanesulfonate	L-PFDS	599>80	599>99	d_3-N-MeFOSAA
Sodium 1H, 1H, 2H, 2H-perfluoro-1-hexanesulfonate	4:2FTS	327>307	327>80	M2-4:2FTS
Sodium 1H, 1H, 2H, 2H-perfluoro-1-octanesulfonate	6:2FTS	427>407	427>80	M2-6:2FTS
Sodium 1H, 1H, 2H, 2H-perfluoro-1-decanesulfonate	8:2FTS	527>507	527>81	M2-8:2FTS

Table S5. Ionic PFAS measured in ambient air: Extracted internal standards (EIS) ion transitions.

Full PFAS EIS Name	PFAS EIS Abbreviation	Quantitative transition
2,3,3,3-Tetrafluoro-2(1,1,2,2,3,3,3-heptafluoropropoxy)-^{13}C3-propanoic acid	M3HFPO-DA	287>169
Perfluoro-n-[$^{13}C_4$] butanoic acid	MPFBA	217>172
Perfluoro-n-[2,3,4-^{13}C3] butanoic acid	M3PFBA	216>172
Perfluoro-n-[$^{13}C_5$] pentanoic acid	M5PFPeA	268>223
Perfluoro-n-[1,2,3,4,6-$^{13}C_5$] hexanoic acid	M5PFHxA	318>273
Perfluoro-n-[1,2-$^{13}C_2$] hexanoic acid	MPFHxA*	315>270
Perfluoro-n-[1,2,3,4-$^{13}C_5$] heptanoic acid	M4PFHpA	367>322
Perfluoro-n-[1,2-$^{13}C_8$] octanoic acid	M2PFOA	415>370
Perfluoro-n-[$^{13}C_8$] octanoic acid	M8PFOA	421>376
Perfluoro-n-[$^{13}C_9$] nonanoic acid	M9PFNA	472>427
Perfluoro-n-[1,2,3,4,5,6-$^{13}C_6$] decanoic acid	M6PFDA	519>474
Perfluoro-n-[1,2-$^{13}C_2$] decanoic acid	MPFDA*	515>470
Perfluoro-n-[1,2,3,4,5,6,7-$^{13}C_6$] undecanoic acid	M7PFUdA	570>525
Perfluoro-n-[1,2-$^{13}C_2$] dodecanoic acid	MPFDoA	615>570
Perfluoro-n-[1,2-$^{13}C_2$] tetradecanoic acid	MPFTeDA	715>670
Perfluror-1-[$^{13}C_8$] octanesulfonamide	M8FOSA	506>78
N—methyl-d_3-perfluoro-1-octancesulfonamidoacetic acid	d_3-N-MeFOSAA	573>419
N- ethyl-d_5-perfluroro-1-octanesulfonamidoacetic acid	d_5-N-Et-FOSAA	589>419
Sodium perfluoro-1-[2,3,4-$^{13}C_3$] butanesulfonate	M3PFBS	302>80
Sodium perfluoro1-[1,2,3-$^{13}C_3$] hexanesulfonate	M3PFHxS	402>80
Potassium perfluoro-1-[$^{13}C_8$] octanesulfonate	M4PFOS	503>80
Potassium perfluoro-1-[1,2,3,4-$^{13}C_8$] octanesulfonate	M8PFOS	507>80
Sodium 1H, 1H, 2H, 2H-perfluoro-1-[1,2-$^{13}C_2$] hexanesulfonate	M2-4:2FTS	329>309
Sodium 1H, 1H, 2H, 2H-perfluoro-1-[1,2-$^{13}C_2$] octanesulfonate	M2-6:2FTS	429>409
Sodium 1H, 1H, 2H, 2H-perfluoro-1-[1,2-$^{13}C_2$] decanesulfonate	M2-8:2FTS	529>509

* No confirmation ions were monitored.

Table S6. Ionic and neutral PFAS measured in ambient air: Spike recoveries.

PFAS Type (Family)	PFAS Abbreviation	Spike Recovery (%)
Ionic (PFCA)	PFBA	98.6
	PFPeA	92.9
	PFHxA	93.5
	PFHpA	95.3
	PFOA	97.0
	PFNA	97.1
	PFDA	98.8
	PFUnA	97.1
	PFDoA	96.3
	PFTrDA	98.7
	PFTeDA	95.9
Ionic (PFSA)	PFBS	95.8
	PFPeS	90.1
	PFHxS	96.3, 78.5*
	PFHpS	92.9
	PFOS	94.6, 92.4*
	PFNS	95.6
	PFDS	88.4
Ionic (Precursors)	N-MeFOSAA	97.4
	N-EtFOSAA	97.4
	PFOSA	92.0
	4:2 FTS	92.3
	6:2 FTS	124.2
	8:2 FTS	100.7
Neutral	N-MeFOSA	78.7
	N-EtFOSA	77.2
	N-MeFOSE	87.0
	N-EtFOSE	91.6
	4:2 FTOH	50.4
	6:2 FTOH	59.2
	8:2 FTOH	80.9

* Linear and branched recoveries presented separately.

Table S7. Ionic PFAS measured in aqueous and solid matrices: Target analytes, labeled analogues, and extracted internal standards.

Full Compound Name	Compound Abbreviation	CAS No.	Extracted Internal Standard
Perfluoro-n-butanoic acid	PFBA	375-22-4	$^{13}C_4$-PFBA
Perfluoro-n-pentanoic acid	PFPeA	2706-90-3	$^{13}C_5$-PFPeA
Perfluororhexanoic acid	PFHxA	307-24-4	$^{13}C_5$-PFHxA
Perfluoroheptanoic acid	PFHpA	374-85-9	$^{13}C_4$-PFHpA
Perfluorooctanoic acid	PFOA	335-67-1	$^{13}C_8$-PFOA
Perfluorononanoic acid	PFNA	375-95-1	$^{13}C_9$-PFNA
Perfluorodecanoic acid	PFDA	335-76-2	$^{13}C_6$-PFDA
Perfluoroundecanoic acid	PFUnA	2058-94-8	$^{13}C_7$-PFUnA
Perfluorododecanoic acid	PFDoA	307-55-1	$^{13}C_2$-PFDoA
Perfluorotridecanoic acid	PFTrA	72629-94-8	$^{13}C_2$-PFTeDA
Perfluorotetradecanoic acid	PFTeDA (PFTA)	376-06-7	$^{13}C_2$-PFTeDA
N-methylperfluorooctanesulfonamidoacetic acid	NMeFOSAA	2355-31-9	d3-MeFOSAA
N-ethylperfluorooctanesulfonamidoacetic acid	NEtFOSAA	2991-50-6	d5-EtFOSAA
Perfluoro-1-octanesulfonamide	PFOSA	754-91-6	$^{13}C_8$-FOSA
Perfluororbutanesulfonic acid	PFBS	375-73-5	$^{13}C_3$-PFBS
Perfluororpentanesulfonic acid	PFPeS	2706-91-4	$^{13}C_3$-PFHxS
Perfluororhexanesulfonic acid	PFHxS	3781-99-6	$^{13}C_3$-PFHxS
Perfluororheptanesulfonic acid	PFHpS	375-99-6	$^{13}C_3$-PFHxS
Perfluorooctanesulfonic acid	PFOS	1763-23-1	$^{13}C_8$-PFOS
Perfluorornonanesulfonic acid	PFNS	98789-57-2	$^{13}C_8$-PFOS
Perfluororordecaanesulfonic acid	PFDS	2806-15-7	$^{13}C_8$-PFOS
1H,1H,2H,2H-Perfluorohexane sulfonate	4:2 FTS	757124-24-4	$^{13}C_2$-4:2FTS
1H,1H,2H,2H-Perfluorooctane sulfonate	6:2 FTS	27619-97-2	$^{13}C_2$-6:2FTS
1H,1H,2H,2H-Perfluorodecane sulfonate	8:2 FTS	39108-34-4	$^{13}C_2$-8:2FTS
3-perfluoropropyl propanoic acid	3:3 FTCA	356-02-5	$^{13}C_5$-PFHxA
3-perfluoropentyl propanoic acid	5:3 FTCA	914637-49-3	$^{13}C_8$-PFOA
3-perfluoroheptyl propanoic acid	7:3 FTCA	812-70-4	$^{13}C_6$-PFDA
Hexafluoropropylene oxide dimer acid	HFPO-DA	13252-13-6	$^{13}C_3$-HFPO-DA
4,8-dioxa-3H-perfluorononanoic acid	ADONA	919005-14-4	$^{13}C_3$-HFPO-DA
11-chloroeicosafluoro-3-oxaundecane-1-sulfonic acid	11Cl-PF3OUdS	763051-92-9	$^{13}C_3$-HFPO-DA
9-chlorohexadecafluoro-3-oxanone-1-sulfonic acid	9Cl-PF3ONS	756426-58-1	$^{13}C_3$-HFPO-DA
Labeled Analogues			
Perfluoro-n-[1,2,3,4-$^{13}C^4$]butanoic acid	$^{13}C_4$-PFBA	BDO-2105	$^{13}C_3$-PFBA
Perfluoro-n-[$^{13}C^5$]pentanoic acid	$^{13}C_5$-PFPeA	BDO-2216	$^{13}C_3$-PFBA
Perfluoro-n-[1,2,3,4,6-$^{13}C_5$]hexanoic acid	$^{13}C_5$-PFHxA	BDO-2217	$^{13}C_2$-PFOA
Perfluoro-n-[1,2,3,4-$^{13}C_4$]hepetanoic acid	$^{13}C_4$-PFHpA	BDO-2218	$^{13}C_2$-PFOA
Perfluoro-n-[$^{13}C_8$]octanoic acid	$^{13}C_8$-PFOA	BDO-2219	$^{13}C_2$-PFOA
Perfluoro[$^{13}C_9$]nonanoic acid	$^{13}C_9$-PFNA	BDO-2221	$^{13}C_2$-PFOA
Perfluoro[1,2,3,4,5,6-$^{13}C_6$]decanoic acid	$^{13}C_6$-PFDA	BDO-2222	$^{13}C_2$-PFDA
Perfluoro[1,2,3,4,5,6,7-$^{13}C_7$]undecanoic acid	$^{13}C_7$-PFUnA	BDO-2223	$^{13}C_2$-PFDA
Perfluoro[1,2-$^{13}C_2$]dodecanoic acid	$^{13}C_2$-PFDoA	BDO-2112	$^{13}C_2$-PFDA
Perfluoro[1,2-$^{13}C_2$]tetradecanoic acid	$^{13}C_2$-PFTeDA	BDO-2224	$^{13}C_2$-PFDA
N-methyl-d3-perfluorooctanesulfonamidoacetic acid	d3-MeFOSAA	BDO-2125	$^{13}C_4$-PFOS
N-ethyl-d5-perfluorooctanesulfonamidoacetic acid	d5-EtFOSAA	BDO-2126	$^{13}C_4$-PFOS
Perfluoro[$^{13}C_8$]octanesulfonamide	$^{13}C_8$-FOSA	BDO-2225	$^{13}C_4$-PFOS
perfluoro[2,3,4-$^{13}C_3$] butanesulfonic acid	$^{13}C_3$-PFBS	BDO-2226	$^{13}C_4$-PFOS

Full Compound Name	Compound Abbreviation	CAS No.	Extracted Internal Standard
perfluoro[1,2,3-$^{13}C_3$]hexanesulfonic acid	$^{13}C_3$-PFHxS	BDO-2227	$^{13}C_4$-PFOS
perfluoro[13C_8]octanesulfonic acid	$^{13}C_8$-PFOS	BDO-2228	$^{13}C_4$-PFOS
1H,1H,2H,2H-perfluoro[1,2-$^{13}C_2$]hexanesulfonate	$^{13}C_2$-4:2FTS	BDO-2229	$^{13}C_4$-PFOS
1H,1H,2H,2H-perfluoro[1,2-$^{13}C_2$]octanesulfonate	$^{13}C_2$-6:2FTS	BDO-2230	$^{13}C_4$-PFOS
1H,1H,2H,2H-perfluoro[1,2-$^{13}C_2$]decanesulfonate	$^{13}C_2$-8:2FTS	BDO-2220	$^{13}C_4$-PFOS
[$^{13}C_3$]Hexafluoropropylene oxide dimer acid	$^{13}C_3$-HFPO-DA	BDO-2276	$^{13}C_2$-PFOA
Internal Standards			
Perfluoro[2,3,4-$^{13}C_3$]butanoic Acid	$^{13}C_3$-PFBA	BDO-2231	NA
Perfluoro[1,2-$^{13}C_2$]octanoic acid	$^{13}C_2$-PFOA	BDO-2107	NA
Perfluoro[1,2-$^{13}C_2$]decanoic acid	$^{13}C_2$-PFDA	BDO-2110	NA
Perfluoro[1,2,3,4-$^{13}C_4$]octanesulfonic acid	$^{13}C_4$-PFOS	BDO-2121	NA
Potential Interferences			
Taurodeoxycholic acid	TDCA	1180-95-6	NA

Table S8. Ionic PFAS measured in aqueous and solid matrices: Native and mass labeled ion transitions.

Native Analyte	Quantitative Transition	Qualitative Transition
PFBA	213>169	NA
PFPeA	263>219	NA
PFHxA	313>269	313>119
PFHpA	363>319	363>169
PFOA	413>369	413>169
PFNA	463>419	463>219
PFDA	513>469	513>219
PFUnA	563>519	563>269
PFDoA	613>569	613>319
PFTrA	663>619	663>169
PFTeDA	713>669	713>169
NMeFOSAA	570>419	570>512
NEtFOSAA	584>419	584>483
PFOSA	498>78	498>83
PFBS	299>80	299>99
PFPeS	349>99	349>80
PFHxS	399>80	399>99
PFHpS	449>80	449>99
PFOS	499>80	499>99
PFNS	549>99	549>80
PFDS	599>80	599>99
4:2 FTS	327>307	327>80
6:2 FTS	427>407	427>81
8:2 FTS	527>507	527>487
3:3 FTCA	241>177	NA
5:3 FTCA	341>237	NA
7:3 FTCA	441>337	NA
HFPO-DA	285>169	285>118
ADONA	377>251	377>85
11Cl-PF3OUdS	631>451	631>83
9Cl-PF3ONS	531>351	531>83

Mass Labeled Analyte	Quantitative Transition	Qualitative Transition
$^{13}C_4$-PFBA	217>172	NA
$^{13}C_5$-PFPeA	268>223	NA
$^{13}C_5$-PFHxA	318>273	NA
$^{13}C_4$-PFHpA	367>322	NA
$^{13}C_8$-PFOA	421>376	NA
$^{13}C_9$-PFNA	472>427	NA
$^{13}C_6$-PFDA	519>474	NA
$^{13}C_7$-PFUnA	570>525	NA
$^{13}C_2$-PFDoA	615>570	NA
$^{13}C_2$-PFTeDA	715>670	NA
d3-MeFOSAA	573>419	NA
d5-EtFOSAA	589>419	NA
$^{13}C_8$-FOSA	506>78	NA
$^{13}C_3$-PFBS	302>99	NA
$^{13}C_3$-PFHxS	402>99	NA
$^{13}C_8$-PFOS	507>99	NA
$^{13}C_2$-4:2FTS	329>81	NA
$^{13}C_2$-6:2FTS	429>81	NA
$^{13}C_2$-8:2FTS	529>81	NA
$^{13}C_3$-HFPO-DA	287>169	NA
$^{13}C_3$-PFBA	216>172	NA
$^{13}C_2$-PFOA	415>370	NA
$^{13}C_2$-PFDA	515>470	NA
$^{13}C_4$-PFOS	503>99	NA
TCDA	NA	499>107

Table S9. IC method for analysis of IF in aqueous matrices and extracts of solid matrices.

IC System	Dionex DX-500		
Mobile Phase	KOH in 18.2 MΩ*cm ultra-high purity water		
KOH gradient	**Time (min)**	**KOH Concentration (mM)**	**Hold/Ramp**
	0.000	0.50	Hold
	3.000	0.50	
	3.100	50.00	Cleanout
	5.000	50.00	
	5.010	0.50	Re-equilibrate
	19.000	0.50	
Flow Rate	2.0 mL/min		
Injection Volume	10 µL		
Guard Column	Dionex IonPac® AG11, 4 x 50 mm		
Analytical Column	Dionex IonPac® AS11, 4 x 250 mm		
Anion Trap Column	Dionex CR-ATC, 4 mm		
Detector Mode	Suppressed Conductivity		
Suppressor	Dionex AERS 500, 4 mm		
Suppression Current	50 mA		

Table S10. Ionic PFAS measured in stack gas: Native and mass labeled ion transitions.

Native Analyte	Quantitative Transition	Qualitative Transition
PFBA	212.9>169	NA
PFBS	298.9>80	298.9>99
PFPeA	262.9>219	NA
4:2 FTS	327>307	NA
PFHxA	313>269	313>119
PFHpA	363>319	363>169
PFPeS	349>80	349>99
PFHxS	399>80	399>99
6:2 FTS	427>407	NA
PFOA	413>369	413>169
PFHpS	449>80	449>99
PFNA	463>419	463>169
PFOS	499>80	499>99
PFNS	549>80	549>99
PFDoS	699>80	699 >99
PFDA	513>469	513>169
8:2 FTS	527>507	NA
10:2 FTS	627>607	NA
PFOSA	498>78	NA
N-MeFOSAA	570>419	NA
PFDS	599>80	599>99
PFUdA	563>519	563>169
N-EtFOSAA	584>419	NA
PFDoA	613>569	613>169
PFTrDA	663>619	663>169
PFTeDA	713>169	713>219
PFHxDA	813>769	813>169
PFODA	913>869	913>169
HFPO-DA	285>169	329 >169
DONA	377>251	377>85
9Cl-PF3ONS	531>351	NA
11Cl-PF3OUdS	631>451	NA
Me-FOSE	616>59	NA
Me-FOSA	512>169	NA
Et-FOSE	630>59	NA
Et-FOSA	526>169	NA

Mass Labeled analyte	Qualitative Transition	Qualitative Transition
$^{13}C_4$-PFBA	217>172	NA
$^{13}C_3$-PFBS	301.9>83 301.9>80*	NA
$^{13}C_5$-PFPeA	267.9 > 223	NA
M2-4:2FTS	329 > 81	NA
$^{13}C_2$-PFHxA	315 > 270	NA
$^{13}C_4$-PFHpA	367>322	NA
$^{18}O_2$-PFHxS	403>84	NA
M2-6:2FTS	429>81	NA
$^{13}C_4$-PFOA	417>372	NA
$^{13}C_2$-PFOA	415>370	NA
$^{13}C_5$-PFNA	468>423	NA
$^{13}C_4$-PFOS	503>80	NA
$^{13}C_2$-PFDA	515>470	NA
M2-8:2FTS	529>81	NA
$^{13}C_8$-PFOSA	506>78	NA
d3-MeFOSAA	573>419	NA
$^{13}C_2$-PFUdA	565>520	NA
d5-EtFOSAA	589>419	NA
$^{13}C_2$-PFDoA	615>570	NA
$^{13}C_2$-PFTeDA	715>670	NA
$^{13}C_2$-PFHxDA	815>770	NA
M2-4:2FTS	329>81	NA
$^{13}C_3$-HFPO-DA	287>169	NA
$^{13}C_8$-PFOA	421 >376	NA
$^{13}C_8$-PFOS	507>99	NA
$^{13}C_8$-FOSA	506>78	NA
d7-MeFOSE	623>59	NA
d3-MeFOSA	515>169	NA
d9-EtFOSE	639>59	NA
d5-EtFOSA	531>169	NA

* Initial and secondary laboratories (see Text S4) had different quantitative transitions. Both presented here.

Table S11. Raw Influent central tendency concentrations and mass flows for PFAS and IF.

Compound	Max NC (ng/L)	Max MDL (ng/L)	Max LOQ (ng/L)	Qualifier*	Concentration (ng/L)		Mass Flow (mg/day)	
					Mean	Uncertainty (± 1 std dev)	Mean	Uncertainty (± 1 std dev)
PFBA †	1.25	0.55	6.1		19.6	29.8	1.28E+03	1.97E+03
PFPeA †	0.137	0.32	6.1		6.33	7.56	416	476
PFHxA	0.205	0.65	6.1		22.3	7.12	1.62E+03	661
PFHpA	0.081	0.32	6.1	J	5.48	0.728	393	65.5
PFOA	0.59	0.62	6.1		15.9	2.5	1.10E+03	54.2
PFNA	0.12	0.38	6.1	J	1.48	0.285	107	26.4
PFDA	0.08	0.17	6.1	J	0.536	0.178	38.7	15.8
PFUnA	0.091	0.27	6.1	U	5.56E-03	0.0915	0.451	6.75
PFDoA	0.001	0.23	6.1	U	0.0752	0.12	4.95	8.17
PFTrDA	ND	0.18	6.1	U	0.0311	0.0861	2.05	6.04
PFTeDA	ND	0.89	6.1	U	0.0566	0.0911	3.72	6.12
ΣPFCA	--	--	--		71.8	35	4.97E+03	1.87E+03
PFBS	0.005	0.17	6.1		12.3	11.5	853	758
PFPeS †	0.131	0.32	6.1	ND	ND	0	ND	0
PFHxS	0.139	0.13	6.1	J	4.74	1.42	341	114
PFHpS †	0.126	1.04	6.1	U	0.0646	0.31	3.51	20.9
PFOS	0.074	0.54	6.1		14.9	7.4	1.09E+03	610
PFNS †	ND	0.44	6.1	ND	ND	0	ND	0
PFDS †	0.057	0.33	6.1	ND	ND	0	ND	0
PFDoS §	--	--	--	--	--	--	--	--
ΣPFSA	--	--	--		32	10.9	2.28E+03	741
NMeFOSAA	0.137	0.43	6.1	U	0.243	0.292	16.8	19.7
NEtFOSAA	0.151	0.61	6.1	U	0.232	0.294	15.6	18.3
PFOSA †	0.105	0.56	6.1	ND	ND	0	ND	0
4:2 FTS †	ND	0.61	6.1	ND	ND	0	ND	0
6:2 FTS †	0.561	0.65	6.1	J	5.29	3.8	387	301
8:2 FTS †	0.137	0.73	6.1	U	0.158	0.213	10.7	13.7
10:2 FTS §	--	--	--	--	--	--	--	--
ΣPrecursors	--	--	--	J	5.92	3.89	430	306
HFPO-DA ‡	ND	0.3	6.1		7.53	2.47	528	98.6
Adona ‡	ND	0.33	6.1	ND	ND	0	ND	0
11Cl-PF3OUdS ‡	ND	0.28	6.1	ND	ND	0	ND	0
9Cl-PF3ONS ‡	ND	0.33	6.1	ND	ND	0	ND	0
ΣNew Alternatives	--	--	--		7.53	2.47	528	98.6
ΣPFAS	--	--	--		117	39.1	8.21E+03	1.73E+03
Inorganic Fluoride	5.09E+04	6.28E+04	1.00E+05		1.06E+06	6.71E+04	7.59E+07	4.81E+06

† Compound not measured in potable water.
§ Compound only measured in stack gas.
‡ Compound not measured in ambient air.
* ND: The compound was not detected or had a mean concentration less than zero following NC correction.
U: The mean concentration following NC correction is > zero (0) and ≤ the maximum MDL.
J: The mean concentration following NC correction is > the maximum MDL and ≤ the maximum LOQ.
Summed PFAS are qualified following the "highest order" individual pollutant qualifier (Text S4).

Table S12. Treated Water central tendency concentrations and mass flows for PFAS and IF.

Compound	Max NC (ng/L)	Max MDL (ng/L)	Max LOQ (ng/L)	Qualifier*	Concentration (ng/L)		SSI Influent. Mass Flow (mg/day)		WWTP Effluent Mass Flow (mg/day)	
					Mean	Uncert. (± 1 std dev)	Mean	Uncert. (± 1 std dev)	Mean	Uncert. (± 1 std dev)
PFBA †	0.582	0.51	5.68		72	75.9	259	273	5.14E+03	5.43E+03
PFPeA †	0.21	0.3	5.68		8.15	6.4	29.3	23.1	565	411
PFHxA	0.188	0.6	5.68		26.5	3.64	95.4	13.3	1.89E+03	125
PFHpA	0.072	0.3	5.68	J	4.63	0.917	16.7	3.34	328	29.4
PFOA	1.74	0.58	5.68		12.1	3.64	43.6	13.2	852	132
PFNA	0.115	0.35	5.68	J	1.25	0.247	4.5	0.901	88.7	7.63
PFDA	0.158	0.16	5.68	J	0.815	0.248	2.93	0.893	58.2	18.5
PFUnA	0.107	0.25	5.68	ND	ND	0.064	ND	0.23	ND	4.86
PFDoA	0.063	0.22	5.68	ND	ND	0.0218	ND	0.0783	ND	1.57
PFTrDA	0.084	0.17	5.68	ND	ND	7.88E-03	ND	0.0283	ND	0.569
PFTeDA	0.081	0.83	5.68	ND	ND	0.0944	ND	0.339	ND	6.81
ΣPFCA	--	--	--		125	78.8	451	284	8.92E+03	5.50E+03
PFBS	0.155	0.16	5.68		5.87	1.52	21.1	5.53	413	27.8
PFPeS †	0.091	0.3	5.68	ND	ND	0	ND	0	ND	0
PFHxS	0.136	0.13	5.68	J	3.88	1.01	13.9	3.69	272	14
PFHpS †	0.075	0.97	5.68	ND	ND	0.0768	ND	0.276	ND	5.57
PFOS	0.096	0.5	5.68		10.1	2.4	36.4	8.75	714	63.1
PFNS †	0.107	0.41	5.68	ND	ND	0	ND	0	ND	0
PFDS †	0.056	0.31	5.68	ND	ND	9.54E-03	ND	0.0343	ND	0.688
PFDoS §	--	--	--	--	--	--	--	--	--	--
ΣPFSA	--	--	--		19.9	4.89	71.5	17.8	1.40E+03	95.8
NMeFOSAA	0.187	0.4	5.68	J	0.862	0.305	3.1	1.11	60.4	11.5
NEtFOSAA	0.161	0.57	5.68	U	0.232	0.0765	0.833	0.277	16.5	5.32
PFOSA †	0.121	0.52	5.68	ND	ND	0.222	ND	0.798	ND	16
4:2 FTS †	0.132	0.57	5.68	ND	ND	0.0256	ND	0.0921	ND	1.82
6:2 FTS †	0.149	0.6	5.68	J	1.95	1.05	7.03	3.77	140	77.2
8:2 FTS †	ND	0.68	5.68	U	5.83E-03	0.0162	0.0209	0.0581	0.452	1.18
10:2 FTS §	--	--	--	--	--	--	--	--	--	--
ΣPrecursors	--	--	--	J	3.05	1.14	11	4.1	217	77.6
HFPO-DA ‡	0.1	0.28	5.68		18.6	6.93	67	25.2	1290	255
Adona ‡	0.06	0.31	5.68	ND	ND	0	ND	0	ND	0
11Cl-PF3OUdS ‡	0.071	0.26	5.68	ND	ND	0	ND	0	ND	0
9Cl-PF3ONS ‡	0.055	0.31	5.68	ND	ND	0	ND	0	ND	0
ΣNew Alternatives	--	--	--		18.6	6.93	67	25.2	1.29E+03	255
ΣPFAS	--	--	--		167	82.5	601	298	1.18E+04	5.49E+03
Inorganic Fluoride	5.08E+04	6.28E+04	1.00E+05		8.15E+05	1.93E+05	2.93E+06	6.93E+05	5.74E+07	1.38E+07

† Compound not measured in potable water.
§ Compound only measured in stack gas.
‡ Compound not measured in ambient air.
* ND: The compound was not detected or had a mean concentration less than zero following NC correction.
U: The mean concentration following NC correction is > zero (0) and ≤ the maximum MDL.
J: The mean concentration following NC correction is > the maximum MDL and ≤ the maximum LOQ.
Summed PFAS are qualified following the "highest order" individual pollutant qualifier (Text S4).

Table S13. Venturi/Tray Scrubber central tendency concentrations and mass flows for PFAS and IF.

Compound	Max NC (ng/L)	Max MDL (ng/L)	Max LOQ (ng/L)	Qualifier*	Concentration (ng/L)		Mass Flow (mg/day)	
					Mean	Uncertainty (± 1 std dev)	Mean	Uncertainty (± 1 std dev)
PFBA †	1.03	0.54	5.95	ND	ND	0	ND	0
PFPeA †	0.21	0.31	5.95		8.97	4.54	27.4	13.9
PFHxA	0.188	0.63	5.95		23.8	3.77	72.8	11.8
PFHpA	0.072	0.31	5.95	J	3.75	0.84	11.5	2.62
PFOA	0.11	0.61	5.95		10.1	2.35	30.9	7.31
PFNA	0.115	0.37	5.95	J	0.784	0.165	2.4	0.515
PFDA	0.158	0.17	5.95	J	0.334	0.0631	1.02	0.195
PFUnA	0.107	0.26	5.95	ND	ND	0.0638	ND	0.195
PFDoA	0.063	0.23	5.95	ND	ND	0.0342	ND	0.105
PFTrDA	0.084	0.18	5.95	ND	ND	0.0551	ND	0.169
PFTeDA	0.081	0.87	5.95	U	0.0353	0.272	0.109	0.831
ΣPFCA	--	--	--		47.8	8.41	146	26.2
PFBS	0.133	0.17	5.95	J	5.4	1.42	16.5	4.4
PFPeS †	0.091	0.31	5.95	ND	ND	0.201	ND	0.614
PFHxS	0.136	0.13	5.95	J	4.36	1.43	13.3	4.42
PFHpS †	0.075	1.01	5.95	ND	ND	0.0621	ND	0.19
PFOS	0.096	0.52	5.95		7.36	1.7	22.5	5.27
PFNS †	0.107	0.43	5.95	ND	ND	2.31E-03	ND	7.06E-03
PFDS †	0.056	0.32	5.95	ND	ND	0	ND	0
PFDoS §	--	--	--	--	--	--	--	--
ΣPFSA	--	--	--		17.1	4.17	52.4	13
NMeFOSAA	0.187	0.42	5.95	U	0.328	0.263	1.01	0.812
NEtFOSAA	0.161	0.6	5.95	U	0.109	0.0707	0.335	0.218
PFOSA †	0.121	0.55	5.95	ND	ND	0.191	ND	0.585
4:2 FTS †	0.132	0.6	5.95	ND	ND	0.0364	ND	0.111
6:2 FTS †	0.114	0.63	5.95	J	2.69	0.74	8.23	2.29
8:2 FTS †	ND	0.71	5.95	U	0.18	0.0978	0.549	0.297
10:2 FTS §	--	--	--	--	--	--	--	--
ΣPrecursors	--	--	--	J	3.31	0.929	10.1	2.89
HFPO-DA ‡	0.1	0.3	5.95		18.7	4.89	57.1	15.2
Adona ‡	0.06	0.32	5.95	ND	ND	8.08E-03	ND	0.0247
11Cl-PF3OUdS ‡	0.071	0.27	5.95	ND	ND	0	ND	0
9Cl-PF3ONS ‡	0.055	0.32	5.95	ND	ND	0	ND	0
ΣNew Alternatives	--	--	--		18.7	4.89	57.1	15.2
ΣPFAS	--	--	--		86.9	17.9	266	55.7
Inorganic Fluoride	5.08E+04	6.28E+04	1.00E+05		8.68E+05	1.97E+05	2.65E+06	6.03E+05

† Compound not measured in potable water.
§ Compound only measured in stack gas.
‡ Compound not measured in ambient air.
* ND: The compound was not detected or had a mean concentration less than zero following NC correction.
U: The mean concentration following NC correction is > zero (0) and ≤ the maximum MDL.
J: The mean concentration following NC correction is > the maximum MDL and ≤ the maximum LOQ.
Summed PFAS are qualified following the "highest order" individual pollutant qualifier (Text S4).

Table S14. Wet Ash Slurry central tendency concentrations and mass flows for PFAS and IF.

Compound	Max NC (ng/L)	Max MDL (ng/L)	Max LOQ (ng/L)	Qualifier*	Concentration (ng/L)		Mass Flow (mg/day)	
					Mean	Uncertainty (± 1 std dev)	Mean	Uncertainty (± 1 std dev)
PFBA †	0.209	0.54	5.95		15.1	2.77	8.25	1.8
PFPeA †	0.142	0.31	5.95		11.4	1.14	6.23	0.885
PFHxA	0.144	0.63	5.95		26.8	4.38	14.6	2.81
PFHpA	0.195	0.31	5.95	J	3.87	0.894	2.11	0.535
PFOA	0.155	0.61	5.95		12.5	3.04	6.82	1.8
PFNA	0.202	0.37	5.95	J	1.03	0.185	0.561	0.121
PFDA	0.157	0.17	5.95	J	0.407	0.233	0.222	0.131
PFUnA	0.162	0.26	5.95	U	0.0119	0.171	6.47E-03	0.0934
PFDoA	0.149	0.23	5.95	ND	ND	0.0153	ND	8.34E-03
PFTrDA	0.191	0.18	5.95	U	0.0137	0.102	7.45E-03	0.0559
PFTeDA	0.232	0.87	5.95	U	0.0203	0.087	0.0111	0.0474
ΣPFCA	--	--	--		71.2	10.7	38.8	5.85
PFBS	0.17	0.17	5.95	J	5.45	0.934	2.97	0.596
PFPeS †	0.082	0.31	5.95	J	0.522	0.293	0.284	0.163
PFHxS	0.154	0.13	5.95	J	3.97	1.1	2.17	0.64
PFHpS †	0.14	1.01	5.95	U	2.83E-03	0.0655	1.54E-03	0.0359
PFOS	0.123	0.52	5.95		9.92	2.54	5.41	1.49
PFNS †	0.019	0.43	5.95	ND	ND	0	ND	0
PFDS †	0.071	0.32	5.95	U	0.0226	0.221	0.0123	0.121
PFDoS §	--	--	--	--	--	--	--	--
ΣPFSA	--	--	--		19.9	4.82	10.8	2.63
NMeFOSAA	0.259	0.42	5.95	U	0.254	0.111	0.139	0.067
NEtFOSAA	0.268	0.6	5.95	U	0.0106	0.139	5.77E-03	0.076
PFOSA †	0.219	0.55	5.95	U	0.0378	0.194	0.0206	0.106
4:2 FTS †	0.069	0.6	5.95	ND	ND	0	ND	0
6:2 FTS †	0.082	0.63	5.95		22.2	42.9	12.1	23.4
8:2 FTS †	ND	0.71	5.95	U	0.322	0.494	0.176	0.27
10:2 FTS §	--	--	--	--	--	--	--	--
ΣPrecursors	--	--	--		22.8	43	12.4	23.5
HFPO-DA ‡	0.13	0.3	5.95		22.5	6.6	12.3	3.8
Adona ‡	0.091	0.32	5.95	ND	ND	0	ND	0
11Cl-PF3OUdS ‡	0.044	0.27	5.95	ND	ND	0	ND	0
9Cl-PF3ONS ‡	0.038	0.32	5.95	ND	ND	0.103	ND	0.0561
ΣNew Alternatives	--	--	--		22.5	6.6	12.3	3.6
ΣPFAS	--	--	--		136	44.7	74.3	24.4
Inorganic Fluoride	5.08E+04	6.28E+04	1.00E+05		3.02E+07	7.82E+06	1.64E+07	4.26E+06

† Compound not measured in potable water.
§ Compound only measured in stack gas.
‡ Compound not measured in ambient air.
* ND: The compound was not detected or had a mean concentration less than zero following NC correction.
U: The mean concentration following NC correction is > zero (0) and ≤ the maximum MDL.
J: The mean concentration following NC correction is > the maximum MDL and ≤ the maximum LOQ.
Summed PFAS are qualified following the "highest order" individual pollutant qualifier (Text S4).

Table S15. Potable Water central tendency concentrations and mass flows for PFAS and IF.

Compound	Max NC (ng/L)	Max MDL (ng/L)	Max LOQ (ng/L)	Qualifier*	Concentration (ng/L)		Mass Flow (mg/day)	
					Mean	Uncertainty (± 1 std dev)	Mean	Uncertainty (± 1 std dev)
PFBA †	--	--	--	--	--	--	--	--
PFPeA †	--	--	--	--	--	--	--	--
PFHxA	0.285	0.25	2.67	J	1.35	0.107	2.53E-03	2.26E-04
PFHpA	0.099	0.25	2.67	J	1.28	0.114	2.41E-03	2.34E-04
PFOA	0.219	0.21	2.67		4.51	0.305	8.48E-03	6.43E-04
PFNA	0.082	0.13	2.67	J	0.348	0.0385	6.56E-04	7.96E-05
PFDA	0.093	0.12	2.67	U	0.0309	0.0169	5.80E-05	3.09E-05
PFUnA	0.083	0.11	2.67	ND	ND	0.0136	ND	2.54E-05
PFDoA	0.087	0.15	2.67	ND	ND	0	ND	0
PFTrDA	0.08	0.11	2.67	ND	ND	0.0111	ND	2.08E-05
PFTeDA	0.086	0.24	2.67	ND	ND	0	ND	0
ΣPFCA	--	--	--		7.51	0.499	0.0141	1.08E-03
PFBS	0.06	0.13	2.67	J	0.751	0.068	1.41E-03	1.41E-04
PFPeS †	--	--	--	--	--	--	--	--
PFHxS	0.059	0.13	2.67	J	0.569	0.0566	1.07E-03	1.16E-04
PFHpS †	--	--	--	--	--	--	--	--
PFOS	0.135	0.16	2.67	J	0.996	0.068	1.87E-03	1.42E-04
PFNS †	--	--	--	--	--	--	--	--
PFDS †	--	--	--	--	--	--	--	--
PFDoS §	--	--	--	--	--	--	--	--
ΣPFSA	--	--	--	J	2.32	0.165	4.36E-03	3.52E-04
NMeFOSAA	0.154	0.21	2.67	ND	ND	0.0349	ND	6.53E-05
NEtFOSAA	0.115	0.18	2.67	ND	ND	0.0328	ND	6.14E-05
PFOSA †	--	--	--	--	--	--	--	--
4:2 FTS †	--	--	--	--	--	--	--	--
6:2 FTS †	--	--	--	--	--	--	--	--
8:2 FTS †	--	--	--	--	--	--	--	--
10:2 FTS §	--	--	--	--	--	--	--	--
ΣPrecursors	--	--	--	ND	ND	0	ND	0
HFPO-DA ‡	0.062	0.1	2.67	U	0.0457	0.0119	8.60E-05	2.32E-05
Adona ‡	0.067	0.13	2.67	ND	ND	0.0145	ND	2.73E-05
11Cl-PF3OUdS ‡	0.072	0.11	2.67	ND	ND	5.37E-03	ND	1.01E-05
9Cl-PF3ONS ‡	0.068	0.13	2.67	ND	ND	5.07E-03	ND	9.53E-06
ΣNew Alternatives	--	--	--	U	0.0457	0.0119	8.60E-05	2.32E-05
ΣPFAS	--	--	--		9.88	0.642	0.0186	1.39E-03
Inorganic Fluoride	5.08E+04	6.28E+04	1.00E+05		6.42E+05	6.37E+04	1.21E+03	120

† Compound not measured in potable water.
§ Compound only measured in stack gas.
‡ Compound not measured in ambient air.
* ND: The compound was not detected or had a mean concentration less than zero following NC correction.
U: The mean concentration following NC correction is > zero (0) and ≤ the maximum MDL.
J: The mean concentration following NC correction is > the maximum MDL and ≤ the maximum LOQ.
Summed PFAS are qualified following the "highest order" individual pollutant qualifier (Text S4).

Table S16. Mercury Scrubber central tendency concentrations and mass flows for PFAS and IF.

Compound	Max NC (ng/L)	Max MDL (ng/L)	Max LOQ (ng/L)	Qualifier*	Concentration (ng/L)		Mass Flow (mg/day)	
					Mean	Uncertainty (± 1 std dev)	Mean	Uncertainty (± 1 std dev)
PFBA †	28.2	4.59	51		64.9	74.9	0.122	0.14
PFPeA †	0.27	0.3	5.81	J	2.32	0.622	4.36E-03	1.19E-03
PFHxA	0.301	0.62	5.81	J	4.62	1.01	8.69E-03	1.93E-03
PFHpA	0.253	0.3	5.81	J	0.811	0.285	1.53E-03	5.35E-04
PFOA	1.1	0.59	5.81	J	2.01	1.06	3.79E-03	2.00E-03
PFNA	0.205	0.36	5.81	U	0.0663	0.139	1.25E-04	2.62E-04
PFDA	0.204	0.16	5.81	ND	ND	0.104	ND	1.97E-04
PFUnA	0.195	0.26	5.81	ND	ND	0.0517	ND	9.75E-05
PFDoA	0.108	0.22	5.81	ND	ND	9.57E-03	ND	1.80E-05
PFTrDA	0.084	0.17	5.81	ND	ND	0	ND	0
PFTeDA	0.093	0.85	5.81	ND	ND	0	ND	0
ΣPFCA	--	--	--		74.7	76.3	0.14	0.143
PFBS	0.133	0.16	5.81	J	0.685	0.469	1.29E-03	8.79E-04
PFPeS †	0.224	0.3	5.81	ND	ND	0.149	ND	2.79E-04
PFHxS	0.25	0.13	5.81	J	0.764	0.438	1.44E-03	8.24E-04
PFHpS †	0.231	0.99	5.81	ND	ND	0.0763	ND	1.44E-04
PFOS	0.13	0.51	5.81	J	2.09	0.881	3.92E-03	1.65E-03
PFNS †	0.107	0.42	5.81	ND	ND	0	ND	0
PFDS †	0.147	0.31	5.81	ND	ND	0.0127	ND	2.39E-05
PFDoS §	--	--	--	--	--	--	--	--
ΣPFSA	--	--	--	J	3.53	1.43	6.64E-03	2.69E-03
NMeFOSAA	0.251	0.41	5.81	ND	ND	0.158	ND	2.97E-04
NEtFOSAA	0.252	0.58	5.81	ND	ND	0.146	ND	2.77E-04
PFOSA †	0.121	0.53	5.81	ND	ND	0	ND	0
4:2 FTS †	0.132	0.58	5.81	ND	ND	0.0522	ND	9.82E-05
6:2 FTS †	0.114	0.62	5.81	J	4.4	10.4	8.24E-03	0.0195
8:2 FTS †	0.138	0.7	5.81	ND	ND	0.0697	ND	1.31E-04
10:2 FTS §	--	--	--	--	--	--	--	--
ΣPrecursors	--	--	--	J	4.4	10.4	8.24E-03	0.0195
HFPO-DA ‡	0.1	0.29	5.81	J	2.16	1.06	4.07E-03	2.01E-03
Adona ‡	0.06	0.31	5.81	ND	ND	0	ND	0
11Cl-PF3OUdS ‡	0.071	0.27	5.81	ND	ND	0	ND	0
9Cl-PF3ONS ‡	0.055	0.31	5.81	ND	ND	0	ND	0
ΣNew Alternatives	--	--	--	J	2.16	1.06	4.07E-03	2.01E-03
ΣPFAS	--	--	--		84.8	82.9	0.159	0.155
Inorganic Fluoride	5.08E+04	6.28E+04	1.00E+05		6.42E+05	6.37E+04	2.57E+03	1.39E+03

† Compound not measured in potable water.
§ Compound only measured in stack gas.
‡ Compound not measured in ambient air.
* ND: The compound was not detected or had a mean concentration less than zero following NC correction.
U: The mean concentration following NC correction is > zero (0) and ≤ the maximum MDL.
J: The mean concentration following NC correction is > the maximum MDL and ≤ the maximum LOQ.
Summed PFAS are qualified following the "highest order" individual pollutant qualifier (Text S4).

Table S17. Grit central tendency concentrations and mass flows for PFAS and IF.

Compound	Max NC (ng/g)	Max MDL (ng/g)	Max LOQ (ng/g)	Qualifier*	Concentration (ng/g)**		Mass Flow (mg/day)	
					Mean	Uncertainty (± 1 std dev)	Mean	Uncertainty (± 1 std dev)
PFBA †	0.49	0.99	6.8	U	0.915	1.54	0.31	0.612
PFPeA †	0.135	0.61	6.8	ND	ND	0	ND	0
PFHxA	0.112	0.97	6.8	U	0.383	0.99	0.137	0.389
PFHpA	ND	0.69	6.8	ND	ND	0	ND	0
PFOA	ND	0.83	6.8	U	0.0225	0.045	9.53E-03	0.0191
PFNA	0.078	0.67	6.8	ND	ND	0	ND	0
PFDA	0.001	0.63	6.8	ND	ND	0	ND	0
PFUnA	0.104	0.63	6.8	ND	ND	0	ND	0
PFDoA	0.011	0.83	6.8	ND	ND	0	ND	0
PFTrDA	0.083	0.38	6.8	ND	ND	0	ND	0
PFTeDA	0.018	1.47	6.8	ND	ND	0	ND	0
ΣPFCA	--	--	--	U	1.32	2.46	0.457	0.965
PFBS	0.059	0.48	6.8	ND	ND	0	ND	0
PFPeS †	0.116	0.6	6.8	ND	ND	0	ND	0
PFHxS	0.021	1.1	6.8	ND	ND	0	ND	0
PFHpS †	0.058	1.06	6.8	ND	ND	0	ND	0
PFOS	0.059	0.94	6.8	ND	ND	0	ND	0
PFNS †	0.044	0.76	6.8	ND	ND	0	ND	0
PFDS †	ND	0.33	6.8	ND	ND	0	ND	0
PFDoS §	--	--	--	--	--	--	--	--
ΣPFSA	--	--	--	ND	ND	0	ND	0
NMeFOSAA	0.068	1.39	6.8	ND	ND	0	ND	0
NEtFOSAA	0.179	1.02	6.8	ND	ND	0.12	ND	0.0471
PFOSA †	0.109	0.57	6.8	ND	ND	0	ND	0
4:2 FTS †	0.156	1.63	6.8	ND	ND	0	ND	0
6:2 FTS †	0.068	1.09	6.8	ND	ND	0.005	ND	2.12E-03
8:2 FTS †	ND	1.96	6.8	ND	ND	0	ND	0
10:2 FTS §	--	--	--	--	--	--	--	--
ΣPrecursors	--	--	--	ND	ND	0	ND	0
HFPO-DA ‡	ND	0.87	6.8	ND	ND	0	ND	0
Adona ‡	ND	1.13	6.8	ND	ND	0	ND	0
11Cl-PF3OUdS ‡	0.052	0.71	6.8	ND	ND	0	ND	0
9Cl-PF3ONS ‡	0.033	0.65	6.8	ND	ND	0	ND	0
ΣNew Alternatives	--	--	--	ND	ND	0	ND	0
ΣPFAS	--	--	--	U	1.32	2.46	0.457	0.965
Inorganic Fluoride	229	410	1.03E+03		2.59E+03	788	1.02E+03	365

† Compound not measured in potable water.
§ Compound only measured in stack gas.
‡ Compound not measured in ambient air.
* ND: The compound was not detected or had a mean concentration less than zero following NC correction.
U: The mean concentration following NC correction is > zero (0) and ≤ the maximum MDL.
J: The mean concentration following NC correction is > the maximum MDL and ≤ the maximum LOQ.
Summed PFAS are qualified following the "highest order" individual pollutant qualifier (Text S4).
** Units are presented on a dry weight basis, corrected for the average sample-specific moisture content of 21.0%.

Table S18. Sewage Sludge central tendency concentrations and mass flows for PFAS and IF.

Compound	Max NC (ng/g)*	Max MDL (ng/g)*	Max LOQ (ng/g)*	Qualifier*	Concentration (ng/g)**		Mass Flow (mg/day)	
					Mean	Uncertainty (± 1 std dev)	Mean	Uncertainty (± 1 std dev)
PFBA †	0.39	3.56	24.4	ND	ND	0	ND	0
PFPeA †	0.135	2.2	24.4	J	3.82	1.78	60.3	33
PFHxA	0.112	3.46	24.4	J	5.52	0.993	91	11.1
PFHpA	ND	2.49	24.4	U	6.67E-03	0.0231	0.119	0.405
PFOA	ND	2.98	24.4	U	0.915	0.273	16.3	4.32
PFNA	0.078	2.39	24.4	U	0.214	0.155	ND	2.73
PFDA	0.001	2.24	24.4	U	0.454	0.0838	8.14	2.03
PFUnA	0.104	2.24	24.4	U	0.719	0.268	6.46	4.99
PFDoA	0.011	2.98	24.4	U	0.489	0.145	8.26	3.57
PFTrDA	0.083	1.37	24.4	U	0.285	0.191	0.0555	3.6
PFTeDA	0.018	5.27	24.4	ND	ND	0.0173	ND	0.341
ΣPFCA	--	--	--	J	12.4	2.5	191	40.9
PFBS	0.059	1.71	24.4	ND	ND	0	ND	0
PFPeS †	0.116	2.15	24.4	ND	ND	0	ND	0
PFHxS	0.021	3.95	24.4	U	0.0919	0.391	0.746	8.24
PFHpS †	0.058	3.8	24.4	ND	ND	0	ND	0
PFOS	0.059	3.37	24.4	J	15	1.11	265	29.6
PFNS †	0.044	2.73	24.4	ND	ND	0	ND	0
PFDS †	ND	1.17	24.4	ND	ND	0	ND	0
PFDoS §	--	--	--	--	--	--	--	--
ΣPFSA	--	--	--	J	15.1	1.17	266	34.3
NMeFOSAA	0.068	4.98	24.4	U	2.08	0.35	32.9	5.55
NEtFOSAA	0.052	3.66	24.4	U	1.71	0.27	27.2	4.44
PFOSA †	0.109	2.05	24.4	ND	ND	0	ND	0
4:2 FTS †	0.156	5.85	24.4	ND	ND	0	ND	0
6:2 FTS †	0.068	3.9	24.4	ND	ND	0.0331	ND	0.681
8:2 FTS †	ND	7.02	24.4	ND	ND	0	ND	0
10:2 FTS §	--	--	--	--	--	--	--	--
ΣPrecursors	--	--	--	U	3.78	0.496	60.1	7.04
HFPO-DA ‡	ND	3.12	24.4	ND	ND	0	ND	0
Adona ‡	0.101	4.05	24.4	ND	ND	0	ND	0
11Cl-PF3OUdS ‡	0.052	2.54	24.4	ND	ND	0	ND	0
9Cl-PF3ONS ‡	0.033	2.34	24.4	ND	ND	0	ND	0
ΣNew Alternatives	--	--	--	ND	ND	0	ND	0
ΣPFAS	--	--	--	J	31.3	3.72	517	67.9
Inorganic Fluoride	ND	--	3.81E+03		9.90E+03	1.92E+03	1.75E+05	2.69E+04

† Compound not measured in potable water.
§ Compound only measured in stack gas.
‡ Compound not measured in ambient air.
* ND: The compound was not detected or had a mean concentration less than zero following NC correction.
U: The mean concentration following NC correction is > zero (0) and ≤ the maximum MDL.
J: The mean concentration following NC correction is > the maximum MDL and ≤ the maximum LOQ.
Summed PFAS are qualified following the "highest order" individual pollutant qualifier (Text S4).
** Units are presented on a dry weight basis, corrected for the average sample-specific moisture content of 77.5%.

Table S19. Stack Gas central tendency concentrations and mass flows for PFAS, IF, and Total Fluoride.

Compound	Max NC (ng/m^3)	Max MDL (ng/m^3)	Max LOQ (ng/m^3)	Quali-fier*	Concentration (ng/m^3)**		Mass Flow (mg/day)	
					Mean	Uncertainty (± 1 std dev)	Mean	Uncertainty (± 1 std dev)
PFBA †	22.1	2.71	5.56		21.5	45.1	8.7	18
PFPeA †	1.2	0.274	1.36		1.55	1.24	0.614	0.511
PFHxA	16.6	0.454	1.35	J	1.21	1.43	0.474	0.4
PFHpA	23.7	0.277	1.16		1.23	2.07	0.481	0.596
PFOA	8.65	0.509	1.3	J	0.668	0.569	0.262	0.152
PFNA	0.102	0.364	1.68	U	0.226	0.0622	0.0885	0.0225
PFDA	8.38	0.062	0.697	J	0.431	1.04	0.167	0.294
PFUnA	0.0955	0.513	1.41	U	0.0771	0.0719	0.0304	0.03
PFDoA	0.0669	0.548	2.62	U	0.146	0.168	0.0568	0.0652
PFTrDA	0.0601	0.725	2.32	U	0.102	0.198	0.0392	0.0767
PFTeDA	0.087	1.05	2.56	U	0.13	0.186	0.0505	0.0722
ΣPFCA	--	--	--		27.3	42.4	11	17.9
PFBS	2.08	0.189	1.21	U	0.163	0.185	0.0637	0.049
PFPeS †	0.0496	1.14	2.32	U	0.0536	0.0831	0.0209	0.0322
PFHxS	0.225	0.523	1.77	U	0.154	0.138	0.0604	0.055
PFHpS †	0.451	0.046	0.232	U	0.0203	0.0277	7.86E-03	0.0108
PFOS	0.692	0.362	1.26	J	0.362	0.338	0.143	0.138
PFNS †	1.06	0.107	0.229	U	0.0122	0.0245	4.77E-03	9.59E-03
PFDS †	0.751	0.129	0.46	U	0.0232	0.0464	9.02E-03	0.0182
PFDoS §	1.49	1.52	3.25	U	0.0904	0.141	0.0348	0.0547
ΣPFSA	--	--	--	J	0.878	0.319	0.345	0.0993
NMeFOSAA	0.0797	1.45	2.79	U	0.39	0.41	0.152	0.158
NEtFOSAA	0.0797	18.6	38.3	U	1.92	2.96	0.768	1.18
PFOSA †	0.0569	0.946	2.56	U	0.212	0.389	0.0816	0.151
4:2 FTS †	0.0624	1.01	2.56	U	0.0834	0.0751	0.0323	0.0287
6:2 FTS †	4.25	3.28	3.78	U	1.96	3.43	0.766	1.34
8:2 FTS †	0.533	0.412	1.25		1.3	2.62	0.509	1.03
10:2 FTS §	0.179	1.58	3.11	U	0.266	0.371	0.104	0.145
ΣPrecursors	--	--	--		6.12	5.21	2.41	2.07
HFPO-DA ‡	610	10.5	35.7		488	827	196	331
Adona ‡	0.0262	1.59	3.25	U	0.11	0.117	0.0425	0.0453
11Cl-PF3OUdS ‡	0.0106	0.869	2.75	U	0.104	0.0783	0.0405	0.0301
9Cl-PF3ONS ‡	0.0496	0.301	1.12	U	0.0142	0.0367	5.54E-03	0.0143
ΣNew Alternatives	--	--	--		488	827	196	331
ΣPFAS	--	--	--		523	869	210	349
Inorganic Fluoride	3.83E+03	1.58E+04	3.21E+04	U	9.95E+03	7.55E+03	4.08E+03	2.98E+03
Total Fluorine	3.39E+08	2.02E+07	4.05E+07	U	1.23E+07	2.45E+07	5.08E+06	1.02E+07

† Compound not measured in potable water.
§ Compound only measured in stack gas.
‡ Compound not measured in ambient air.
* ND: The compound was not detected or had a mean concentration less than zero following NC correction.
U: The mean concentration following NC correction is > zero (0) and ≤ the maximum MDL.
J: The mean concentration following NC correction is > the maximum MDL and ≤ the maximum LOQ.
Summed PFAS are qualified following the "highest order" individual pollutant qualifier (Text S4).
** Concentration units are reported at 1 atm, 25°C.

Table S20. Ambient Air results, Ionic PFAS.

Compound	Max NC (pg/m³)	MDL (pg/m³)	LOQ (pg/m³)	Quali-fier*	Concentration (pg/m³)**		Mass Flow (mg/day)	
					Mean	Uncertainty (± 1 std dev)	Mean	Uncertainty (± 1 std dev)
PFBA †	1.76	1.48	1.73		16	2.42	6.26	0.939
PFPeA †	0.465	0.393	1.73	ND	ND	0.643	ND	0.253
PFHxA	0.181	0.425	1.73		3.4	1.81	1.34	0.725
PFHpA	0.0744	0.194	0.26		1.88	0.866	0.739	0.345
PFOA	0.264	0.559	1.73		26.3	31.9	10.3	12.5
PFNA	ND	0.155	0.173		1.08	0.312	0.424	0.122
PFDA	ND	0.159	0.173		0.814	0.164	0.319	0.0663
PFUnA	0.0219	0.167	0.173		0.294	0.0698	0.116	0.0284
PFDoA	ND	0.201	0.26	J	0.23	0.108	0.0904	0.042
PFTrDA	0.155	0.172	0.26	U	0.031	0.0264	0.0121	0.0106
PFTeDA	0.175	0.368	1.73	U	0.0961	0.0385	0.0377	0.015
ΣPFCA	--	--	--		50.1	34.3	19.7	13.5
PFBS	0.231	0.261	0.307	ND	ND	0	ND	0
PFPeS †	ND	0.0971	0.163	ND	ND	0	ND	0
PFHxS	4.01E-03	0.0376	0.0596		0.224	0.0925	0.0877	0.0355
PFHpS †	ND	0.171	0.247	ND	ND	0	ND	0
PFOS	0.101	0.115	0.19		2.15	0.824	0.843	0.325
PFNS †	ND	0.145	0.166	ND	ND	0	ND	0
PFDS †	ND	0.0981	0.167	U	1.66E-03	4.70E-03	6.59E-04	1.85E-03
PFDoS §	--	--	--	--	--	--	--	--
ΣPFSA	--	--	--		2.37	0.884	0.931	0.347
NMeFOSAA	ND	0.084	0.173		0.203	0.0843	0.0799	0.0338
NEtFOSAA	ND	0.187	0.26		2.2	2.22	0.863	0.868
PFOSA †	0.0906	0.26	0.26		0.87	0.305	0.341	0.12
4:2 FTS †	ND	0.0912	0.162	ND	ND	0	ND	0
6:2 FTS †	0.245	1.24	1.65	U	0.153	0.189	0.0594	0.0724
8:2 FTS †	ND	0.103	0.166		0.305	0.0803	0.12	0.0323
10:2 FTS §	--	--	--	--	--	--	--	--
ΣPrecursors	--	--	--		3.73	2.45	1.46	0.956
HFPO-DA ‡	--	--	--	--	--	--	--	--
Adona ‡	--	--	--	--	--	--	--	--
11Cl-PF3OUdS ‡	--	--	--	--	--	--	--	--
9Cl-PF3ONS ‡	--	--	--	--	--	--	--	--
ΣNew Alternatives	--	--	--	--	--	--	--	--
ΣPFAS	--	--	--		56.2	34.8	22.1	13.7
Inorganic Fluoride	--	--	--	--	--	--	--	--

† Compound not measured in potable water.
§ Compound only measured in stack gas.
‡ Compound not measured in ambient air.
* ND: The compound was not detected or had a mean concentration less than zero following NC correction.
U: The mean concentration following NC correction is > zero (0) and ≤ the maximum MDL.
J: The mean concentration following NC correction is > the maximum MDL and ≤ the maximum LOQ.
Summed PFAS are qualified following the "highest order" individual pollutant qualifier (Text S4).
** Concentration units are reported at 1 atm, 25°C.

Table S21. Ambient Air Results, Neutral PFAS

Compound	Max NC (pg/m^3)	MDL/LOQ (pg/m^3) *	Qualifier	Concentration (pg/m^3)	
				Mean	Uncertainty (± 1 std dev)
4:2 FTOH	0	17.3	ND	0	0
6:2 FTOH	0	8.67		696	411
8:2 FTOH	0	17.3		58.5	30.9
Et-FOSA	0	3.47	U	1.25	1.42
Me-FOSA	0	3.47	U	0.600	0.909
Me-FOSE	0	8.67	U	6.37	11.5
Et-FOSE	0	17.3		17.4	32.5

* For the measure of neutral PFAS in ambient air, MDLs were estimated as the LOQ. Thus, concentrations < MDL = LOQ were U-qualified.

Table S22. Impact of stack gas emissions on ambient air ionic PFAS concentrations.

PFAS	Day One (pg/m^3)				Day Two (pg/m^3)				Ambient Air Analysis MDL (pg/m^3)
	Stack Gas	Upwind, South	Downwind, North	Downwind Stack Contribution (%)[a]	Stack Gas	Upwind, North	Downwind, South	Downwind Stack Contribution (%)[b]	
PFBA	42,413	17.8	13.6	0.118 (0.9)	636	15.3	17.2	0.0110 (0.1)	1.48
PFPeA	2427	ND	0.440	0.00674 (1.5)	677	ND	ND	0.0117 (NA)[c]	0.393
PFHxA	822	3.87	4.71	0.00228 (<0.05)	1597	4.22	0.814	0.0275 (3.4)	0.425
PFHpA	386	1.50	2.75	0.00107 (<0.05)	2106	2.24	1.04	0.0363 (3.5)	0.194
PFOA	694	7.72	53.0	0.00193 (<0.05)	642	37.4	6.91	0.0111 (0.2)	0.559
PFNA	244	0.804	1.30	0.00068 (0.1)	208	1.40	0.821	0.00358 (0.4)	0.155
PFDA	48.9	0.803	0.906	0.000136 (<0.05)	813	0.862	0.683	0.0140 (2.1)	0.159
PFUnA	95.3	0.301	0.336	0.000265 (0.1)	58.9	0.328	0.213	0.00102 (0.5)	0.167
PFDoA	101	0.236	0.188	0.000281 (0.1)	191	0.261	0.236	0.00329 (1.4)	0.201
PFTrDA	22.5	0.0292	0.0347	0.0000624 (0.2)	181	ND	0.0628	0.00312 (5)	0.172
PFTeDA	74.9	0.109	0.0690	0.000208 (0.3)	186	0.0623	0.144	0.00320 (2.2)	0.368
ΣPFCA	47,329	33.1	77.3	0.131 (0.2)	7296	62.1	28.1	0.126 (0.4)	
PFBS	116	ND	ND	0.000321 (NA)	210	ND	ND	0.00362 (NA)	0.261
PFPeS	29.0	ND	ND	0.0000806 (NA)	78.1	ND	ND	0.00135 (NA)	0.0971
PFHxS	263	0.280	0.0935	0.000730 (0.8)	44.4	0.207	0.316	0.000765 (0.2)	0.038
PFHpS	29.3	ND	ND	0.0000814 (NA)	11.2	ND	ND	0.000194 (NA)	0.171
PFOS	281	3.12	1.26	0.000780 (0.1)	444	1.55	2.67	0.00765 (0.3)	0.115
PFNS	24.5	ND	ND	0.0000680 (NA)	0.0	ND	ND	0 (NA)	0.145
PFDS	46.4	ND	0.00664	0.000129 (1.9)	0.0	ND	ND	0 (NA)	0.0981
ΣPFSA	788	3.40	1.36	0.00219 (0.2)	788	1.76	2.98	0.0136 (0.5)	
NMeFOSAA	95.8	0.318	0.151	0.000266 (0.2)	685	0.182	0.162	0.0118 (7.3)	0.0840
NEtFOSAA	3143	0.241	3.50	0.00873 (0.2)	687	4.90	0.174	0.0119 (6.8)	0.187
PFOSA	27.2	0.684	1.03	0.0000756 (<0.05)	397	1.20	0.560	0.00684 (1.2)	0.260
4:2 FTS	35.7	ND	ND	0.0000991 (NA)	131	ND	ND	0.00226 (NA)	0.0912
6:2 FTS	889	0.151	ND	0.00247 (NA)	3029	0.194	0.327	0.0522 (16)	1.24
8:2 FTS	65.4	0.394	0.258	0.000182 (0.1)	2533	0.242	0.324	0.0437 (13.5)	0.103
ΣPrecursors	4256	1.79	4.94	0.0118 (0.2)	7463	6.72	1.55	0.129 (8.3)	
ΣPFAS	52,373	38.3	83.6	0.145 (0.2)	15,546	70.5	32.7	0.268 (0.8)	

[a] The estimated Day One downwind ambient air concentration contribution from the stack plume as calculated per the dispersion modeling dilution of $2.8*10^{-6}$.

[b] The estimated Day Two downwind ambient air concentration contribution from the stack plume as calculated per the dispersion modeling dilution of $1.7*10^{-5}$.

[c] *NA* downwind stack contribution percentages indicate the compound was not detected at the downwind ambient monitoring site.

Table S23. Impact of onsite neutral PFAS emissions on downwind ambient air concentrations

PFAS	Day One (pg/m^3)			Day Two (pg/m^3)			Ambient Air Analysis LOQ
	Upwind (South)	Downwind (North)	Difference[a]	Upwind (North)	Downwind (South)	Difference[a]	
4:2 FTOH	ND	ND	NA	ND	ND	NA	17.3
6:2 FTOH	525	1064	539	1038	158	-881	8.67
8:2 FTOH	36.5	65.7	29.1	102	29.5	-72.9	17.3
Et-FOSA	0.730	1.3	0.561	3.0	ND	NA	3.47
Me-FOSA	0.589	1.2	0.615	0.609	ND	NA	3.47
Me-FOSE	14.6	0.236	-14.3	0.640	10.1	9.41	8.67
Et-FOSE	38.3	ND	NA	ND	31.4	NA	17.3

[a] Difference = Downwind concentration minus upwind concentration.

Table S24. Point estimates and statistical confidence for NMFs of various PFAS families and inorganic fluoride at both the WWTP and SSI levels.

				95% confidence interval of the point estimate (mg/day)		p-value [b]	
Level of aggregation	**Compound Family or Compound**	**NMF [a] (mg/day)**	**Uncertainty (± 1 std dev) (mg/day)**	**Lower bound**	**Upper bound**	**Un-adjusted**	**Adjusted**
WWTP	PFCA	4004	5808	-14323	22331	0.54	1
	PFSA	-872	748	-3599	1854	0.35	1
	Precursors	-198	315	-1076	680	0.56	1
	New Alternatives	976	596	-752	2703	0.18	0.92
	Net PFAS	3909	5815	-14266	22084	0.55	1
	Inorganic fluoride	-2,059,026	16,508,755	-54,597,253	50,479,202	0.91	0.91
SSI	PFCA	-446	297	-1391	498	0.23	0.79
	PFSA	-274	34	-380	-168	**0.0034**	**0.017**
	Precursors	-46	28	-135	43	0.20	0.79
	New Alternatives	199	321	-823	1220	0.58	0.79
	Net PFAS	-568	452	-2005	869	0.30	0.79
	Inorganic fluoride	15,993,644	4,217,698	2,571,047	29,416,242	**0.032**	**0.032**

a A positive NMF indicates that the WWTP/SSI is a source of the compound/compound family to the external environment (land, water, and/or air); a negative NMF represents a sink.

b p-values < 0.05 (shown in bold) indicate that the corresponding point estimate of the NMF is statistically significantly different from 0 at the 95% confidence level. The adjusted p-values was derived via the Holm-Bonferroni method(Holm 1979), which adjusts for the fact that multiple tests are completed simultaneously (e.g., all PFCA or all SSI compounds together, etc.) and is a more conservative approach that protects against false positives.

Table S25. Point estimates and statistical confidence for NMFs of the individual PFAS compounds at the WWTP level.

				95% confidence interval of the point estimate (mg/day)		p-value [b]	
Compound Family	**PFAS**	**NMF [a] (mg/day)**	**Uncertainty (±1 std dev) (mg/day)**	**Lower bound**	**Upper bound**	**Un-adjusted**	**Adjusted**
PFCA	PFBA †	3872	5778	-14486	22231	0.55	1.0
	PFPeA †	156	629	-1799	2110	0.82	1.0
	PFHxA	284	672	-1592	2159	0.70	1.0
	PFHpA	-62	72	-271	147	0.44	1.0
	PFOA	-237	143	-643	169	0.18	1.0
	PFNA	-17	27	-105	71	0.57	1.0
	PFDA	20	24	-51	91	0.47	1.0
	PFUnA	-0.41	6.8	-20	19	0.95	1.0
	PFDoA	-4.9	8.2	-30	20	0.59	1.0
	PFTrDA	-2.0	6.0	-20	16	0.76	1.0
	PFTeDA	-3.7	6.1	-22	15	0.59	1.0
PFSA	PFBS	-437	759	-2578	1705	0.60	1.0
	PFPeS †	0.31	0.15	-0.19	0.80	0.14	1.0
	PFHxS	-66	115	-470	338	0.61	1.0
	PFHpS †	-3.5	21	-68	61	0.88	1.0
	PFOS	-366	614	-2074	1341	0.58	1.0
	PFNS †	0.0048	0.0096	-0.026	0.035	0.65	1.0
	PFDS †	0.021	0.12	-0.36	0.40	0.87	1.0
	PFDoS §	0.035	0.055	-0.14	0.21	0.57	1.0
Precursors	NMeFOSAA	44	23	-21	108	0.13	1.0
	NEtFOSAA	1.7	19	-52	55	0.93	1.0
	PFOSA †	0.10	0.17	-0.43	0.63	0.58	1.0
	4:2 FTS †	0.032	0.029	-0.059	0.12	0.34	1.0
	6:2 FTS †	-234	311	-1104	636	0.49	1.0
	8:2 FTS †	-9.6	14	-49	30	0.53	1.0
	10:2 FTS §	0.10	0.15	-0.36	0.57	0.53	1.0
New Alternatives	HFPO-DA ‡	976	596	-752	2703	0.18	1.0
	Adona ‡	0.043	0.045	-0.10	0.19	0.42	1.0
	11Cl-PF3OUdS ‡	0.040	0.030	-0.055	0.14	0.27	1.0
	9Cl-PF3ONS ‡	0.0055	0.014	-0.040	0.051	0.73	1.0

a A positive NMF indicates that the WWTP is a source of the compound/compound family to the external environment (land, water, and/or air); a negative NMF represents a sink.

b p-values < 0.05 (shown in bold) indicate that the corresponding point estimate of the NMF is statistically significantly different from 0 at the 95% confidence level. The adjusted p-values was derived via the Holm-Bonferroni method(Holm 1979), which adjusts for the fact that multiple tests are completed simultaneously (e.g., all PFCA or all SSI compounds together, etc.) and is a more conservative approach that protects against false positives.

Table S26. Point estimates and statistical confidence for NMFs of the individual PFAS compounds at the SSI level.

				95% confidence interval of the point estimate (mg/day)		p-value [b]	
Compound Family	**PFAS**	**NMF [a] (mg/day)**	**Uncertainty (±1 std dev) (mg/day)**	**Lower bound**	**Upper bound**	**Un-adjusted**	**Adjusted**
PFCA	PFBA †	-242	271	-1106	622	0.44	1
	PFPeA †	-55	30	-148	37	0.15	1
	PFHxA	-99	12	-135	-62	**0.0031**	0.089
	PFHpA	-2.7	1.9	-8.8	3.4	0.25	1
	PFOA	-22	9.2	-51	7.4	0.098	1
	PFNA	-1.5	0.51	-3.1	0.16	0.064	1
	PFDA	-9.7	2.5	-18	-1.7	**0.030**	0.79
	PFUnA	-6.4	5.0	-22	9.5	0.29	1
	PFDoA	-8.2	3.5	-19	3.0	0.10	1
	PFTrDA	-0.0089	3.6	-11	11	1.00	1
	PFTeDA	0.17	0.82	-2.4	2.8	0.85	1
PFSA	PFBS	-1.6	2.3	-8.9	5.7	0.54	1
	PFPeS †	0.31	0.15	-0.19	0.80	0.14	1
	PFHxS	0.86	8.9	-27	29	0.93	1
	PFHpS †	0.0094	0.040	-0.12	0.14	0.83	1
	PFOS	-274	30	-366	-182	**0.0022**	0.066
	PFNS †	0.0048	0.0096	-0.026	0.035	0.65	1
	PFDS †	0.021	0.12	-0.36	0.40	0.87	1
	PFDoS §	0.035	0.055	-0.14	0.21	0.57	1
Precursors	NMeFOSAA	-35	5.8	-53	-17	**0.0083**	0.23
	NEtFOSAA	-27	4.7	-44	-10	**0.017**	0.46
	PFOSA †	0.10	0.17	-0.43	0.63	0.58	1
	4:2 FTS †	0.032	0.029	-0.059	0.12	0.34	1
	6:2 FTS †	14	25	-65	93	0.61	1
	8:2 FTS †	1.2	1.3	-2.8	5.2	0.41	1
	10:2 FTS §	0.10	0.15	-0.36	0.57	0.53	1
New Alternatives	HFPO-DA ‡	198	321	-823	1220	0.58	1
	Adona ‡	0.043	0.045	-0.10	0.19	0.42	1
	11Cl-PF3OUdS ‡	0.040	0.030	-0.055	0.14	0.27	1
	9Cl-PF3ONS ‡	0.0055	0.014	-0.040	0.051	0.73	1

a A positive NMF indicates that the SSI is a source of the compound/compound family to the external environment (land, water, and/or air); a negative NMF represents a sink.

b p-values < 0.05 (shown in bold) indicate that the corresponding point estimate of the NMF is statistically significantly different from 0 at the 95% confidence level. The adjusted p-values was derived via the Holm-Bonferroni method(Holm 1979), which adjusts for the fact that multiple tests are completed simultaneously (e.g., all PFCA or all SSI compounds together, etc.) and is a more conservative approach that protects against false positives.

Table S27. Population-normalized[a] effluent mass flows ± uncertainties, µg/day/person (%), for PFAS at the WWTP level.

Individual PFAS	Wet Ash Slurry[b,c]			Grit[b]			Stack Gas[b,c]			Treated Water[b]			Total	
	Mass Flow	Uncert-ainty	%[d]	Mass Flow	Uncert-ainty	%[d]	Mass Flow	Uncert-ainty	%[d]	Mass Flow	Uncert-ainty	%[d]	Mass Flow	Uncert-ainty
PFBA	0.0165	0.00360	<0.1	0.00252	0.00497	<0.1	0.0174	0.0360	<0.1	41.8	44.2	99.9	41.8	44.2
PFPeA	0.0125	0.00177	0.3	0	0	0	0.00123	0.00102	<0.1	4.59	3.34	99.7	4.61	3.34
PFHxA	0.0292	0.00562	0.2	0.00111	0.00316	<0.1	0.000949	0.000802	<0.1	15.4	1.01	99.8	15.4	1.01
PFHpA	0.00422	0.00107	0.2	0	0	0	0.000963	0.00119	<0.1	2.67	0.239	99.8	2.67	0.240
PFOA	0.0137	0.00360	0.2	7.75E-05	0.000155	<0.1	0.000525	0.000304	<0.1	6.93	1.07	99.8	6.94	1.07
PFNA	0.00112	0.000242	0.2	0	0	0	0.000177	4.50E-05	<0.1	0.721	0.0620	99.8	0.723	0.0620
PFDA	0.000445	0.000263	0.1	0	0	0	0.000335	0.000589	0.1	0.474	0.151	99.8	0.474	0.151
PFUnA	1.30E-05	0.000187	17.6	0	0	0	6.08E-05	6.00E-05	82.4	0	0.0395	0	7.38E-05	0.000181
PFDoA	0	1.67E-05	0	0	0	0	0.000114	0.000131	100	0	0.0128	0	0.000114	0.000131
PFTrDA	1.49E-05	0.000112	16.0	0	0	0	7.85E-05	0.000154	84.0	0	0.00462	0	9.35E-05	0.000176
PFTeDA	2.22E-05	9.50E-05	18.0	0	0	0	0.000101	0.000145	82.0	0	0.0554	0	0.000123	0.000142
ΣPFCA	0.0777	0.0117	0.1	0.00372	0.00785	<0.1	0.0219	0.0358	<0.1	72.5	44.7	99.9	72.6	44.7
PFBS	0.00595	0.00119	0.2	0	0	0	0.000127	9.81E-05	<0.1	3.36	0.226	99.8	3.36	0.227
PFPeS	0.000570	0.000327	93.1	0	0	0	4.19E-05	6.45E-05	6.9	0	0	0	0.000611	0.000309
PFHxS	0.00434	0.00128	0.2	0	0	0	0.000121	0.000110	0.0	2.22	0.114	99.8	2.22	0.118
PFHpS	3.09E-06	7.19E-05	16.4	0	0	0	1.57E-05	2.16E-05	83.6	0	0.0453	0	1.88E-05	8.09E-05
PFOS	0.0108	0.00299	0.2	0	0	0	0.000287	0.000276	<0.1	5.81	0.513	99.8	5.82	0.515
PFNS	0	0	0	0	0	0	9.54E-06	1.92E-05	100	0	0	0	9.54E-06	1.92E-05
PFDS	2.47E-05	0.000242	57.7	0	0	0	1.81E-05	3.63E-05	42.3	0	0.00560	0	4.27E-05	0.000237
PFDoS §	--	--	--	--	--	--	6.97E-05	0.000110	100	--	--	--	6.97E-05	0.000110
ΣPFSA	0.0217	0.00527	0.2	0	0	0	6.90E-04	1.99E-04	<0.1	11.4	0.779	99.8	11.4	0.786
NMeFOSAA	0.000277	0.000134	0.1	0	0	0	0.000303	0.000317	0.1	0.491	0.0939	99.9	0.492	0.0938
NEtFOSAA	1.16E-05	0.000152	<0.1	0	0.000383	0	0.00154	0.00236	1.1	0.134	0.0433	98.9	0.136	0.0428
PFOSA	4.13E-05	0.000212	20.2	0	0	0	0.000163	0.000303	79.8	0	0.130	0	0.000205	0.000334
4:2 FTS	0	0	0	0	0	0	6.48E-05	5.76E-05	100	0	0.0148	0	6.48E-05	5.76E-05
6:2 FTS	0.0242	0.0469	2.1	0	1.72E-05	0	0.00153	0.00268	0.1	1.14	0.628	97.8	1.16	0.625
8:2 FTS	0.000352	0.000541	7.0	0	0	0	0.00102	0.00205	20.2	0.00368	0.00963	72.8	0.00505	0.0112
10:2 FTS §	--	--	--	--	--	--	0.000208	0.000291	100	--	--	--	0.000208	0.000291
ΣPrecursors	0.0249	0.0470	1.4	0	0	0	0.00483	0.00414	0.3	1.77	0.631	98.3	1.80	0.625
HFPO-DA	0.0245	0.00761	0.2	0	0	0	0.393	0.663	3.6	10.5	2.07	96.2	10.9	2.74
ADONA	0	0	0	0	0	0	8.52E-05	9.07E-05	100	0	0	0	8.52E-05	9.07E-05
11Cl-PF3OUdS	0	0	0	0	0	0	8.11E-05	6.02E-05	100	0	0	0	8.11E-05	6.02E-05
9Cl-PF3ONS	0	0.000112	0	0	0	0	1.11E-05	2.87E-05	100	0	0	0	1.11E-05	2.87E-05
ΣNew Alts.	0.0245	0.00720	0.2	0	0	0	0.393	0.663	3.6	10.5	2.07	96.2	10.9	2.74
ΣPFAS	0.149	0.0488	0.2	0.00372	0.00785	<0.1	0.420	0.699	0.4	96.2	44.7	99.4	96.8	44.8

[a] Total population served by the WWTP is estimates to be approximately 123,000.

[b] The wet ash slurry and grit are disposed of by landfilling; stack gas is emitted to the atmosphere; and treated water is discharged to the aquatic environment.

[c] Emission rates for wet ash slurry and stack gas were scaled by the SSI duty cycle (25%) for the year 2019, as only approximately ¼ of the time that the WWTP was continuously operated did the SSI emit ash or stack gas.

[d] Percent of the total effluent mass flow (summed across the four matrices) from the given matrix.

§ Compound only measured in stack gas.

Supplementary Figures

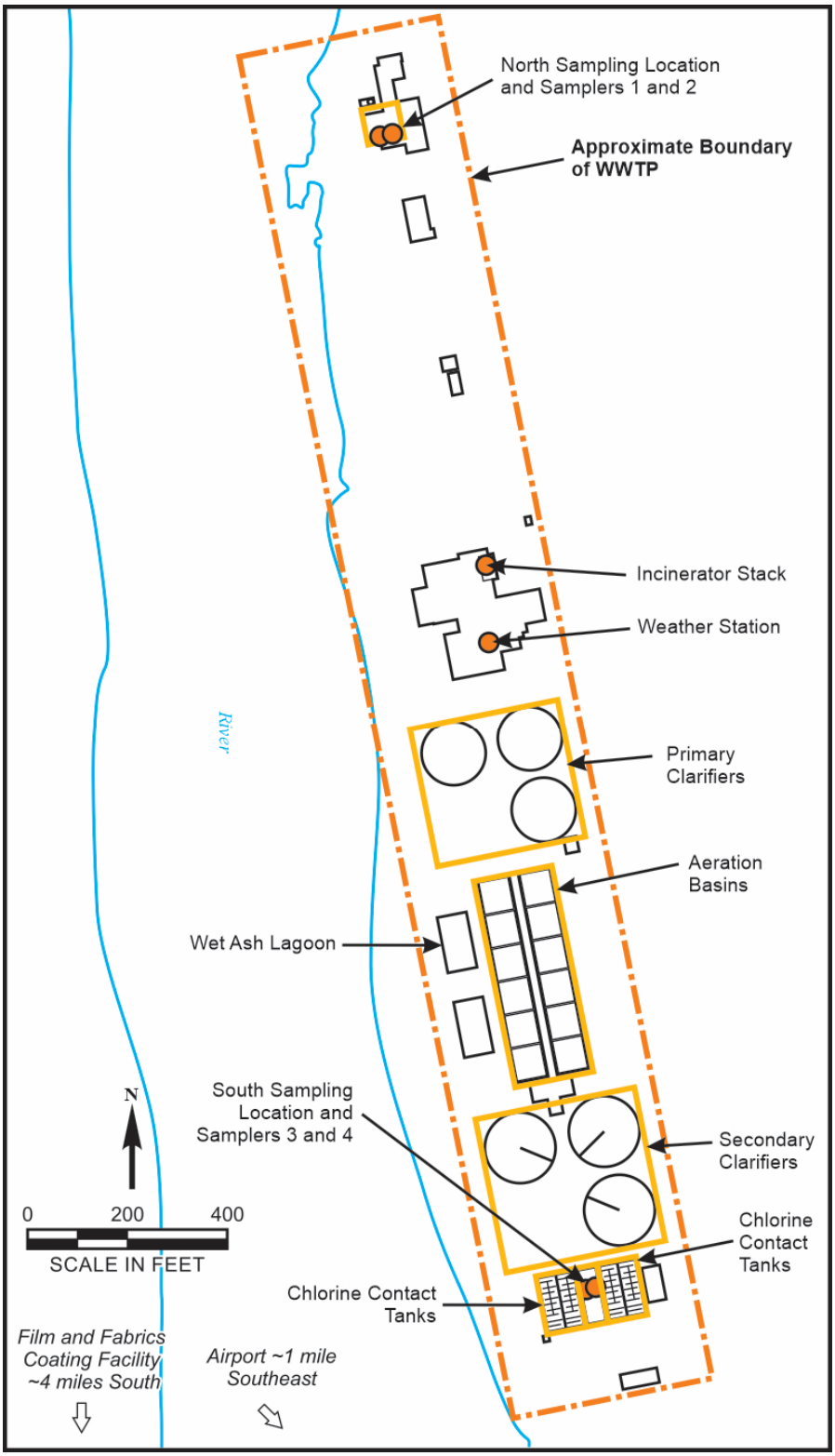

Figure S1. Aerial schematic of the WWTP's boundary and main features. Locations of ambient air sampling, incinerator stack sampling, and the portable weather station are illustrated by orange circles.

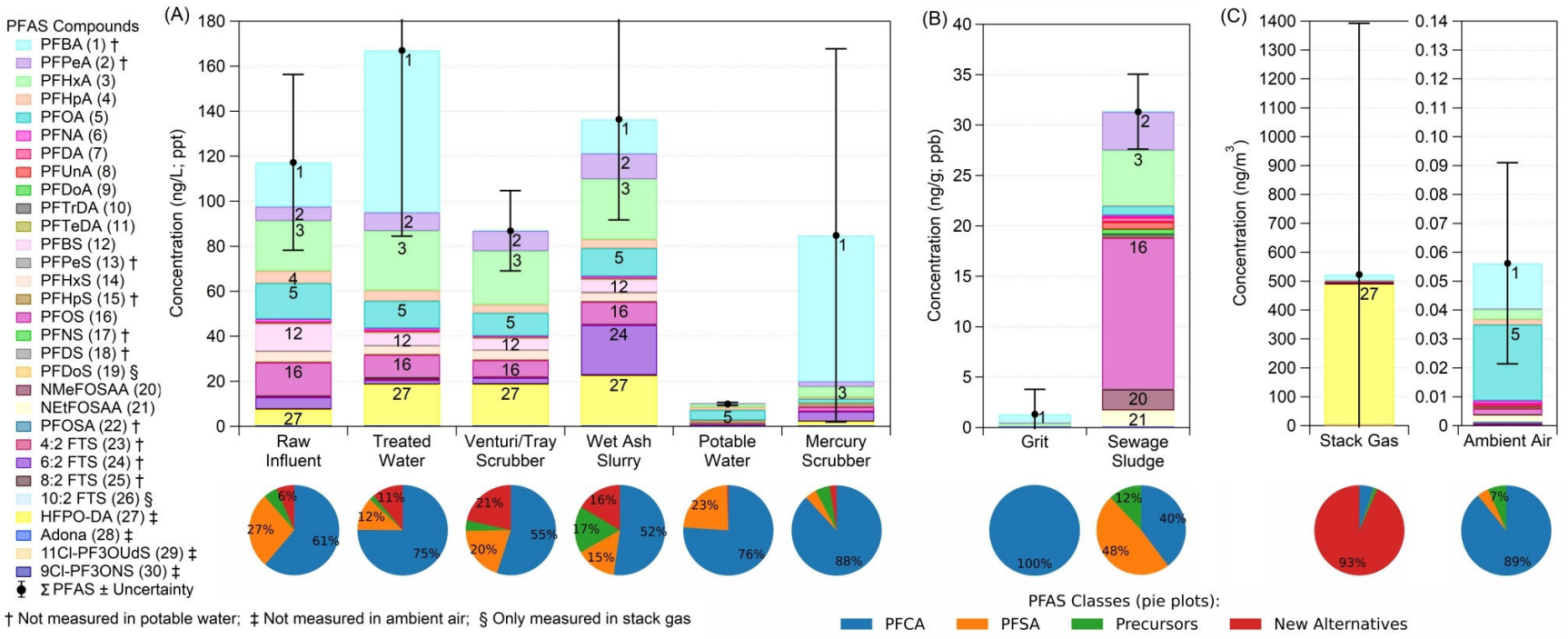

Figure S2. Study average PFAS concentrations and uncertainties (error bars; ±1σ) for each of the aqueous (A), solid (B), and air (C) matrices. Individual PFAS concentration contributions are illustrated by the different colored stacked bars, while the larger contributing individual PFAS are further identified via numbers labeled on the bar and linked back to the legend. The various symbols (†, §, ‡) in the legend identify individual PFAS not measured in the specified matrices. The total height of the stacked bar for each matrix indicates the average total sum PFAS concentration and the black error bars provide uncertainty estimates (±1σ). Note that the stack gas y-axis is scaled 10^4 times larger than the ambient air y-axis in subplot (C). Pie plots below each stacked bar show relative contributions of PFCAs (blue), PFSAs (orange), precursors (green), and new alternatives (red) to the total sum PFAS for each matrix.

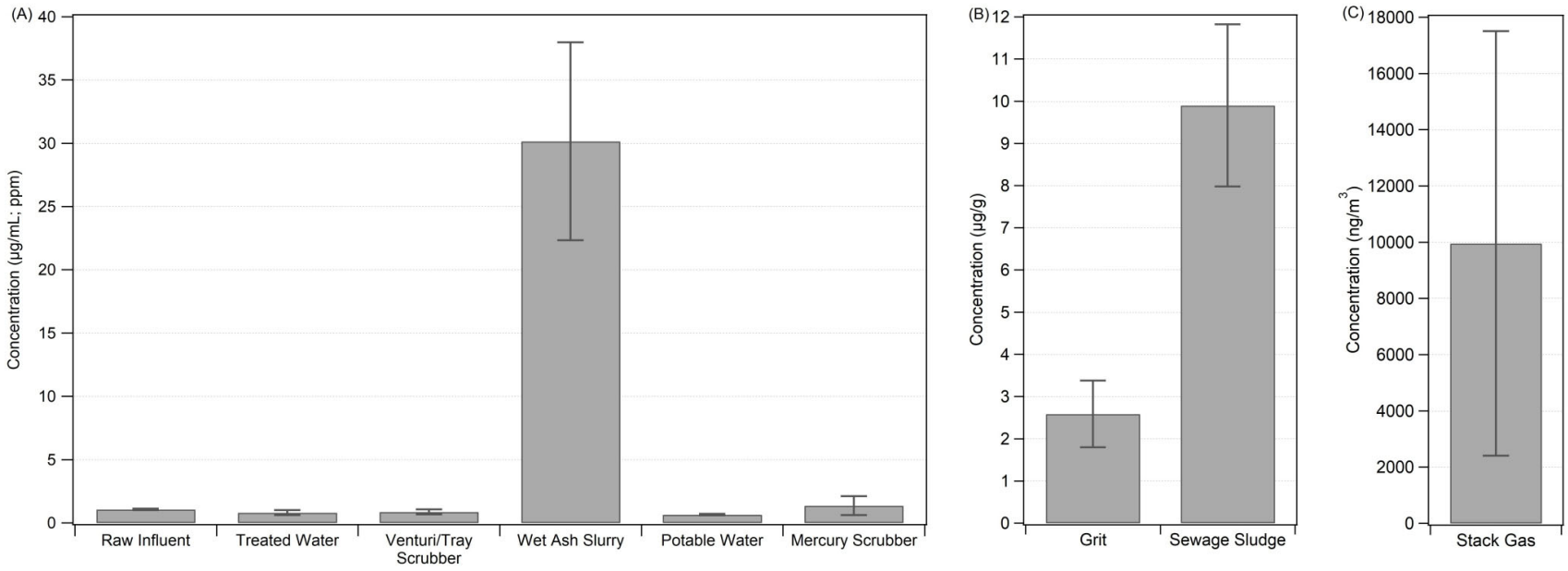

Figure S3. Study average inorganic fluoride concentrations and uncertainties (error bars; ±1σ) for various aqueous (A), solid (B), and stack gas (C) matrices. Inorganic fluoride was not measured in the ambient air matrix or in the solid phase of the wet ash slurry. To convert reported fluoride concentrations to hydrogen fluoride, multiplication by the stoichiometric adjustment factor of 1.053 is required ($HF = F^- * 1.053$).

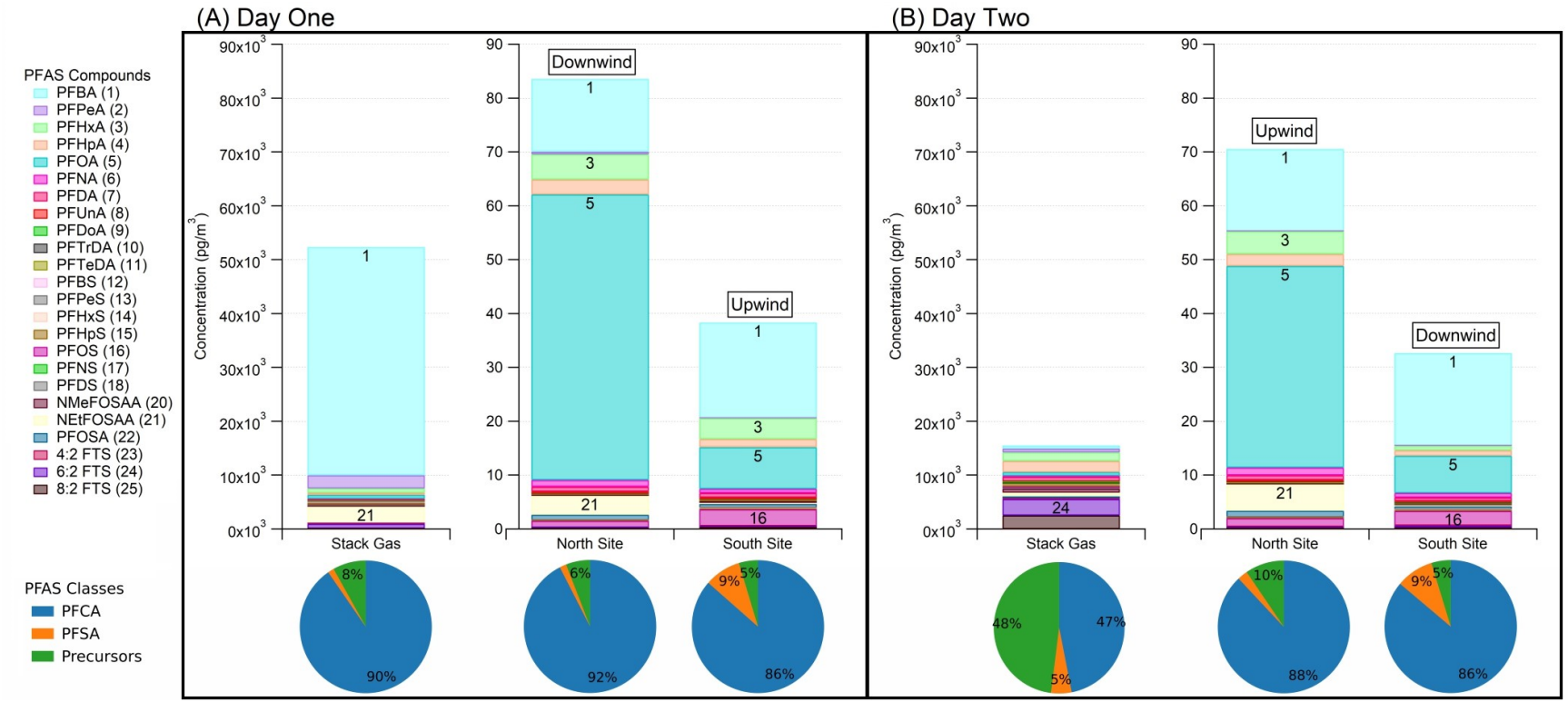

Figure S4. PFAS concentrations from the incinerator stack gas and the North and South ambient air sampling locations for both Day One (A) and Day Two (B) of the study. Individual PFAS concentration contributions are illustrated by the different colored stacked bars, while the larger contributing individual PFAS are further identified via numbers labeled on the bar and linked back to the legend. Only PFAS measured in both the ambient air and stack gas matrices are included. The total height of each stacked bar indicates the total PFAS concentration. Pie plots below each stacked bar show relative contributions of PFCAs (blue), PFSAs (orange), and precursors (green) to the total sum PFAS for each matrix. Note that the stack gas y-axes are scaled 10^3 times larger than the ambient air y-axes in both subplots.

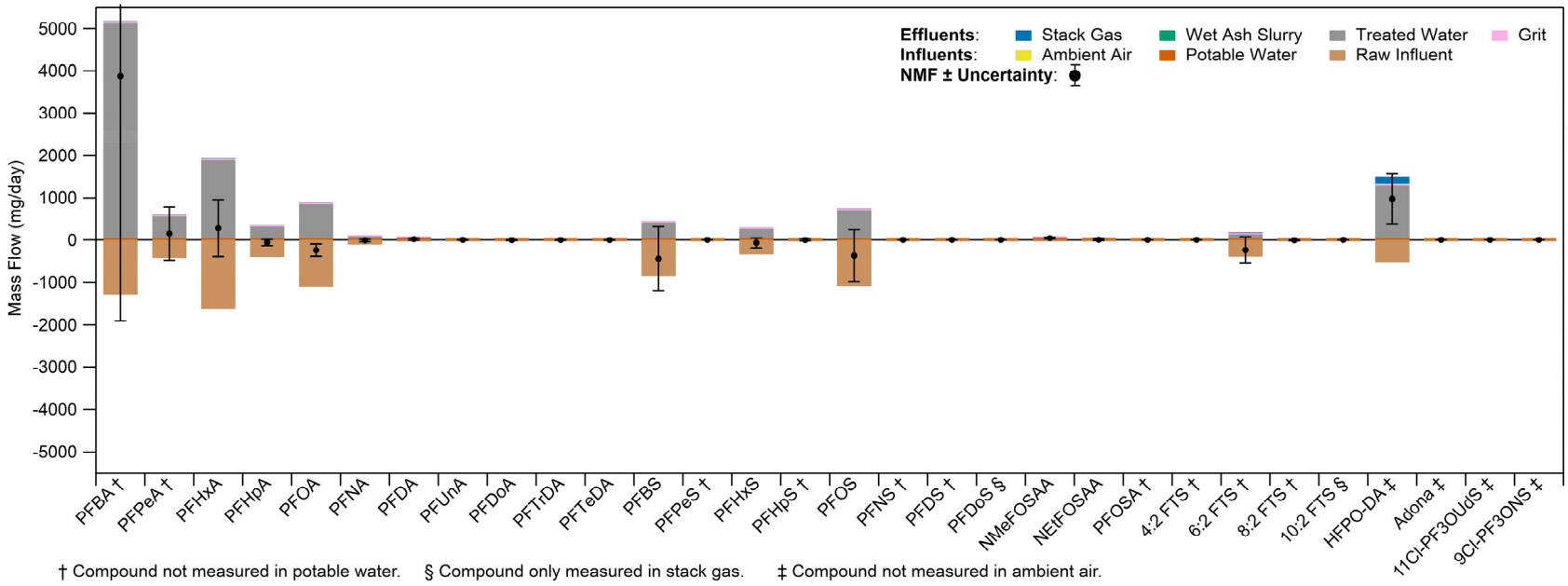

Figure S5. WWTP level study average mass flows and uncertainties for each individual PFAS. Each color indicates a separate influent/effluent source. Influents are shown as negatives and effluents as positives on the y-axis. The black circles represent the NMF for a given pollutant group, i.e., the sum of all effluents minus the sum of all influents. The black error bars represent the NMF uncertainty.

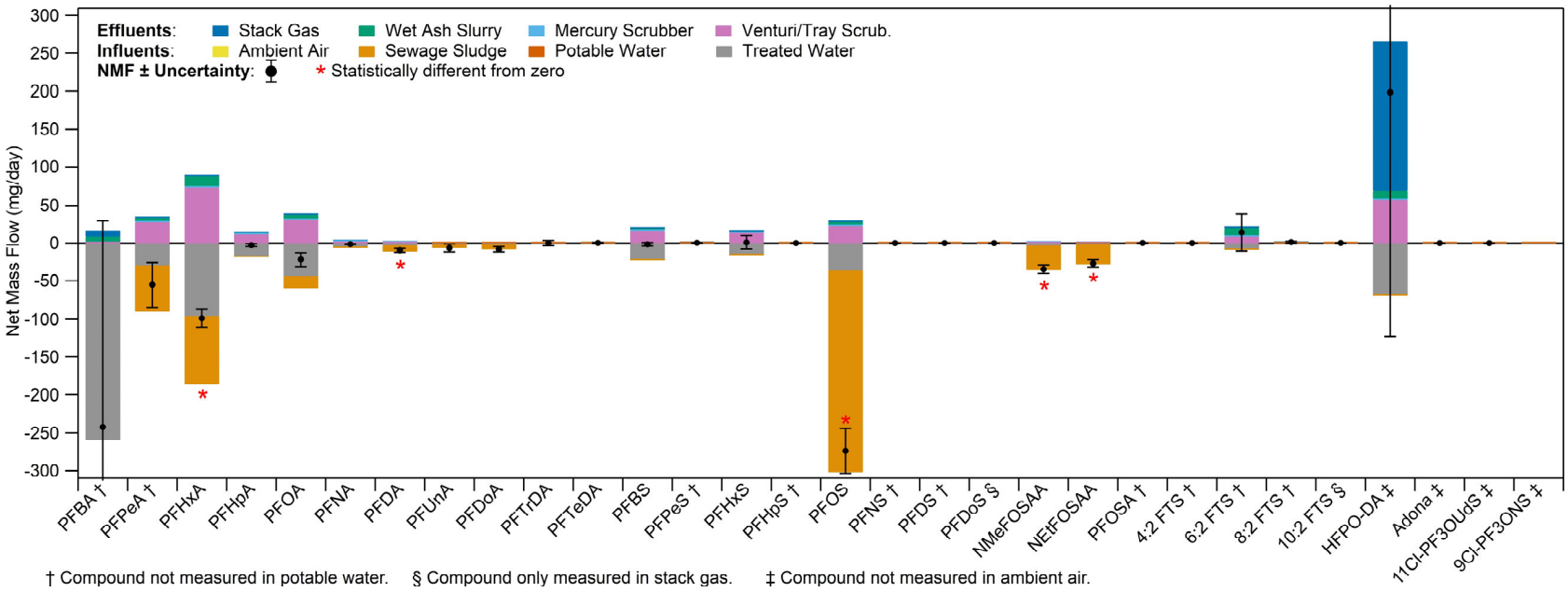

Figure S6. SSI level study average mass flows and uncertainties for each individual PFAS. Each color indicates a separate influent/effluent source. Influents are shown as negatives and effluents as positives on the y-axis. The black circles represent the NMF for a given pollutant group, i.e., the sum of all effluents minus the sum of all influents. The black error bars represent the NMF uncertainty. Red asterisks (*) denote NMFs that are statistically different from zero at the 95% confidence interval.

References

Ahrens, Lutz, Mahiba Shoeib, Tom Harner, Sum Chi Lee, Rui Guo, and Eric J. Reiner. 2011. 'Wastewater Treatment Plant and Landfills as Sources of Polyfluoroalkyl Compounds to the Atmosphere', *Environmental Science & Technology*, 45: 8098-105.

Alinezhad, Ali, Pavankumar Challa Sasi, Ping Zhang, Bin Yao, Alena Kubátová, Svetlana A. Golovko, Mikhail Y. Golovko, and Feng Xiao. 2022. 'An Investigation of Thermal Air Degradation and Pyrolysis of Per- and Polyfluoroalkyl Substances and Aqueous Film-Forming Foams in Soil', *ACS ES&T Engineering*, 2: 198-209.

Arvaniti, O. S., and A. S. Stasinakis. 2015. 'Review on the occurrence, fate and removal of perfluorinated compounds during wastewater treatment', *Sci Total Environ*, 524-525: 81-92.

DoD, U.S., and U.S. DOE. 2009. "DoD Quality Systems Manual Version 5.3." In.

EPA, U.S. 1984. "Quality Assurance Handbook for Air Pollution Measurement Systems: Volume III. Stationary Source Specific Methods." In.

———. 1986. "SW-846 Test Method 0010: Modified Method 5 Sampling Train." In.

———. 2021. "Human Health Toxicity Values for Hexafluoropropylene Oxide (HFPO) Dimer Acid and Its Ammonium Salt (CASRN 13252-13-6 and CASRN 62037-80-3) Also Known as "GenX Chemicals" " In.

———. 2023a. "Method 4-Determination of moisture content in stack gases." In *Title 40, Part 60, Appendix A-3*, edited by Code of Federal Regulation.

———. 2023b. "Method 5-Determination of particulate matter emissions from stationary sources." In *Title 40, Part 60, Appendix A-3*, edited by Code of Federal Regulations.

———. 2023c. "Method 18-Measurement of gaseous organic compound emissions by gas chromatography." In *Title 40, Part 60, Appendix A-6*, edited by Code of Federal Regulation.

———. 2023d. "Method 26A-Determination of hydrogen halide and halogen emissions from stationary sources isokinetic method." In *Title 40, Part 60, Appendix A-8*, edited by Code of Federal Regulations.

Eriksson, U., P. Haglund, and A. Karrman. 2017. 'Contribution of precursor compounds to the release of per- and polyfluoroalkyl substances (PFASs) from waste water treatment plants (WWTPs)', *Journal of Environmental Sciences*, 61: 80-90.

Gallen, C., G. Eaglesham, D. Drage, T. H. Nguyen, and J. F. Mueller. 2018. 'A mass estimate of perfluoroalkyl substance (PFAS) release from Australian wastewater treatment plants', *Chemosphere*, 208: 975-83.

Holm, Sture. 1979. 'A Simple Sequentially Rejective Multiple Test Procedure', *Scandinavian Journal of Statistics*, 6: 65-70.

Kim Lazcano, Rooney, Youn Jeong Choi, Michael L. Mashtare, and Linda S. Lee. 2020. 'Characterizing and Comparing Per- and Polyfluoroalkyl Substances in Commercially Available Biosolid and Organic Non-Biosolid-Based Products', *Environmental Science & Technology*, 54: 8640-48.

Loganathan, Bommanna G., Kenneth S. Sajwan, Ewan Sinclair, Kurunthachalam Senthil Kumar, and Kurunthachalam Kannan. 2007. 'Perfluoroalkyl sulfonates and perfluorocarboxylates in two wastewater treatment facilities in Kentucky and Georgia', *Water Research*, 41: 4611-20.

Sasi, Pavankumar Challa, Ali Alinezhad, Bin Yao, Alena Kubátová, Svetlana A. Golovko, Mikhail Y. Golovko, and Feng Xiao. 2021. 'Effect of granular activated carbon and other porous materials on thermal decomposition of per- and polyfluoroalkyl substances: Mechanisms and implications for water purification', *Water Research*, 200: 117271.

Schulman, Lloyd L., David G. Strimaitis, and Joseph S. Scire. 2000. 'Development and Evaluation of the PRIME Plume Rise and Building Downwash Model', *Journal of the Air & Waste Management Association*, 50: 378-90.
Schultz, Melissa M., Christopher P. Higgins, Carin A. Huset, Richard G. Luthy, Douglas F. Barofsky, and Jennifer A. Field. 2006. 'Fluorochemical Mass Flows in a Municipal Wastewater Treatment Facility', *Environmental Science & Technology*, 40: 7350-57.
Skoog, D.A., D.A West, and F.H. James. 1996. *Fundamentals of Analytical Chemistry* (Saunders College Publishing).
Sun, Mei, Elisa Arevalo, Mark Strynar, Andrew Lindstrom, Michael Richardson, Ben Kearns, Adam Pickett, Chris Smith, and Detlef R. U. Knappe. 2016. 'Legacy and Emerging Perfluoroalkyl Substances Are Important Drinking Water Contaminants in the Cape Fear River Watershed of North Carolina', *Environmental Science & Technology Letters*, 3: 415-19.
Taylor, John. 1997. *Introduction to error analysis, the study of uncertainties in physical measurements*.
Venkatesan, Arjun K., and Rolf U. Halden. 2013. 'National inventory of perfluoroalkyl substances in archived U.S. biosolids from the 2001 EPA National Sewage Sludge Survey', *Journal of Hazardous Materials*, 252-253: 413-18.
Wang, Ning, Jinxia Liu, Robert C. Buck, Stephen H. Korzeniowski, Barry W. Wolstenholme, Patrick W. Folsom, and Lisa M. Sulecki. 2011. '6:2 Fluorotelomer sulfonate aerobic biotransformation in activated sludge of waste water treatment plants', *Chemosphere*, 82: 853-58.
Wang, Yi, Nanyang Yu, Xiaobin Zhu, Huiwei Guo, Jianguo Jiang, Xuebing Wang, Wei Shi, Jichun Wu, Hongxia Yu, and Si Wei. 2018. 'Suspect and Nontarget Screening of Per- and Polyfluoroalkyl Substances in Wastewater from a Fluorochemical Manufacturing Park', *Environmental Science & Technology*, 52: 11007-16.
Willink, R. 2007. 'A generalization of the Welch–Satterthwaite formula for use with correlated uncertainty components', *Metrologia*, 44: 340.
Xiao, Feng, Pavankumar Challa Sasi, Ali Alinezhad, Svetlana A. Golovko, Mikhail Y. Golovko, and Anthony Spoto. 2021. 'Thermal Decomposition of Anionic, Zwitterionic, and Cationic Polyfluoroalkyl Substances in Aqueous Film-Forming Foams', *Environmental Science & Technology*, 55: 9885-94.
Xiao, Feng, Pavankumar Challa Sasi, Bin Yao, Alena Kubátová, Svetlana A. Golovko, Mikhail Y. Golovko, and Dana Soli. 2020. 'Thermal Stability and Decomposition of Perfluoroalkyl Substances on Spent Granular Activated Carbon', *Environmental Science & Technology Letters*, 7: 343-50.
Zhao, Lijie, Patricia K. McCausland, Patrick W. Folsom, Barry W. Wolstenholme, Hongwen Sun, Ning Wang, and Robert C. Buck. 2013. '6:2 Fluorotelomer alcohol aerobic biotransformation in activated sludge from two domestic wastewater treatment plants', *Chemosphere*, 92: 464-70.